SPACE, TELECOMMUNICATIONS AND RADIOSCIENCE LABORATORY

STARLAB
DEPARTMENT OF ELECTRICAL ENGINEERING / SEL
STANFORD UNIVERSITY • STANFORD, CA 94305

# THE ULF/ELF/VLF ELECTROMAGNETIC FIELDS GENERATED IN A SEA OF FINITE DEPTH BY ELEVATED DIPOLE SOURCES



by
A.C. Fraser-Smith
D.M. Bubenik

Final Technical Report E715-2

September 1984



Sponsored by
The Office of Naval Research
through
Contract No. N00014-77-C-0292

The views and conclusions contained in this document are those of the authors and should not be interpreted as necessarily representing the official policies, either expressed or implied, of the Office of Naval Research or the U.S. Government.

UNCLASSIFIED

SECURITY CLASSIFICATION OF THIS PAGE (When Data Entered)

| REPORT DOCUMENTATION PAGE | READ INSTRUCTIONS BEFORE COMPLETING FORM |
|---|---|
| 1. REPORT NUMBER: Final Tech. Report No. E715-2 | 2. GOVT ACCESSION NO.: AD-A149638 |
| | 3. RECIPIENT'S CATALOG NUMBER |
| 4. TITLE (and Subtitle): The ULF/ELF/VLF Electromagnetic Fields Generated in a Sea of Finite Depth by Elevated Dipole Sources. | 5. TYPE OF REPORT & PERIOD COVERED: Final 1 July 1979- 31 Dec. 1982 |
| | 6. PERFORMING ORG. REPORT NUMBER |
| 7. AUTHOR(s): A.C. Fraser-Smith, D.M. Bubenik | 8. CONTRACT OR GRANT NUMBER(s): N00014-77-C-0292 |
| 9. PERFORMING ORGANIZATION NAME AND ADDRESS: Space, Telecommunications and Radioscience Laboratory, Stanford University, Stanford, CA 94305 | 10. PROGRAM ELEMENT, PROJECT, TASK AREA & WORK UNIT NUMBERS: Task Area NR089-121 |
| 11. CONTROLLING OFFICE NAME AND ADDRESS: Office of Naval Research, Code 414, 800 N. Quincy Street, Arlington, Virginia 22217 | 12. REPORT DATE: September 1984 |
| | 13. NUMBER OF PAGES: 96 |
| 14. MONITORING AGENCY NAME & ADDRESS(if different from Controlling Office) | 15. SECURITY CLASS. (of this report): Unclassified |
| | 15a. DECLASSIFICATION/DOWNGRADING SCHEDULE |
| 16. DISTRIBUTION STATEMENT (of this Report): Approval for public release, distribution unlimited | |
| 17. DISTRIBUTION STATEMENT (of the abstract entered in Block 20, if different from Report) | |
| 18. SUPPLEMENTARY NOTES | |
| 19. KEY WORDS (Continue on reverse side if necessary and identify by block number): ULF, ELF, & VLF Electromagnetic Waves; Air-Undersea Communication; VMD, VED, HED, HMD; Sea Floor Effects | |

20. ABSTRACT (Continue on reverse side if necessary and identify by block number)

In this report we complete the presentation of the results of a study of the amplitudes of the quasi-static electromagnetic fields produced in, on, and above the surface of a sea of finite depth by vertically-directed harmonic electric and magnetic dipoles (VED's and VMD's, respectively) and horizontally-directed harmonic electric and magnetic dipoles (HED's and HMD's, respectively). In a previous report and publication we presented numerical data for the fields produced on and above the surface of the sea by the dipole sources when submerged in the sea. We now present data for the fields produced in the sea by

DD FORM 1 JAN 73 1473 EDITION OF 1 NOV 65 IS OBSOLETE

S N 0102-LF-014-6601

UNCLASSIFIED

SECURITY CLASSIFICATION OF THIS PAGE (When Data Entered)

the same dipole sources when they are either on or elevated above the sea surface. The primary purpose of these computations is to determine the conditions under which an electrically-conducting sea bed can produce significant changes in the fields generated by the dipoles, as compared with the fields produced in, on, and above an infinitely deep sea, for frequencies in the ULF, ELF, and VLF bands (frequencies less than 30 kHz). In contrast to our earlier work, where we found substantial floor effects on the fields produced by the submerged dipoles, and particularly strong effects on some of the field components produced by a submerged VED, the present work shows that the fields produced in the sea by elevated dipoles are comparatively little affected by the presence of a sea floor. This result is in fact in agreement with our previously-derived criteria for estimating when a sea floor effect is likely to occur: (1) the sea floor effects are most marked in seas that are electrically shallow, (2) the largest changes in the fields occur when the dipoles are located within one sea water skin depth of the sea floor, and (3) there are essentially no sea floor effects when the dipoles are located more than three sea water skin depths above the floor. These new data and results should prove useful in studies of air-undersea communication at frequencies less than 30 kHz.

# The ULF/ELF/VLF Electromagnetic Fields Generated in a Sea of Finite Depth by Elevated Dipole Sources

by

A.C. Fraser-Smith
D.M. Bubenik[1]

Final Technical Report E715-2


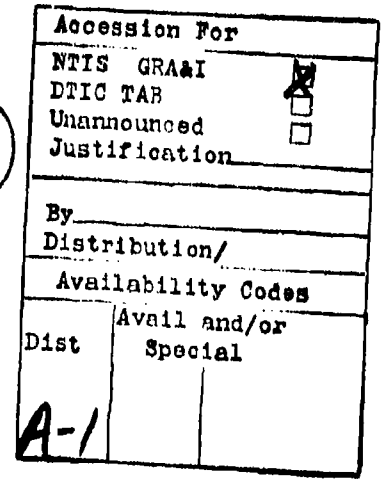


September 1984

Sponsored by
The Office of Naval Research
through
Contract No. N00014-77-C-0292

---

[1]Present Address: Electromagnetic Sciences Laboratory, SRI International, Menlo Park, California 94025

## ACKNOWLEDGEMENTS

We wish to thank Oswald G. Villard, Jr., for his continued support and encouragement during the course of this work, and R. Gracen Joiner of the Office of Naval Research for helpful discussions and for making this work possible.

Support for the work was provided by the Office of Naval Research through Contract No. N00014-77-C-0292.

## ABSTRACT

In this report we complete the presentation of the results of a study of the amplitudes of the quasi-static electromagnetic fields produced in, on, and above the surface of a sea of finite depth by vertically-directed harmonic electric and magnetic dipoles (VED's and VMD's, respectively) and horizontally-directed harmonic electric and magnetic dipoles (HED's and HMD's, respectively). In a previous report and publication we presented numerical data for the fields produced on and above the surface of the sea by the dipole sources when submerged in the sea. We now present data for the fields produced in the sea by the same dipole sources when they are either on or elevated above the sea surface. The primary purpose of these computations is to determine the conditions under which an electrically-conducting sea bed can produce significant changes in the fields generated by the dipoles, as compared with the fields produced in, on, and above an infinitely deep sea, for frequencies in the ULF, ELF, and VLF bands (frequencies less than 30 kHz). In contrast to our earlier work, where we found substantial sea floor effects on the fields produced by the submerged dipoles, and particularly strong effects on some of the field components produced by a submerged VED, the present work shows that the fields produced in the sea by elevated dipoles are comparatively little affected by the presence of a sea floor. This result is in fact in agreement with our previously-derived criteria for estimating when a sea floor effect is likely to occur: (1) the sea floor effects are most marked in seas that are electrically shallow, (2) the largest changes in the fields occur when the dipoles are located within one sea water skin depth of the sea floor, and (3) there are essentially no sea floor effects when the dipoles are located more than three sea water skin depths above the floor. These new data and results should prove useful in studies of air-undersea communication at frequencies less than 30 kHz.

# TABLE OF CONTENTS

## A NOTE ON FREQUENCIES

In this report we use the abbreviation ULF (ultra-low frequencies) for frequencies less than 5 Hz. Pc 1 geomagnetic pulsations are observed in the upper part of this frequency range (0.2 - 5 Hz). ELF (extremely-low frequencies) is used to designate frequencies in the range 5 Hz to 3 kHz, and VLF (very-low frequencies) is used for frequencies in the range 3 to 30 kHz.

# 1. INTRODUCTION

This report extends earlier work in which we gave a broad description of the ultra-low frequency (ULF; frequencies less than 5 Hz) and extremely-low frequency (ELF; frequencies in the range 5 Hz to 3 kHz) electromagnetic fields produced on and above the surface of a sea of finite depth by *submerged* harmonic electric and magnetic dipole sources [*Fraser-Smith and Bubenik*, 1979, 1980]. As we reported at the time, the purpose of this earlier work was to provide new, quantitative information about the effects of a sea floor on the ULF/ELF electromagnetic fields propagating upwards from submerged sources. In addition to providing this information, our work showed that the sea floor effects could be quite large under certain conditions, particularly at frequencies in the ULF range and for a vertical electric dipole source. Among the many applications of these earlier results, we pointed out two specific Navy applications: submarine detection and undersea-to-air communication. The work we now report is particularly relevant to the latter application; our results describe the electromagnetic field amplitudes that can be produced in the sea, and the effects of a sea floor on these amplitudes, for *elevated* (*i.e.*, airborne) dipole sources, and thus the data are applicable to an air-to-undersea communication link.

When combined with our earlier undersea-to-air results, these new air-to-undersea data should provide much of the quantitative information required for studies of two-way air-undersea communication links utilizing frequencies in the ULF, ELF, and VLF ranges. Since radio waves with frequencies above the upper limit of the VLF range (30 kHz) do not penetrate to any significant depth in sea water, the three frequency ranges specifically covered by our analysis should include all of the radio frequencies that have any practical application to communication with moderately or deeply submerged submarines.

In addition to their communication and submarine detection applications, our earlier data [*Fraser-Smith and Bubenik*, 1979, 1980] could well be utilized in geophysical prospecting and in the derivation of effective sea floor conductivities. The new data presented here are less likely to have application in these latter activities, because of the much smaller relative magnitudes of the sea floor effects. However, there is a possible application analogous to submarine detection, namely the detection by electromagnetic means of the presence of overhead aircraft by submerged submarines.

**Table 1:** Representative skin depths (for $\sigma_s = 4.0$ S/m)

| Frequency (Hz) | Skin depth (m) | Frequency (Hz) | Skin depth (m) | Frequency (Hz) | Skin depth (m) |
|---|---|---|---|---|---|
| 10,000 | 2.52 | 100 | 25.2 | 1 | 251.6 |
| 8,000 | 2.81 | 80 | 28.1 | 0.8 | 281.3 |
| 6,000 | 3.25 | 60 | 32.5 | 0.6 | 324.9 |
| 4,000 | 3.98 | 40 | 39.8 | 0.4 | 397.9 |
| 2,000 | 5.63 | 20 | 56.3 | 0.2 | 562.7 |
| 1,000 | 7.96 | 10 | 79.6 | 0.1 | 795.8 |
| 800 | 8.90 | 8 | 89.0 | 0.08 | 889.7 |
| 600 | 10.3 | 6 | 102.7 | 0.06 | 1027.3 |
| 400 | 12.6 | 4 | 125.8 | 0.04 | 1258.2 |
| 200 | 17.8 | 2 | 177.9 | 0.02 | 1779.4 |
| 100 | 25.2 | 1 | 251.6 | 0.01 | 2516.5 |

This report also extends earlier work in which we considered the feasibility of air-to-undersea communication at ULF using airborne loop antennas [*Fraser-Smith et al.*, 1977]. The frequencies in this latter study were largely restricted to 1 Hz and sea floor effects were only briefly considered; in addition, the sources of the ULF fields were limited to loop antennas, *i.e.*, to magnetic dipole sources. In the present work all major categories of dipole sources are covered by the analysis: vertically-directed electric and magnetic dipoles (VED's and VMD's, respectively) and horizontally-directed electric and magnetic dipoles (HED's and HMD's, respectively). Further, as has already been mentioned, all frequencies in the ULF/ELF/VLF range are covered and information is always provided about the possibility of sea floor effects. Despite the limitations of its field data, the earlier work is not superseded since its primary purpose was to use representative ULF field data to assess the feasibility of air-to-undersea communication, whereas the purpose of the present work is to present a wide range of field data for use in such studies.

Our computed values of the ULF/ELF/VLF electromagnetic fields are presented in a frequency-independent parametric form that has two features. First, all distances are measured in units of the sea water skin depth $\delta$, which is given by

$$\delta = (2/\omega\mu_0\sigma_s)^{1/2}, \tag{1.1}$$

where $\omega = 2\pi f$ is the angular frequency, $\mu_0$ is the permeability of free space ($4\pi \times 10^{-7}$ H/m), and $\sigma_s$ is the electrical conductivity of sea water measured in S/m. The second feature is the use of a sea floor conductivity $\sigma_f$ that is measured in units of the sea water conductivity $\sigma_s$. This approach enables the dipole field amplitudes to be presented in a more general form than would otherwise be possible and it avoids the duplication that would result from the use of specific frequencies. A minor disadvantage of the approach is the need for a computation to be made to obtain the actual electric and magnetic field amplitudes from the given field data, which are also in parametric form. However, these computations are comparatively simple and can be made quickly on a hand calculator; worked examples are included in a later section to make the conversion process clear. The same parametric approach was used in some of our earlier work [*Fraser-Smith and Bubenik*, 1979, 1980], and further worked examples are given there. To assist further in the computation, and in the interpretation of the data, representative skin depths for sea water (we assume $\sigma_s = 4.0$ S/m) are listed in Table 1.

In our earlier computations for the undersea-to-air path, we used two different values

of the sea floor conductivity to show the effects produced by the sea floor on the dipole fields (specifically, we used $\sigma_f = 0.1\sigma_s$ and $\sigma_f = 0.01\sigma_s$). If we had used the same approach in this report, we would have had to include nearly 100 figures, which appeared excessive. We therefore restricted our computations to one value of the sea floor conductivity, namely $\sigma_f = 0.1\sigma_s$. While this restriction certainly limits the quantity of our data, it is unlikely to seriously limit studies using the data because of the reduced importance of sea floor effects for the air-to-undersea path. This is consistent with our previous observation that sea floor effects are most pronounced when the dipole sources are close to the sea floor [*Fraser-Smith and Bubenik*, 1979, 1980].

One other possible limitation of our data results from the restriction of the dipole altitudes to the three values $h = 0$, $3.0\delta$, and $10.0\delta$. Because our work is primarily oriented toward air-to-undersea communication with moderately to deeply submerged receivers, the frequencies of most interest lie in the ULF and lower-ELF ranges, where the skin depths vary from a few tens of meters up to many kilometers and the signals can penetrate to considerable depths in the sea water before they become too attenuated to be detected. For these skin depths the restriction of $h$ to a maximum value of $10\delta$ does not seriously limit the range of applicability of our data. However, for frequencies in the VLF range, a maximum value of $10.0\delta$ for $h$ clearly restricts the altitude of the dipole sources to impractically low values for fixed-wing aircraft operation. Fortunately, this is not a serious limitation, because at VLF the depth of any sea of practical importance for air-to-undersea communication is likely to exceed 10 - 100 skin depths and sea floor effects can be ignored (the sea water skin depth varies from a maximum of about 4.6 m at 3 kHz down to 1.4 m at 30 kHz). The sea can then be assumed to be of infinite depth and the VLF fields generated beneath its surface can be calculated with little difficulty using comparatively simple expressions [*e.g., Kraichman*, 1976].

In the following section we list the field expressions for the four dipole types and describe the method of calculation used to obtain the amplitudes of the fields (Section 2). We next briefly describe the results of the computations, which are presented almost entirely in graphical form in six Appendices and which comprise the major part of this report (Section 3 and Appendices). Some of the significance of these results are discussed in the following section (Section 4). A list of references (Section 5) and the six appendices complete the report. In general, the format of the data and the notation are very close to those used in our undersea-to-air work [ *Fraser-Smith and Bubenik*, 1979, 1980]. However, one unavoidable difference arises because of the interchange of rce

and field point locations. In our earlier work we use $h$ to indicate the height of the field point, or receiver, above the sea, and $d$ is used for the depth of the dipole source in the sea. In the present work $h$ is used for the height of the dipole above the sea and $d$ indicates the depth of the field point, or receiver, in the sea. All the other symbols, including $D$, the depth of the sea, have the same meaning as before.

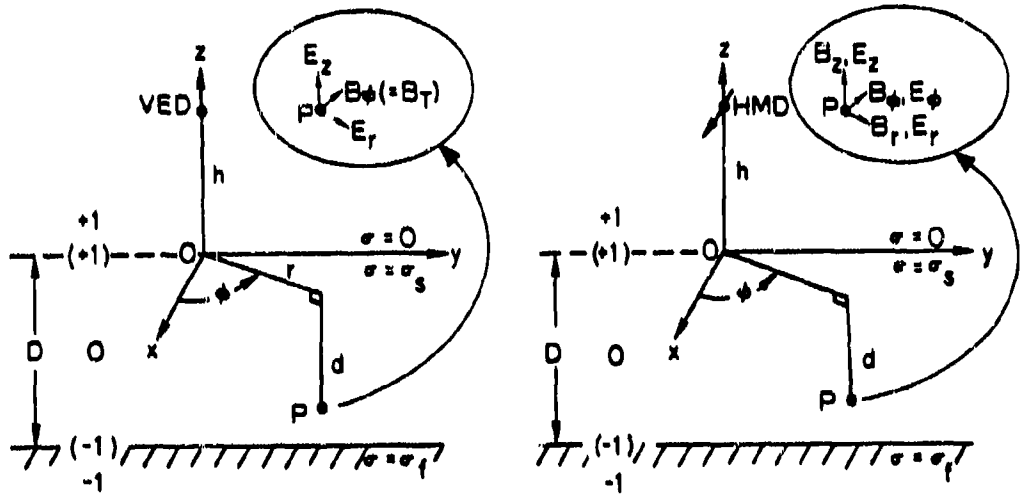


**Figure 1:** The geometry employed in computing the electromagnetic field components produced at point $P$ located at a depth $d$ in a sea of finite depth $D$ ($D \geq d$) by dipole sources located at an altitude $h$ above the surface of the sea. The electromagnetic field components for two dipole sources are illustrated in the figure. On the left are shown the $E_r$, $E_z$ and $B_\phi$ field components produced by a VED source, and on the right are shown the $B_r$, $B_z$, $B_\phi$ and $E_r$, $E_z$, $E_\phi$ components produced by a HMD source.

## 2. FIELD CALCULATIONS

Figure 1 shows the geometry used in the field calculations; except for the interchange of the source and field points, it closely resembles the geometry used earlier for the undersea-to-air link [*Fraser-Smith and Bubenik*, 1979, 1980]. A cylindrical coordinate system $(r,\phi,z)$ is used and the harmonic dipoles, of moment $m$ (magnetic dipole) or $p$ (electric dipole) and angular frequency $\omega$ ($\omega = 2\pi f$), are located at the point (0,0,h). The sea surface is the plane $z = 0$, the sea floor is the plane $z = -D$, and the field measurements are made at the point $P(r,\phi,-d)$, where $D \geq d \geq 0$. The region $z > 0$ is air, assumed to be free space, while the region $z < -D$ is a homogeneous conducting half-space of conductivity $\sigma_f$ representing the sea bed. To simplify the notation in the field expressions, the air, water, and sea bed regions have been labeled +1, 0, and -1, respectively, and the surface and sea floor boundaries are correspondingly denoted by +1 and -1.

It may be noted that the HMD source in Figure 1 is directed along the $x$ axis. This particular geometry, which is also used for the HED, differs from that of *Kraichman* [1976], who oriented his HED along the $x$-direction and his HMD along the $y$-direction.

The expressions for the electromagnetic fields produced by the VED, VMD, HED, and HMD at the point $P$ were derived by using a method adapted from *Morrison et al.*, [1969], and *Kong*, [1975]. The same method was used in our earlier work to obtain the field components produced above the sea by submerged dipole sources. The field expressions for the four dipole types are:

1. Vertical Electric Dipole

$$E_r = -\frac{p}{2\pi\sigma_0}\int_0^\infty \gamma_0 F_{4M}\,\lambda\,d\lambda, \tag{2.1}$$

$$E_z = \frac{p}{2\pi\sigma_0}\int_0^\infty F_{1M}\,\lambda^2\,d\lambda, \tag{2.2}$$

$$B_\phi = \frac{\mu_0 p}{2\pi}\int_0^\infty F_{2M}\,\lambda\,d\lambda. \tag{2.3}$$

2. Vertical Magnetic Dipole

$$E_\phi = -\frac{i\omega\mu_0 m}{2\pi}\int_0^\infty \frac{1}{\gamma_0+\lambda}F_{2E}\lambda^2\,d\lambda, \tag{2.4}$$

$$B_r = -\frac{\mu_0 m}{2\pi}\int_0^\infty \frac{\gamma_0}{\gamma_0+\lambda}F_{4E}\lambda^2\,d\lambda, \tag{2.5}$$

$$B_z = \frac{\mu_0 m}{2\pi}\int_0^\infty \frac{1}{\gamma_0+\lambda}F_{1E}\lambda^3\,d\lambda. \tag{2.6}$$

3. Horizontal Electric Dipole

$$E_r = -\frac{p\cos\phi}{2\pi\sigma_0}\left[\int_0^\infty \gamma_0 F_{3M}\lambda\,d\lambda - \frac{1}{r}\int_0^\infty (\gamma_0 F_{4M} + (\lambda-\gamma_0)F_{2E})\,d\lambda\right], \tag{2.7}$$

$$E_\phi = \frac{p\sin\phi}{2\pi\sigma_0}\left[\int_0^\infty (\gamma_0-\lambda)F_{1E}\lambda\,d\lambda + \frac{1}{r}\int_0^\infty (\gamma_0 F_{4M} + (\lambda-\gamma_0)F_{2E})\,d\lambda\right], \tag{2.8}$$

$$E_z = -\frac{p\cos\phi}{2\pi\sigma_0}\int_0^\infty F_{2M}\lambda^2\,d\lambda, \tag{2.9}$$

$$B_r = \frac{\mu_0 p\sin\phi}{2\pi}\left[\int_0^\infty \frac{\gamma_0}{\gamma_0+\lambda}F_{3E}\lambda\,d\lambda + \frac{1}{r}\int_0^\infty (F_{2M} - \frac{\gamma_0}{\gamma_0+\lambda}F_{4E})\,d\lambda\right], \tag{2.10}$$

$$B_\phi = \frac{\mu_0 p\cos\phi}{2\pi}\left[\int_0^\infty F_{3M}\lambda\,d\lambda - \frac{1}{r}\int_0^\infty (F_{2M} - \frac{\gamma_0}{\gamma_0+\lambda}F_{4E})\,d\lambda\right], \tag{2.11}$$

$$B_z = \frac{\mu_0 p\sin\phi}{2\pi}\int_0^\infty \frac{1}{\gamma_0+\lambda}F_{2E}\lambda^2\,d\lambda. \tag{2.12}$$

4. Horizontal Magnetic Dipole

$$E_r = -\frac{i\omega\mu_0 m\sin\phi}{2\pi}\left[\frac{1}{r}\int_0^\infty \frac{1}{\gamma_0+\lambda}F_{2E}\lambda\,d\lambda\right], \tag{2.13}$$

$$E_\phi = \frac{i\omega\mu_0 m\cos\phi}{2\pi}\left[\int_0^\infty \frac{1}{\gamma_0+\lambda}F_{1E}\lambda^2\,d\lambda - \frac{1}{r}\int_0^\infty \frac{1}{\gamma_0+\lambda}F_{2E}\lambda\,d\lambda\right], \tag{2.14}$$

$$E_z = \frac{\omega^2\mu_0\epsilon_1 m\sin\phi}{2\pi\sigma_0}\int_0^\infty F_{2M}\lambda\,d\lambda, \tag{2.15}$$

$$B_r = -\frac{\mu_0 m \cos\phi}{2\pi}\left[\int_0^\infty \frac{\gamma_0}{\gamma_0+\lambda} F_{3E}\lambda^2\, d\lambda - \frac{1}{r}\int_0^\infty \frac{\gamma_0}{\gamma_0+\lambda} F_{4E}\lambda\, d\lambda\right], \tag{2.16}$$

$$B_\phi = \frac{\mu_0 m \sin\phi}{2\pi}\left[\frac{1}{r}\int_0^\infty \frac{\gamma_0}{\gamma_0+\lambda} F_{4E}\lambda\, d\lambda\right], \tag{2.17}$$

$$B_z = \frac{\mu_0 m \cos\phi}{2\pi}\int_0^\infty \frac{1}{\gamma_0+\lambda} F_{2E}\lambda^3\, d\lambda. \tag{2.18}$$

The following equations also apply

$$F_{1M} = F_{TM}^{(a)} e^{-(\gamma_0 d+\lambda h)} J_0(\lambda r),$$

$$F_{2M} = F_{TM}^{(a)} e^{-(\gamma_0 d+\lambda h)} J_1(\lambda r),$$

$$F_{3M} = F_{TM}^{(b)} e^{-(\gamma_0 d+\lambda h)} J_0(\lambda r),$$

$$F_{4M} = F_{TM}^{(b)} e^{-(\gamma_0 d+\lambda h)} J_1(\lambda r),$$

$$F_{1E} = F_{TE}^{(a)} e^{-(\gamma_0 d+\lambda h)} J_0(\lambda r),$$

$$F_{2E} = F_{TE}^{(a)} e^{-(\gamma_0 d+\lambda h)} J_1(\lambda r),$$

$$F_{3E} = F_{TE}^{(b)} e^{-(\gamma_0 d+\lambda h)} J_0(\lambda r),$$

$$F_{4E} = F_{TE}^{(b)} e^{-(\gamma_0 d+\lambda h)} J_1(\lambda r),$$

where

$$F_{TM}^{(a)} = (1+\rho_{-1TM})/(1-\rho_{-1TM}\rho_{1TM}),$$

$$F_{TM}^{(b)} = (1-\rho_{-1TM})/(1-\rho_{-1TM}\rho_{1TM}),$$

$$F_{TE}^{(a)} = (1 + \rho_{-1TE})/(1 - \rho_{-1TE}\rho_{1TE}),$$

$$F_{TE}^{(b)} = (1 - \rho_{-1TE})/(1 - \rho_{-1TE}\rho_{1TE}),$$

$$\rho_{1TM} = [(Y_1 - Y_0)/(Y_1 + Y_0)]\, e^{-2\gamma_0 d},$$

$$\rho_{-1TM} = [(Y_{-1} - Y_0)/(Y_{-1} + Y_0)]\, e^{2\gamma_0 (d-D)},$$

$$\rho_{1TE} = [(Z_1 - Z_0)/(Z_1 + Z_0)]\, e^{-2\gamma_0 d},$$

$$\rho_{-1TE} = [(Z_{-1} - Z_0)/(Z_{-1} + Z_0)]\, e^{2\gamma_0 (d-D)},$$

$$Y_n = (\sigma_n + i\omega\epsilon_n)/\gamma_n,$$

$$Z_n = i\omega\mu_0/\gamma_n,$$

$$\gamma_n^2 = \lambda^2 - k_n^2,$$

$$k_n^2 = \omega^2\mu_n\epsilon_n - i\omega\mu_n\sigma_n.$$

In the last of these equations the subscript $n$ can take one of the three values 1, 0, or -1, thus specifying the applicable region for the subscripted quantity. Thus $\epsilon_n$ and $\sigma_n$, for example, are the permittivity and electrical conductivity in region $n$. Note that, according to this notation convention, $\sigma_1 = 0$, $\sigma_0 = \sigma_s$, and $\sigma_{-1} = \sigma_f$. The equations are valid for all frequencies. However, in our computations we use the quasi-static approximation (see p. 3-15 of *Kraichman*, [1976]), which is equivalent to neglecting most displacement current terms. Thus, with the single exception of the $\epsilon_1$ occurring in the expression for the electric field component $E_z$ produced by the HMD, we set $\epsilon_1 = \epsilon_0 = \epsilon_{-1} = 0$. This is a commonly used approximation that is applicable when the source-receiver distance is much smaller than one free space wavelength. We discussed the frequency range over which this approximation is valid in our 1980 report [*Fraser-Smith and Bubenik*, 1980] and concluded that the field data only begin to become inaccurate for frequencies above 30 kHz. The same arguments used in that earlier report are applicable here and we conclude that our field data are valid throughout the ULF/ELF/VLF frequency range.

The full field expressions given above were evaluated numerically using the same computational techniques used in our previous work and, in particular, using the same

techniques described by *Bubenik*, [1977]. Both the electric dipole moment $p$ and the magnetic dipole moment $m$ are set equal to unity ($p = 1$ Am, and $m = 1$ Am$^2$). For dipoles of arbitrary moment the field values given in the figures should be multiplied by the moment to obtain the corresponding field magnitudes. We use the milligamma as our unit for the magnetic field (1 m$\gamma$ = 1 picotesla), and the electric field data are presented in units of microvolts/meter.

# 3. RESULTS

The presentation of the results of our field computations follows closely the presentation used in our earlier report on the fields generated in the air by submerged dipoles [*Fraser-Smith and Bubenik*, 1980]. For the VED, these results consist of amplitude data for the radial and vertical electric field components $E_r$ and $E_z$, the maximum electric field vector magnitude $E_{TOTAL}$, and the maximum magnetic field vector magnitude $B_{TOTAL}$ (which represents the azimuthal magnetic field component $B_\phi$). For the VMD, the results consist of amplitude data for the radial and vertical magnetic field components $B_r$ and $B_z$, the net electric field component $E_{TOTAL}$ (which represents the azimuthal electric field component $E_\phi$), and the maximum magnetic field magnitude $B_{TOTAL}$. Also presented are data for the three electric field components ($E_r$, $E_\phi$, $E_z$), three magnetic field components ($B_r$, $B_\phi$, $B_z$), the maximum magnetic field magnitude $B_{TOTAL}$, and the maximum electric field magnitude $E_{TOTAL}$ produced by the elevated HED and HMD along the two principal azimuthal angles $\phi = 0°$ and 90°. Although it is not the primary purpose of the choice, restriction of the azimuthal angles to $\phi = 0°$ and 90° simplifies the presentation of field data for the two horizontal dipoles since not all of the possible field components are produced at each azimuthal angle. Specifically, only one of the horizontal electric components ($E_r$ and $E_\phi$) or one of the horizontal magnetic components ($B_r$ and $B_\phi$) are produced by each of the dipoles when $\phi = 0°$ or 90°, and the vertical field components ($E_z$ and $B_z$) also vanish at one or the other of these angles. We use the notation $E_{HORIZONTAL}$ or $B_{HORIZONTAL}$ for the non-zero horizontal field components. Whether these latter components are radial or azimuthal can be determined quickly by noting the azimuthal angle and by referring to Equations 2.1 - 2.18. Alternatively, the form of the horizontal components can be determined by reference to the following list of non-zero electric and magnetic field quantities produced by each dipole type.

1. VED:

   - The basic field quantities are $E_r$, $E_z$, $B_\phi$.
   - Other field quantities are $E_{TOTAL}$, $E_{HORIZONTAL} = E_r$, $B_{TOTAL} = B_{HORIZONTAL} = B_\phi$.

2. VMD:

- The basic field quantities are $E_\phi$, $B_r$, $B_z$.
- Other field quantities are $E_{\text{TOTAL}} = E_{\text{HORIZONTAL}} = E_\phi$, $B_{\text{HORIZONTAL}} = B_\phi$, $B_{\text{TOTAL}}$.

3. HED, $\phi = 0°$:

- The basic field quantities are $E_r$, $E_z$, $B_\phi$.
- Other field quantities are $E_{\text{TOTAL}}$, $E_{\text{HORIZONTAL}} = E_r$, $B_{\text{TOTAL}} = B_{\text{HORIZONTAL}} = B_\phi$.

4. HED, $\phi = 90°$:

- The basic field quantities are $E_\phi$, $B_r$, $B_z$.
- Other field quantities are $E_{\text{TOTAL}} = E_{\text{HORIZONTAL}} = E_\phi$, $B_{\text{TOTAL}}$, $B_{\text{HORIZONTAL}} = B_r$.

5. HMD, $\phi = 0°$:

- The basic field quantities are $E_\phi$, $B_r$, $B_z$.
- Other field quantities are $E_{\text{TOTAL}} = E_{\text{HORIZONTAL}} = E_\phi$, $B_{\text{TOTAL}}$, $B_{\text{HORIZONTAL}} = B_r$.

6. HMD, $\phi = 90°$:

- The basic field quantities are $E_r$, $E_z$, $B_\phi$.
- Other field quantities are $E_{\text{TOTAL}}$, $E_{\text{HORIZONTAL}} = E_r$, $B_{\text{TOTAL}} = B_{\text{HORIZONTAL}} = B_\phi$.

Notice that there are only three basic electric and magnetic field components for each dipole category.

The presentation of field data is very similar to those used for the results of our submerged dipole computations [*Fraser-Smith*, 1979, 1980]. For each dipole type we first present a series of curves that give the actual fields produced by the elevated dipole in a sea of infinite depth, *i.e.*, without any effects due to the presence of a sea floor. Next, we present additional curves that give the ratios of the fields produced by the dipole in a sea of finite depth $D$ to the fields produced under otherwise identical

conditions in the sea of infinite depth. These latter curves provide an immediate quantitative indication of the presence or absence of sea floor effects, since the absence of a sea floor effect is indicated by a ratio of 1.0. The curves for the infinitely deep sea are presented for three dipole (*i.e.*, transmitter) altitudes ($h/\delta = 0$ (sea surface), 3.0, and 10.0) and for four receiver depths ($d/\delta$ = 0.3, 1.0, 3.0, and 10.0). These data are supplemented by the sea floor effect curves, which are drawn for four sea depths ($D/\delta$ = 0.3, 1.0, 3.0, and 10.0). Only one sea bed electrical conductivity is considered; the value chosen, $\sigma_f = 0.1\ \sigma_s$, is intended to be typical of the values encountered in the first 1 km depth of the sea bed. The reader is referred to the work of *Young and Cox*, [1981], for the results of some recent measurements of sea bed conductivity that support our choice. Note that the subscript has been dropped from $\sigma_s$ when this conductivity appears in the ordinate labels of some of the infinitely-deep-sea figures.

The field data are presented in the following figures:

1. VED; Figures 2 through 9 (Appendix 1).

2. VMD; Figures 10 through 17 (Appendix 2).

3. HED, $\phi = 0°$; Figures 18 through 25 (Appendix 3).

4. HED, $\phi = 90°$; Figures 26 through 33 (Appendix 4).

5. HMD, $\phi = 0°$; Figures 34 through 41 (Appendix 5).

6. HMD, $\phi = 90°$; Figures 42 through 49 (Appendix 6).

The same basic arrangement of figures is used for each dipole category. One small difference occurs in the case of the HMD ($\phi = 90°$), where fewer sea-floor-effect curves are shown. This difference is caused by the comparatively small amplitude of the $E_z$ component. Since $E_{\text{HORIZONTAL}} = E_{\text{TOTAL}}$, to a close approximation, the $E_{\text{HORIZONTAL}}$ curves have been omitted.

To illustrate the use of these data, suppose the source of fields is an HED ($\phi = 90°$) transmitting at 1 Hz and we wish to know $B_z$ at a distance $r/\delta = 100$ and depth $d/\delta$ = 0.3 for a dipole altitude $h/\delta = 10$. Our $B_z$ curves for the HED ($\phi = 90°$) give $B_z \times \delta = 3.8 \times 10^{-2}$ m$\gamma$.m$^2$ (Figure 27). At 1 Hz, $\delta = 251.6$ m and $B_z = 3.0 \times 10^{-7}$ m$\gamma$ for a unit moment dipole and infinitely deep sea. Turning next to Figure 33, we find that the sea floor effect (for $\sigma_f = 0.4$ S/m) varies from negligible (multiplication factor = 1) for a sea depth of 1.0 or more sea water skin depths, *i.e.*, for depths greater than about 250 m,

and doubles the amplitude of the field (multiplicatio  actor = 2) for a depth $D/\delta = 0.3$, at which time our HED source, which is located at a depth of 0.3 sea water skin depths, would be sitting on the sea floor.

## 4. DISCUSSION

In our studies of the ULF/ELF electromagnetic fields generated above a sea of finite depth by submerged harmonic dipoles [*Fraser-Smith and Bubenik*, 1979, 1980] we drew attention to the differing power-law declines with distance of the field components produced by the various dipole sources at large distances. The purpose of this comparison was to identify the dipole types and field components with the greatest potential for undersea-to-air communication. We finally concluded that the $E_z$ field produced by an HED ($\phi = 0°$) was likely to be the most attractive electric field component. Several different factors led to this conclusion, among which the inverse square decline of the amplitude of the field component with distance (at large distances) was perhaps the most influential. We now examine the large-distance variations of the various field components considered in the present study, together with the effects of a sea floor on these components, with the goal, once again, of determining which dipole types and field components are likely to have the greatest potential for communication over long distances.

At horizontal distances greater than $10\delta$ the curves for the ULF/ELF fields produced in an infinitely deep sea by our elevated dipole sources begin to decrease linearly with distance (see Figures 2, 3 [VED]; 10, 11 [VMD]; 18, 19 [HED, $\phi = 0°$]; 26, 27 [HED, $\phi = 90°$]; 34, 35 [HMD, $\phi = 0°$]; 42, 43 [HMD, $\phi = 90°$]). Because of the use that is made of logarithmic scales, the linear decline implies a power law decrease of the fields with distance: the fields decrease with distance as $r^{-n}$, where the power $n$ depends both on the dipole type and on the electric or magnetic field component under consideration. As indicated above, power law decreases of this kind are also observed in the fields produced in the air by submerged dipoles. Further, they are in agreement with the power law variations in approximate expressions for the fields that apply at large source-receiver distances [*Kraichman*, 1976; also see *Bannister*, 1984, for a new series of formulas that apply at measurement distances greater than $10\delta$ from the source].

The values of $n$ for the various field components produced in an infinitely deep sea by our various categories of elevated dipoles are listed in Table 2. It can be seen that $n$ ranges from 5, implying a very rapid decline of the field quantity with distance, down to 2, implying a comparatively slow variation of the field quantity with distance. The

**Table 2:** Values of the power $n$ occurring in the long distance variations $r^{-n}$ observed in the fields produced in the sea by elevated dipole sources. An asterisk indicates that no field component is produced.

| | VMD | VED | HED, $\phi = 0°$ | HED, $\phi = 90°$ | HMD, $\phi = 0°$ | HMD, $\phi = 90°$ |
|---|---|---|---|---|---|---|
| $B_{\mathrm{TOTAL}}$ | 4 | 2 | 3 | 3 | 3 | 3 |
| $E_{\mathrm{TOTAL}}$ | 4 | 2 | 3 | 3 | 3 | 3 |
| $B_r$ | 4 | * | * | 3 | 3 | * |
| $B_\phi$ | * | 2 | 3 | * | * | 3 |
| $B_z$ | 5 | * | * | 4 | 4 | * |
| $E_r$ | * | 2 | 3 | * | * | 3 |
| $E_\phi$ | 4 | * | * | 3 | 3 | * |
| $E_z$ | * | 3 | 4 | * | * | 2 |

distance variations corresponding to these powers of $n$ are all in agreement with the variations predicted by the approximate expressions for the fields tabulated by *Kraichman* [1976] for large source-receiver distances.

Our primary interest is in long-distance air-to-undersea communication, for which field quantities having a $r^{-2}$ distance variation are likely to be most suitable. However, we recognize that there may be situations where a short communication range could be an important requirement. Such a situation might arise, for example, during a naval engagement, where good communication would be important on a local basis but where it would also be particularly desirable that the enemy fleet (presumably more distant) should be denied access to the communication signals. For such limited-range communication the VMD appears to be the most suitable transmitter, since none the fields it produces have an $n$ less than 4 (Table 2), whereas all the other dipole sources produce fields in the sea with a smaller $n$.

Examining the field quantities with $n = 2$ in greater detail, we observe that they are $E_r$ (or, equivalently, $E_{\mathrm{HORIZONTAL}}$) and $B_\phi$ (or, equivalently, $B_{\mathrm{TOTAL}}$) for the VED, and $E_z$ for the HMD ($\phi = 90°$). These three field components would appear to have equivalent potential for long distance communication, but we can conditionally dismiss the $E_z$ component produced by the HMD source because its amplitude is comparatively small (over the distance range considered in our computations it is smaller than the $E_\phi$ component produced by the same source, even though the amplitude of the latter component declines more rapidly with distance). This leaves the VED as the preferred source for long-distance air-to-undersea communication.

The conditionality of our dismissal of the HMD source for long-distance communication follows from the difficulty of comparing the fields produced by electric and magnetic dipole sources. We assume unit moment dipole sources when comparing the magnitudes of the field quantities. However, there are many practical differences between the sources, which influence the magnitude of the dipole moment that can be achieved, and technological advances can also alter the situation. At present there is a possibility that a very powerful HMD source might be developed (*i.e.*, a rotating superconducting loop). If such a development were to occur, our conclusion that the VED is the preferred source for long-distance communication would need to be reexamined.

In our earlier work [*Fraser-Smith and Bubenik*, 1979, 1980] we found that the fields produced above the sea by a VED were subject to exceptionally large sea floor effects:

under certain conditions the $E_r$ field component can be increased by nearly six orders of magnitude. Such large effects are not observed in our results for the elevated VED. Our computations indicate that field enhancements by a factor of two are about the best that can be expected at larger distances ($E_{\mathrm{TOTAL}}$ and $E_{\mathrm{HORIZONTAL}}$) and reductions of field amplitudes to about half their original amplitude can also take place ($B_{\mathrm{TOTAL}}$ and $E_z$). The sea floor effects are therefore not particularly marked and do not influence our conclusion regarding the advantages of a VED as a transmitter.

Taken as a whole, our computations show that the fields produced by all the dipole sources are little affected by the presence of a sea floor except for the $E_z$ component produced by the HED ($\phi = 0°$). In this latter case very substantial enhancements can occur for horizontal distances in the range $5 \leq r/\delta \leq 100$, provided the dipole is located on the sea surface. However, once the dipole is elevated above the sea surface the enhancements rapidly decline to the same order as those for the other dipole categories. It does not appear that sea floor effects are likely to be a substantial factor in air-to-undersea communication.

It is interesting to observe that the criteria we developed in our submerged dipole studies [*Fraser-Smith and Bubenik*, 1979, 1980] for estimating when sea-floor effects are most likely to occur are also valid for the ULF/ELF/VLF fields generated in the sea by elevated dipoles: (1) the sea-floor effects are most marked in seas that are electrically shallow, (2) the largest changes in the fields occur when the dipoles are located within onesea water skin depth of the sea floor, and (3) there are essentially no sea-floor effects when the dipoles are located more than threesea water skin depths above the floor.

## 5. REFERENCES

Bannister, P.R., New formulas that extend Norton's farfield elementary dipole equations to the quasi-nearfield range, *NUSC Tech. Rept. 6888*, Naval Underwater Systems Center, New London, Connecticut, 11 January 1984.

Bubenik, D.M., A practical method for the numerical evaluation of Sommerfeld integrals, *IEEE Trans. Antennas Propagat., AP-25*, 904 - 906, 1977.

Bubenik, D.M., and A.C. Fraser-Smith, ULF/ELF electromagnetic fields generated in a sea of finite depth by a submerged vertically-directed harmonic magnetic dipole, *Radio Sci., 13*, 1011 - 1020, 1978.

Fraser-Smith, A.C., D.M. Bubenik, and O.G. Villard, Jr., Air/undersea communication at ultra-low-frequencies using airborne loop antennas, *Tech. Rept. No. 4207-6*, Radioscience Lab., Stanford Univ., Stanford, California, June 1977.

Fraser-Smith, A.C., and D.M. Bubenik, ULF/ELF electromagnetic fields generated above a sea of finite depth by a submerged vertically-directed harmonic magnetic dipole, *Radio Sci., 14*, 59 - 74, 1979.

Fraser-Smith, A.C., and D.M. Bubenik, Compendium of the ULF/ELF electromagnetic fields generated above a sea of finite depth by submerged harmonic dipoles, *Tech. Rept. E715-1*, Radioscience Lab., Stanford Univ., Stanford, California, January 1980.

Kong, J.A., *Theory of Electromagnetic Wave Propagation in Conducting Media*, 339 pp, Wiley-Interscience, New York, 1975.

Kraichman, M.B., *Handbook of Electromagnetic Propagation in Conducting Media*, U.S. Government Printing Office, Washington, D.C., 1976.

Morrison, H.F., R.J. Phillips, and D.P. O'Brien, Quantitative interpretation of transient electromagnetic fields over a layered half-space, *Geophys. Prospect., 17*, 82 - 101, 1969.

Young, P.D., and C.S. Cox, Electromagnetic active source sounding near the East Pacific Rise, *Geophys. Res. Letters, 8*, 1043 - 1046, 1981.

# APPENDIX 1

## Field Data For The

## VERTICAL ELECTRIC DIPOLE

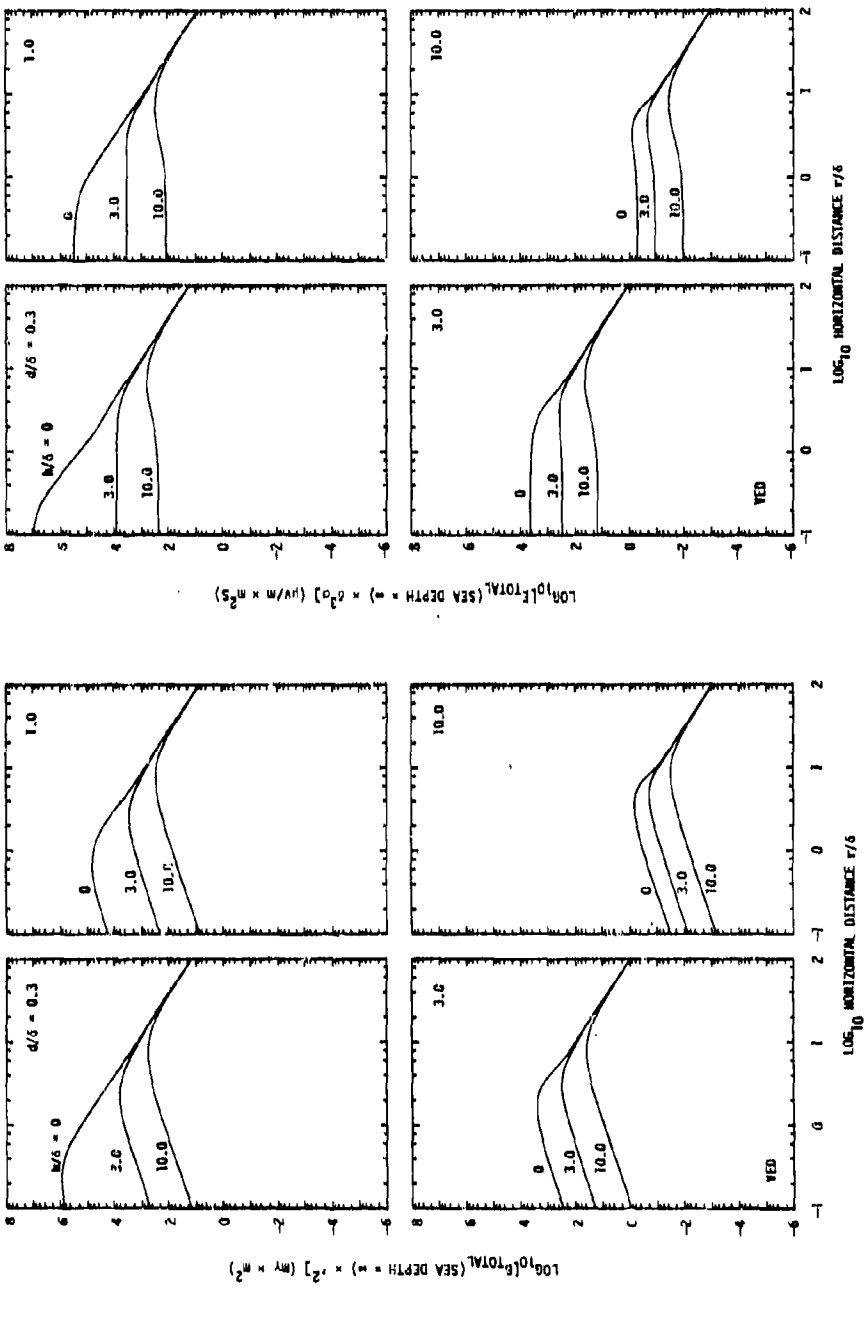


Figure 2. Variation with horizontal distance of the amplitudes of the total magnetic ($B_{TOTAL}$) and electric ($E_{TOTAL}$) fields produced in an infinitely deep sea by a vertically directed harmonic electric dipole (VED) located on and above the surface of the sea.

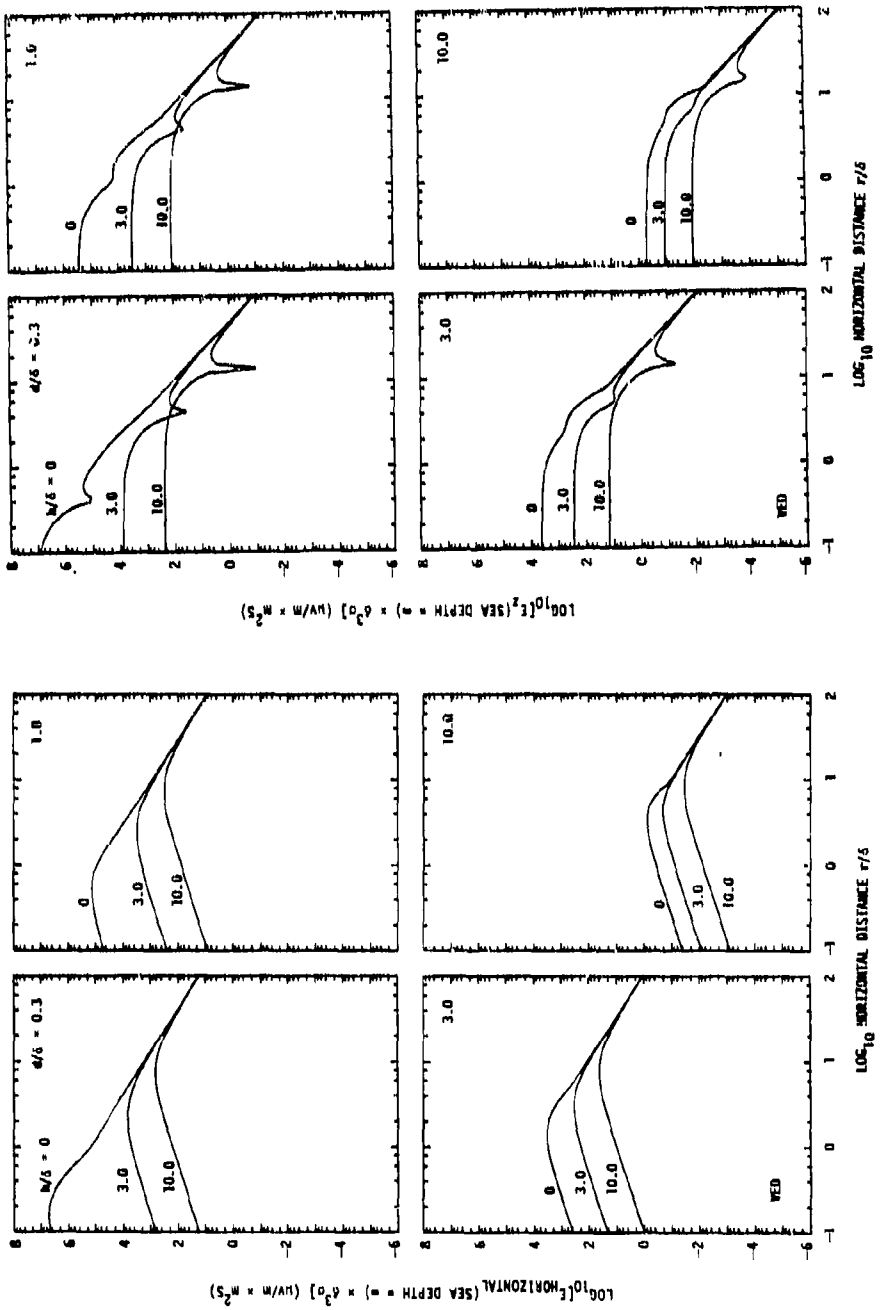


Figure 3. Variation with horizontal distance of the amplitudes of the two electric field components $E_{HORIZONTAL}$ and $E_Z$ produced in an infinitely deep sea by a vertically directed harmonic electric dipole (VED) located on and above the surface of the sea.

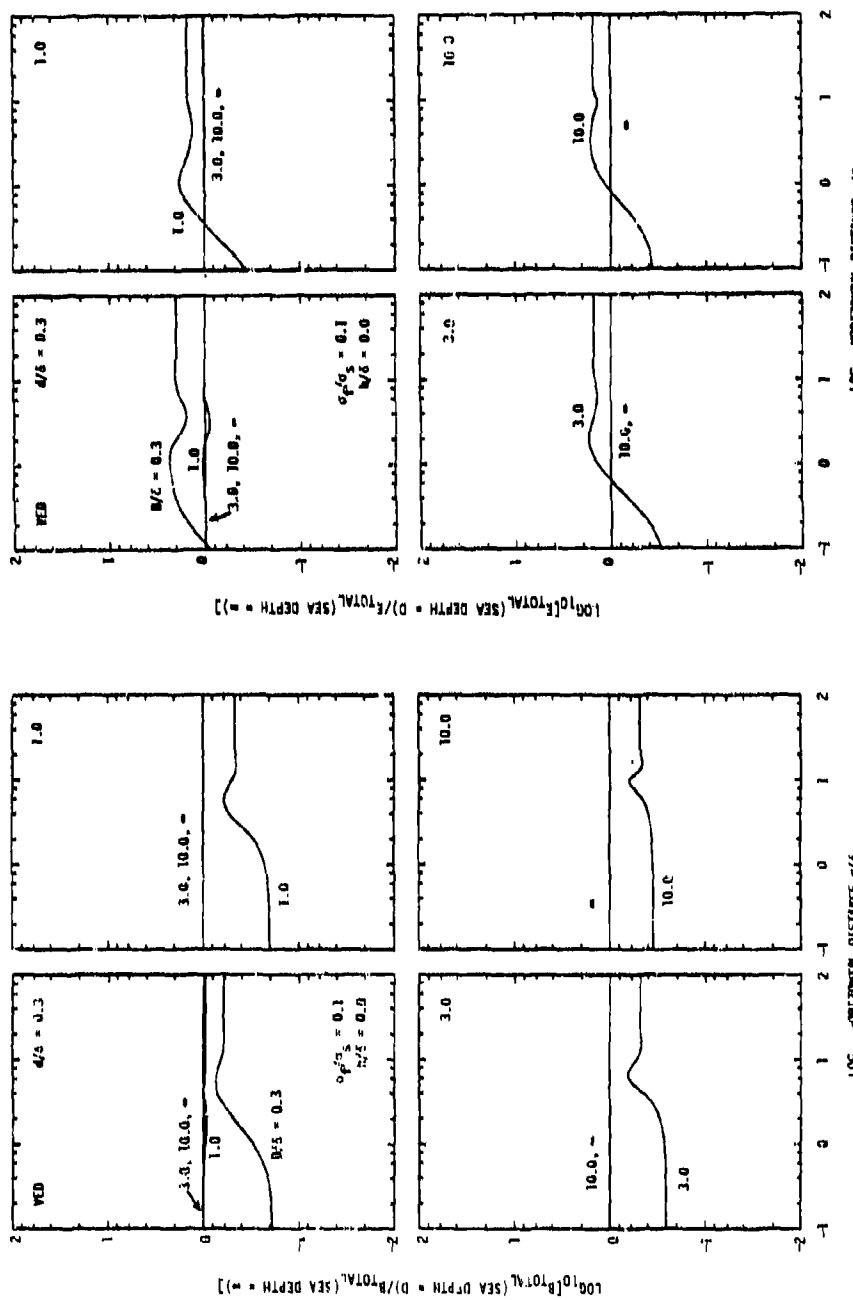


Figure 4. Curves illustrating the changes produced in the magnetic and electric field data presented in Figure 2 for a VED located on the surface of an infinitely deep sea when an electrically conducting sea floor (conductivity $\sigma_f = 0.1\ \sigma_s$, depth D) is introduced.

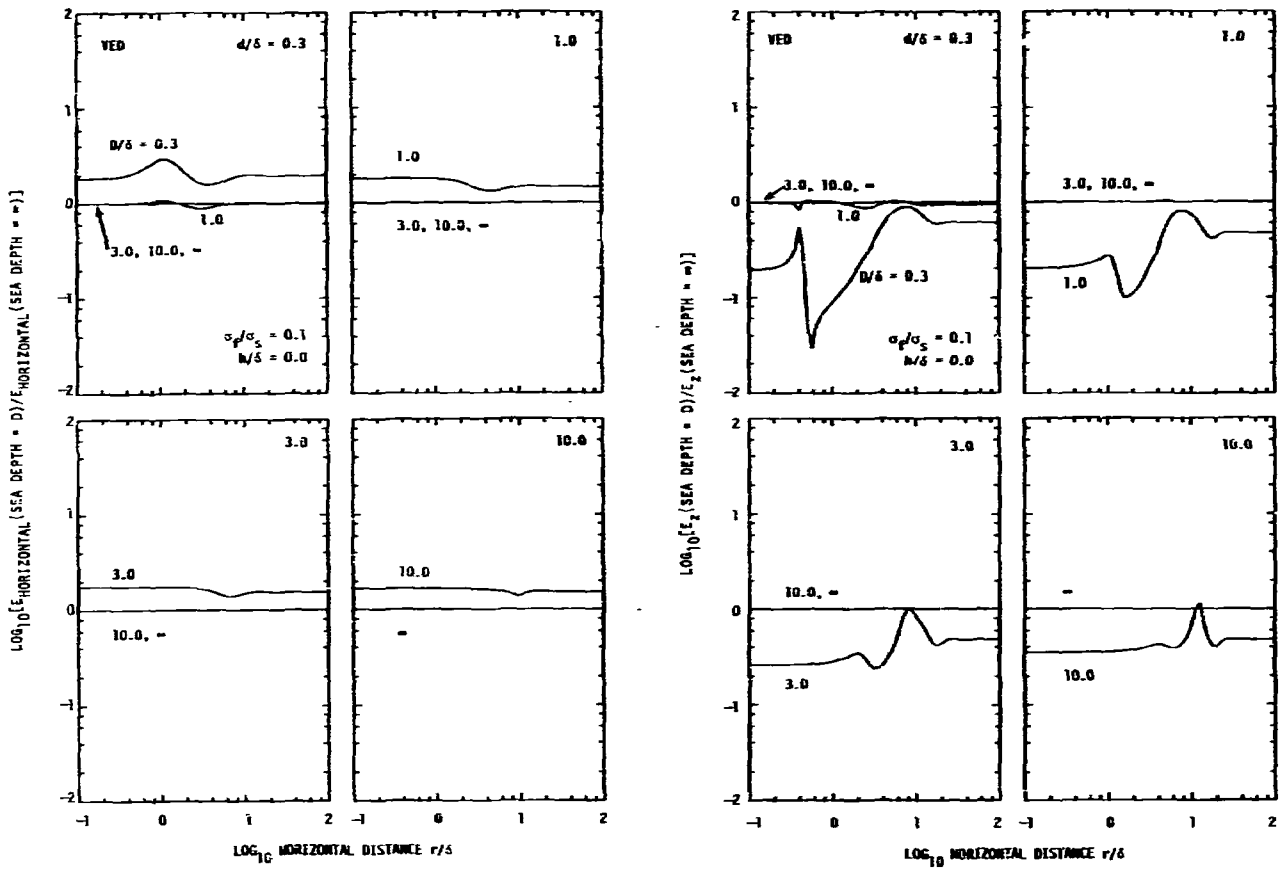


Figure 5. Curves illustrating the changes produced in the electric field component data presented in Figure 3 for a VED located on the surface of an infinitely deep sea when an electrically conducting sea floor (conductivity $\sigma_f = 0.1\ \sigma_s$, depth D) is introduced.

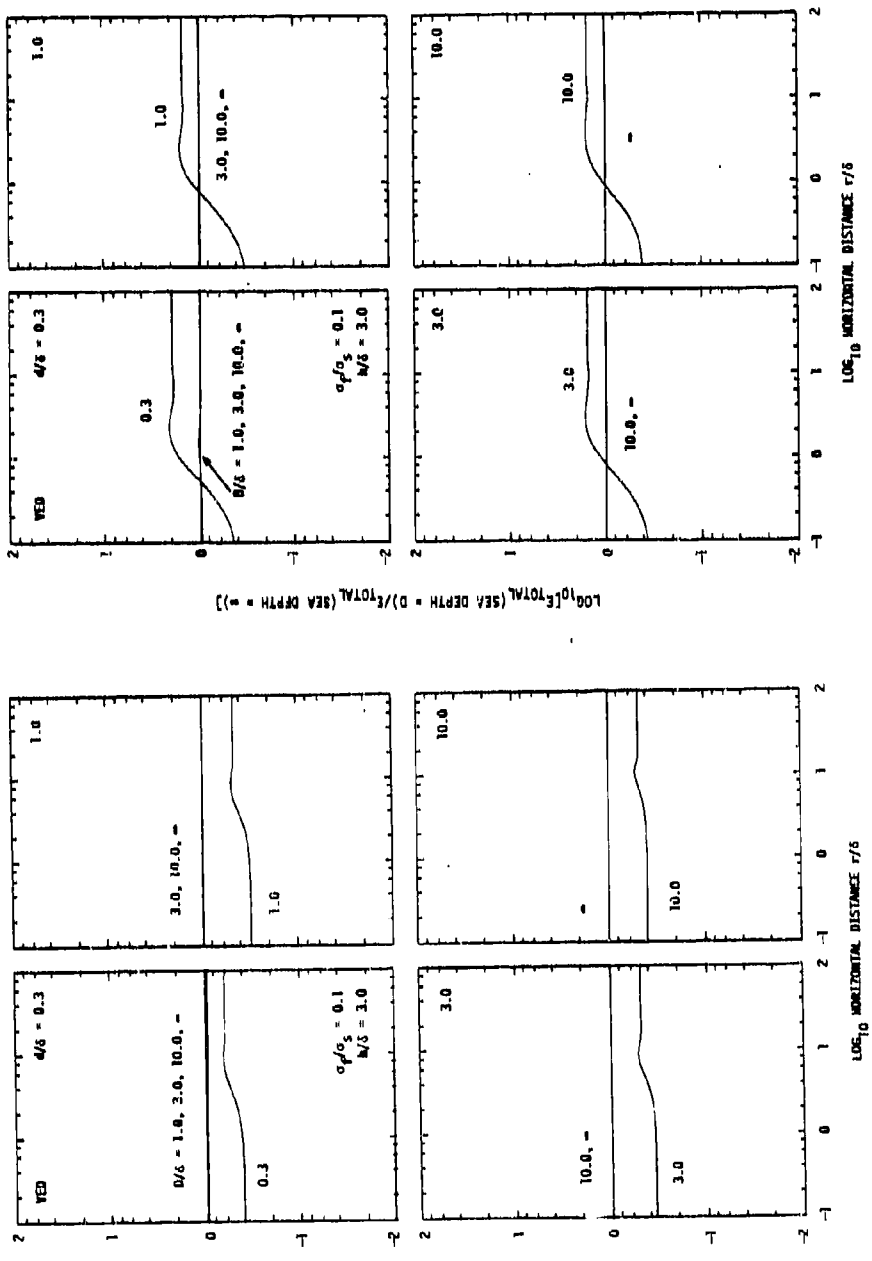


Figure 6. Curves illustrating the changes produced in the magnetic and electric field data presented in Figure 2 for a VED located three sea water skin depths above the surface of an infinitely deep sea ($h/\delta = 3.0$) when an electrically conducting sea floor (conductivity $\sigma_f = 0.1\ \sigma_s$, depth D) is introduced.

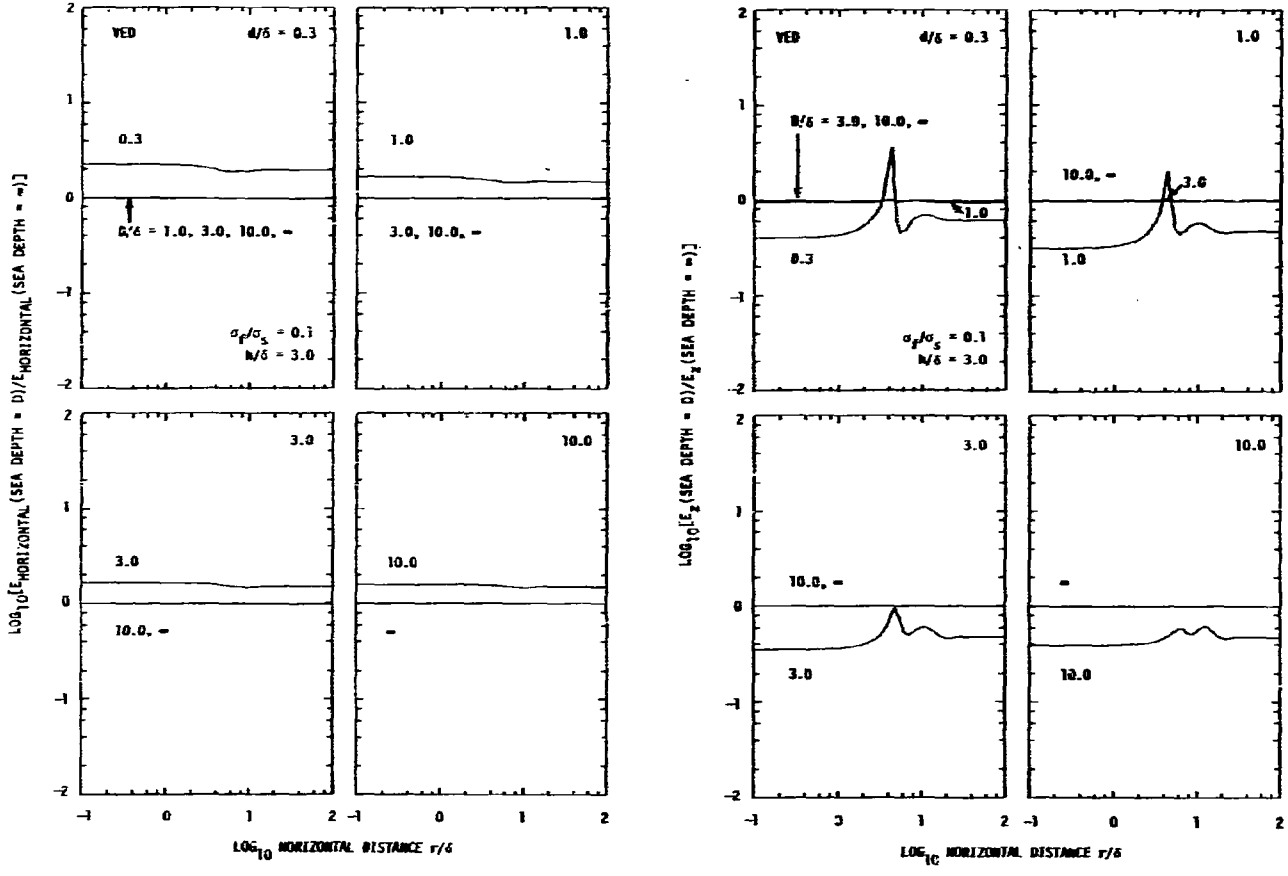


Figure 7. Curves illustrating the changes produced in the electric field component data presented in Figure 3 for a VED located three sea water skin depths above the surface of an infinitely deep sea ($h/\delta = 3.0$) when an electrically conducting sea floor (conductivity $\sigma_f = 0.1\ \sigma_s$, depth D) is introduced.

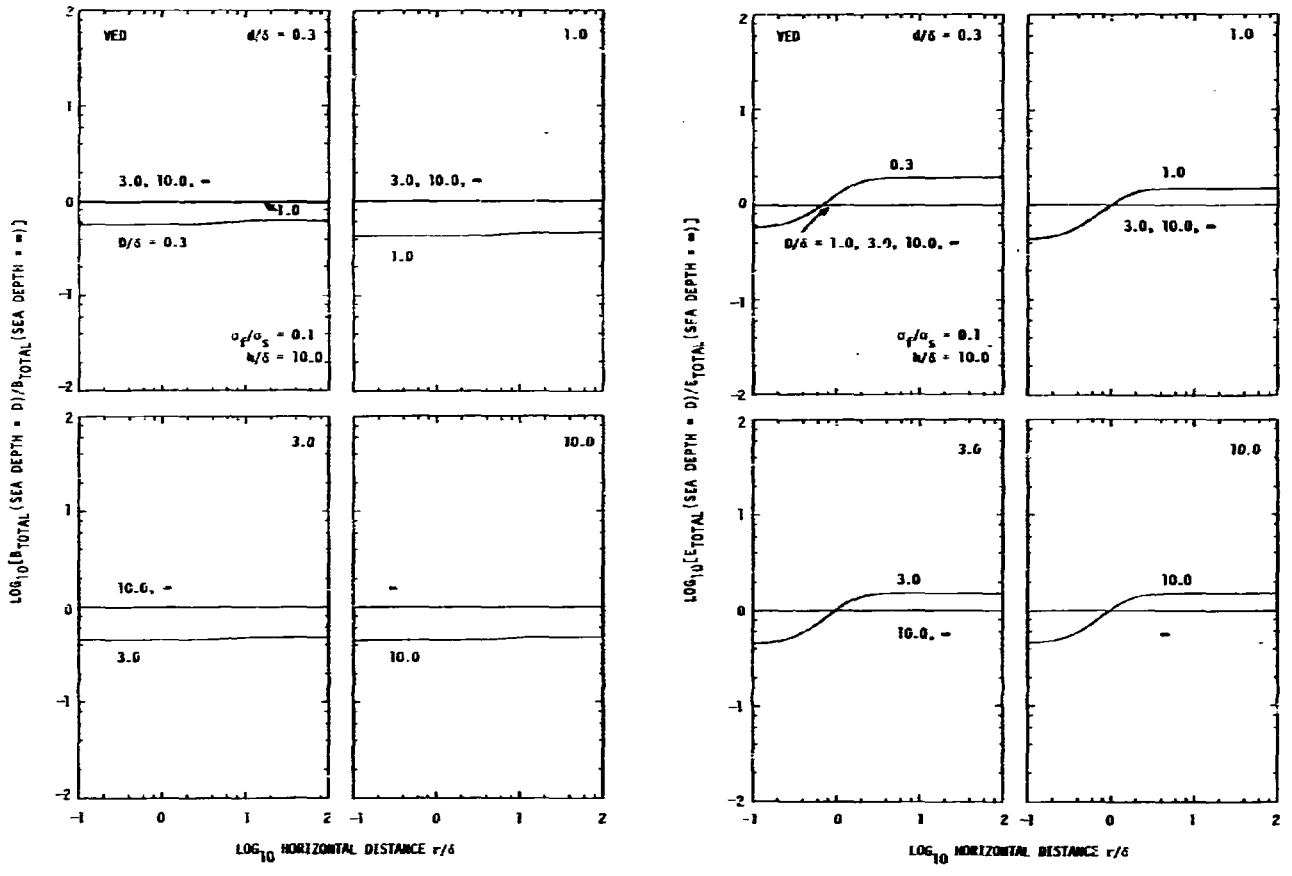


Figure 8. Curves illustrating the changes produced in the magnetic and electric field data presented in Figure 2 for a VED located ten sea water skin depths above the surface of an infinitely deep sea ($h/\delta = 10.0$) when an electrically conducting sea floor (conductivity $\sigma_f = 0.1\ \sigma_s$, depth D) is introduced.

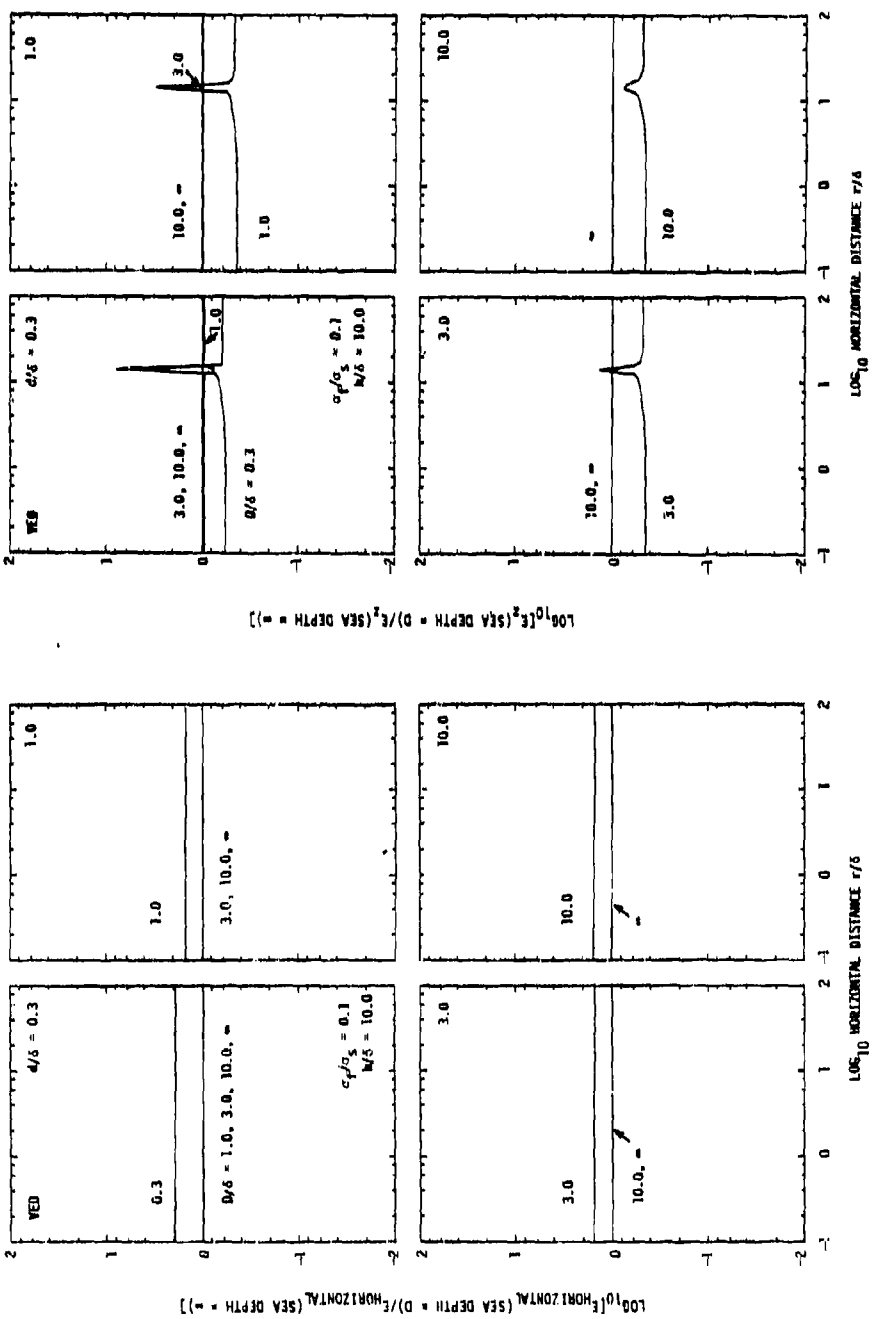


Figure 9. Curves illustrating the changes produced in the electric field component data presented in Figure 3 for a VED located ten sea water skin depths above the surface of an infinitely deep sea ($h/\delta = 10.0$) when an electrically conducting sea floor (conductivity $\sigma_f = 0.1\ \sigma_s$, depth D) is introduced.

# APPENDIX 2

## Field Data For The

## VERTICAL MAGNETIC DIPOLE

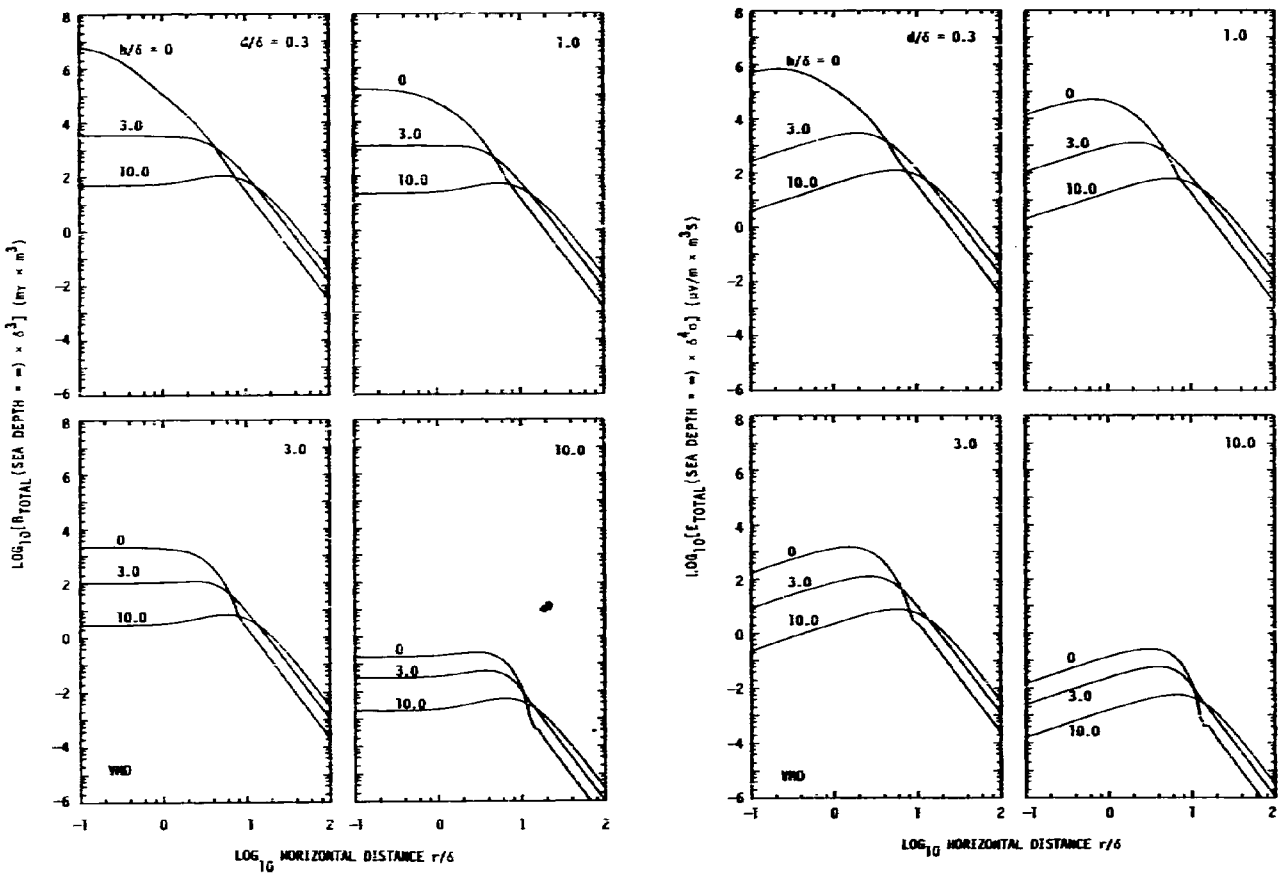


Figure 10. Variation with horizontal distance of the amplitudes of the total magnetic ($B_{TOTAL}$) and electric ($E_{TOTAL}$) fields produced in an infinitely deep sea by a vertically directed harmonic magnetic dipole (VMD) located on and above the surface of the sea.

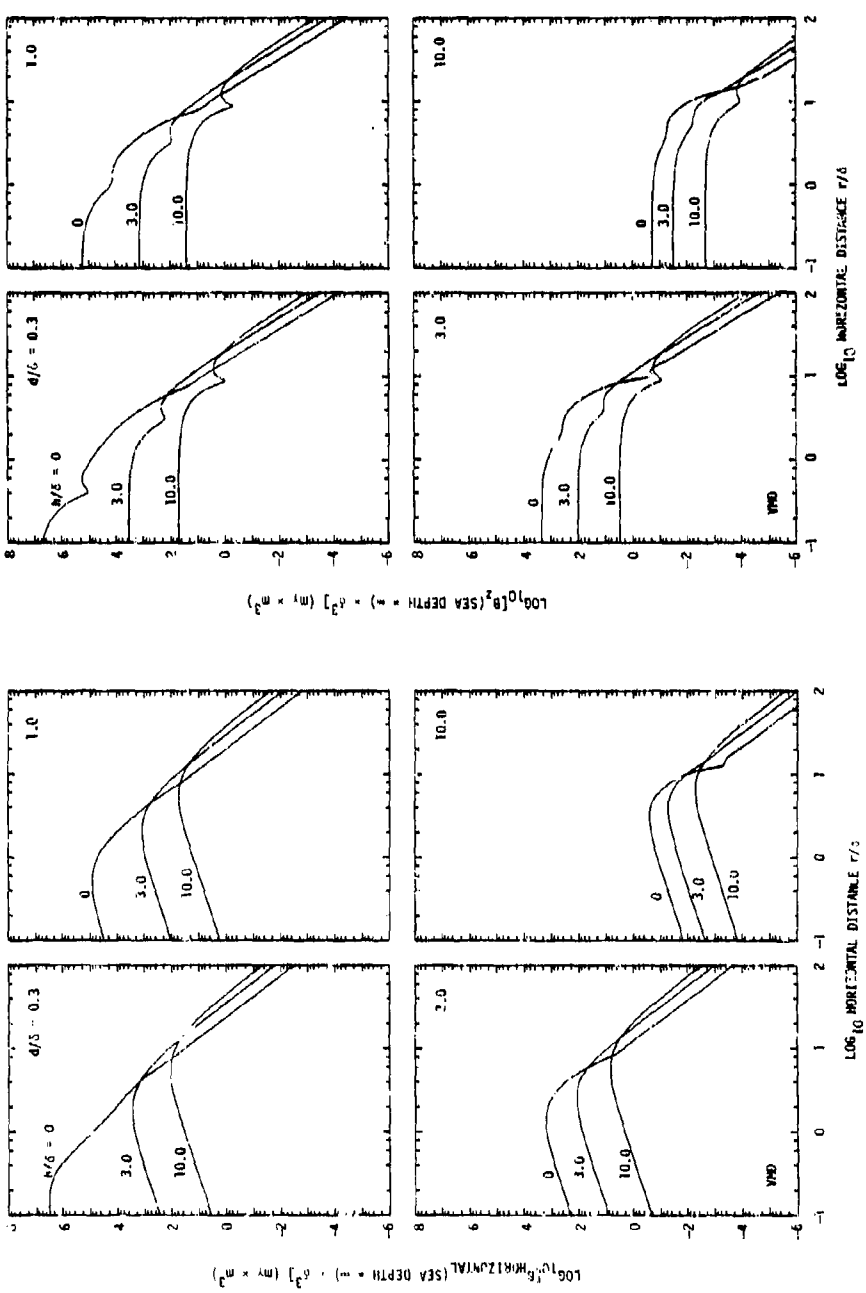


Figure 11. Variation with horizontal distance of the amplitudes of the two magnetic field components $B_{HORIZONTAL}$ and $B_z$ produced in an infinitely deep sea by a vertically directed harmonic magnetic dipole (VMD) located on and above the surface of the sea.

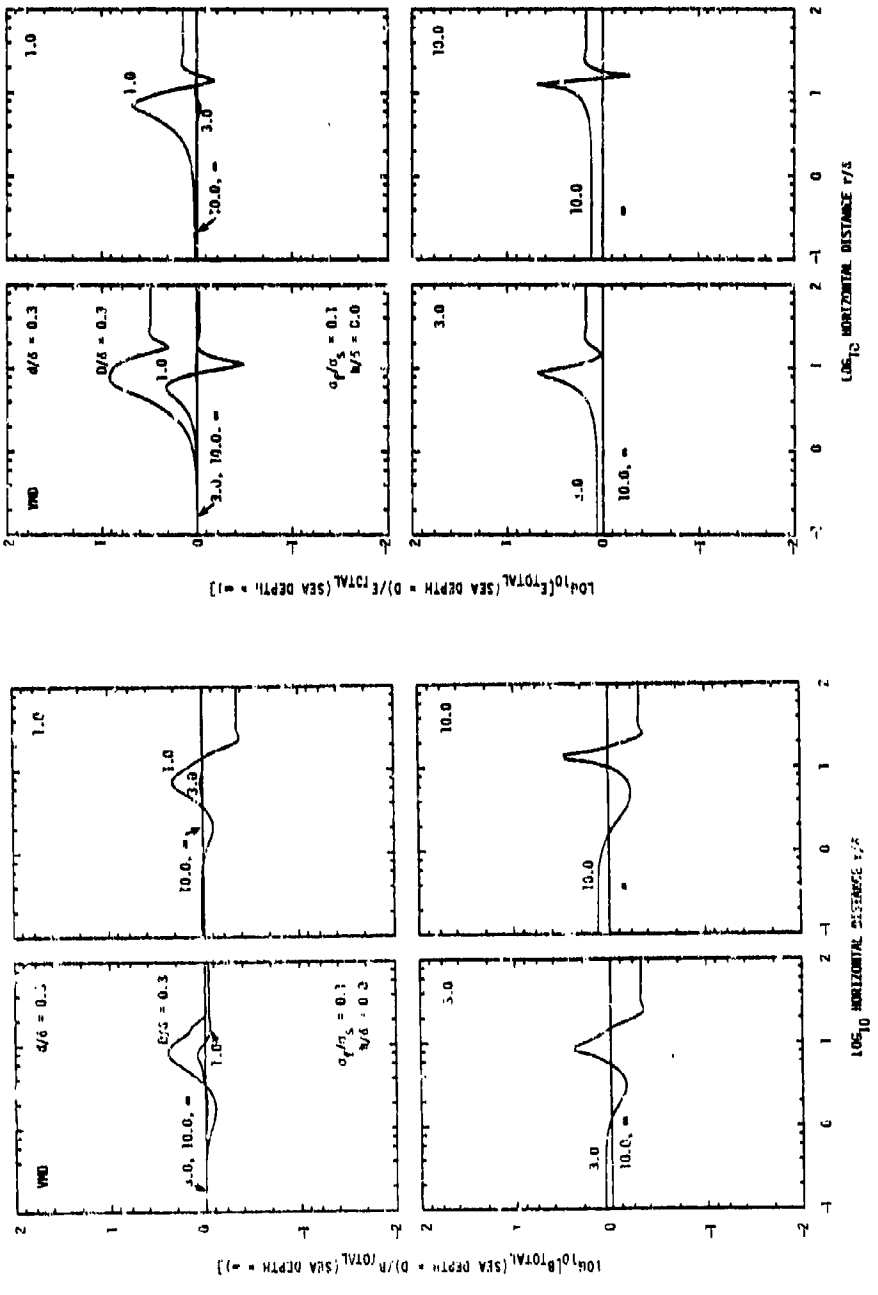


Figure 12. Curves illustrating the changes produced in the magnetic and electric field data presented in Figure 10 for a VMD located on the surface of an infinitely deep sea when an electrically conducting sea floor (conductivity $\sigma_f = 0.1\ \sigma_s$, depth D) is introduced.

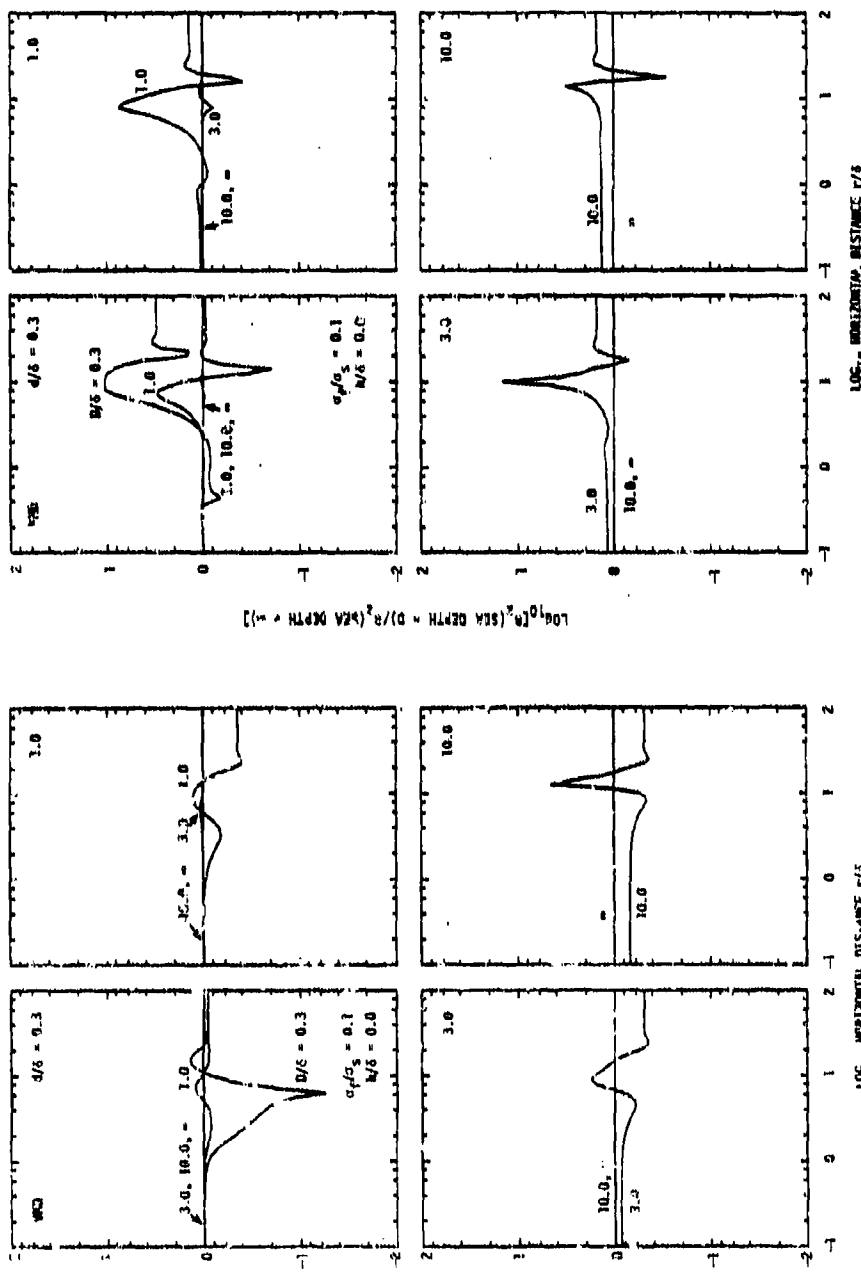

Figure 15. Curves illustrating the changes produced in the magnetic field component data presented in Figure 11 for a VMD located on the surface of an infinitely deep sea when an electrically conducting sea floor (conductivity $\sigma_f = 0.1\ \sigma_s$, depth D) is introduced.

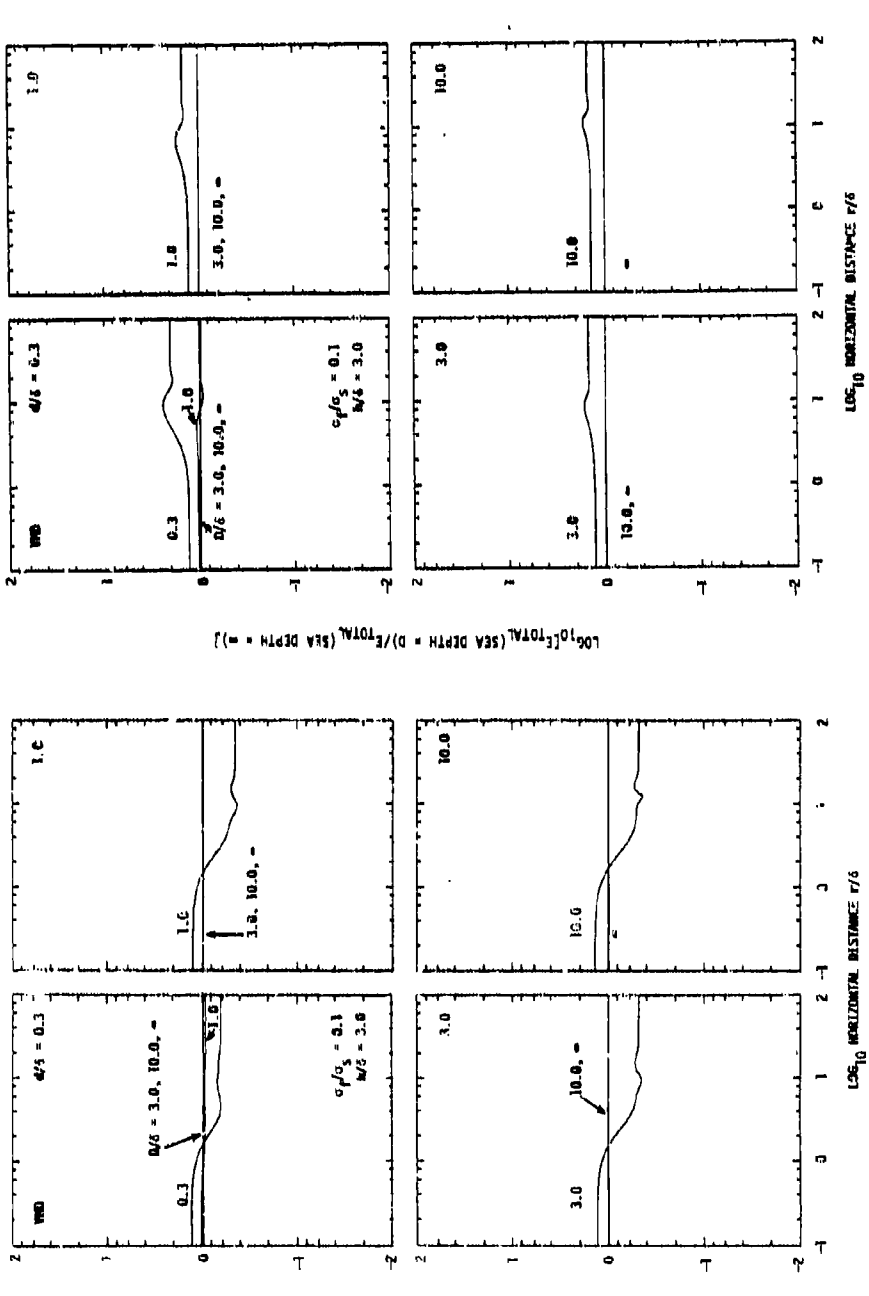


Figure 14. Curves illustrating the changes produced in the magnetic and electric field data presented in Figure 10 for a VMD located three sea water skin depths above the surface of an infinitely deep sea ($h/\delta = 3.0$) when an electrically conducting sea floor (conductivity $\sigma_f = 0.1\ \sigma_s$, depth D) is introduced.

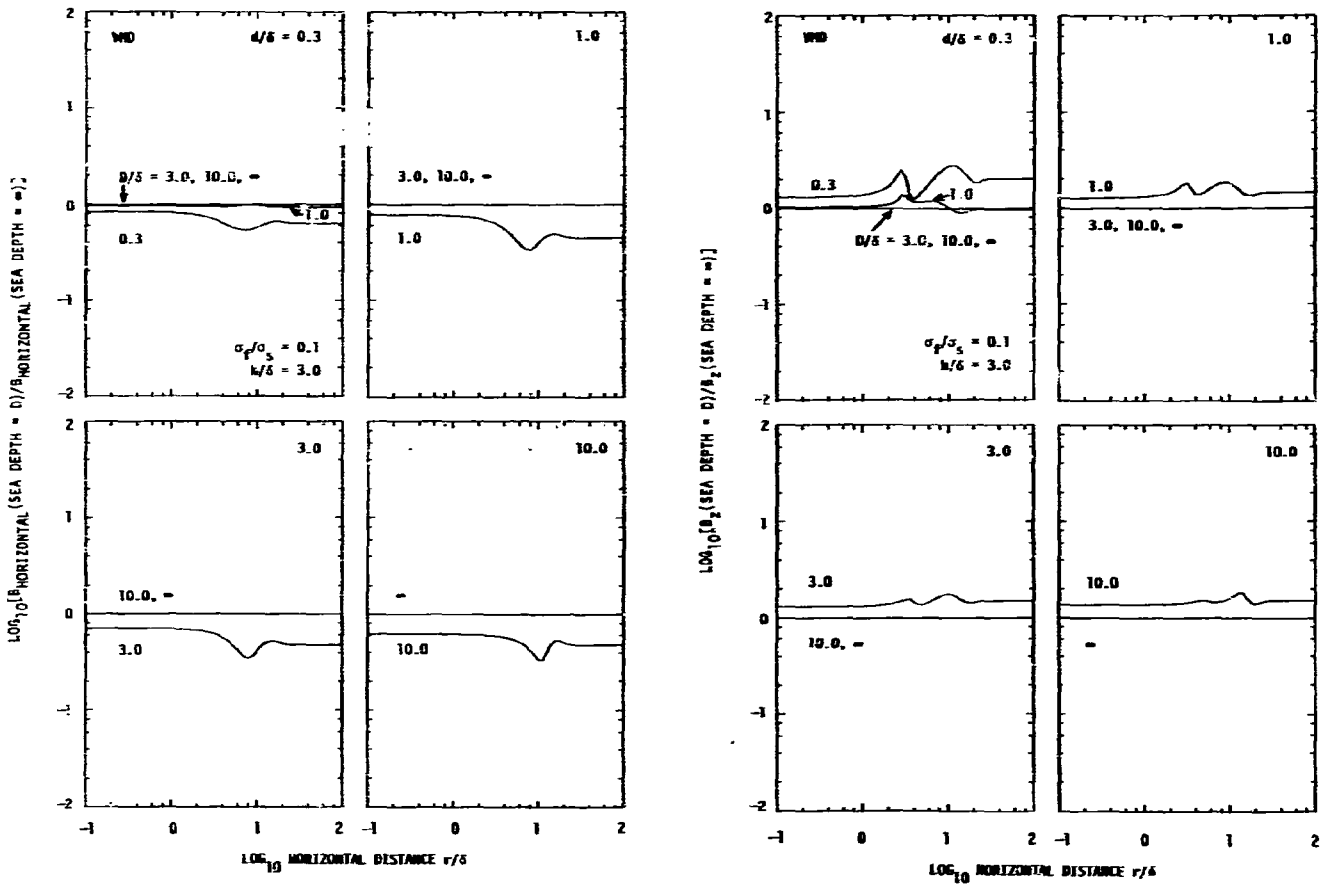


Figure 15. Curves illustrating the changes produced in the magnetic field component data presented in Figure 11 for a VMD located three sea water skin depths above the surface of an infinitely deep sea ($h/\delta = 3.0$) when an electrically conducting sea floor (conductivity $\sigma_f = 0.1\ \sigma_s$, depth D) is introduced.

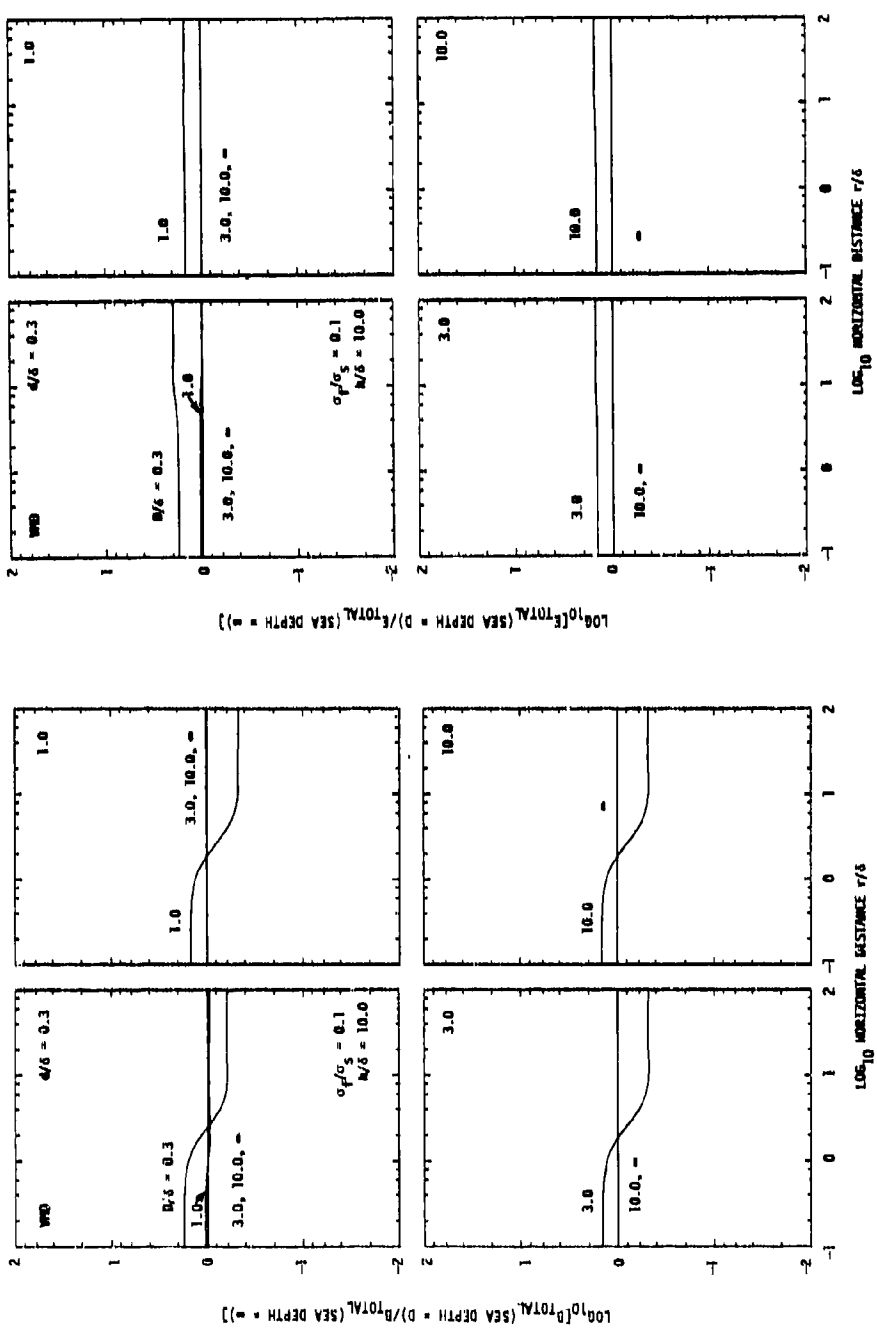


Figure 16. Curves illustrating the changes produced in the magnetic and electric field data presented in Figure 10 for a VMD located ten sea water skin depths above the surface of an infinitely deep sea ($h/\delta = 10.0$) when an electrically conducting sea floor (conductivity $\sigma_f = 0.1\ \sigma_s$, depth D) is introduced.

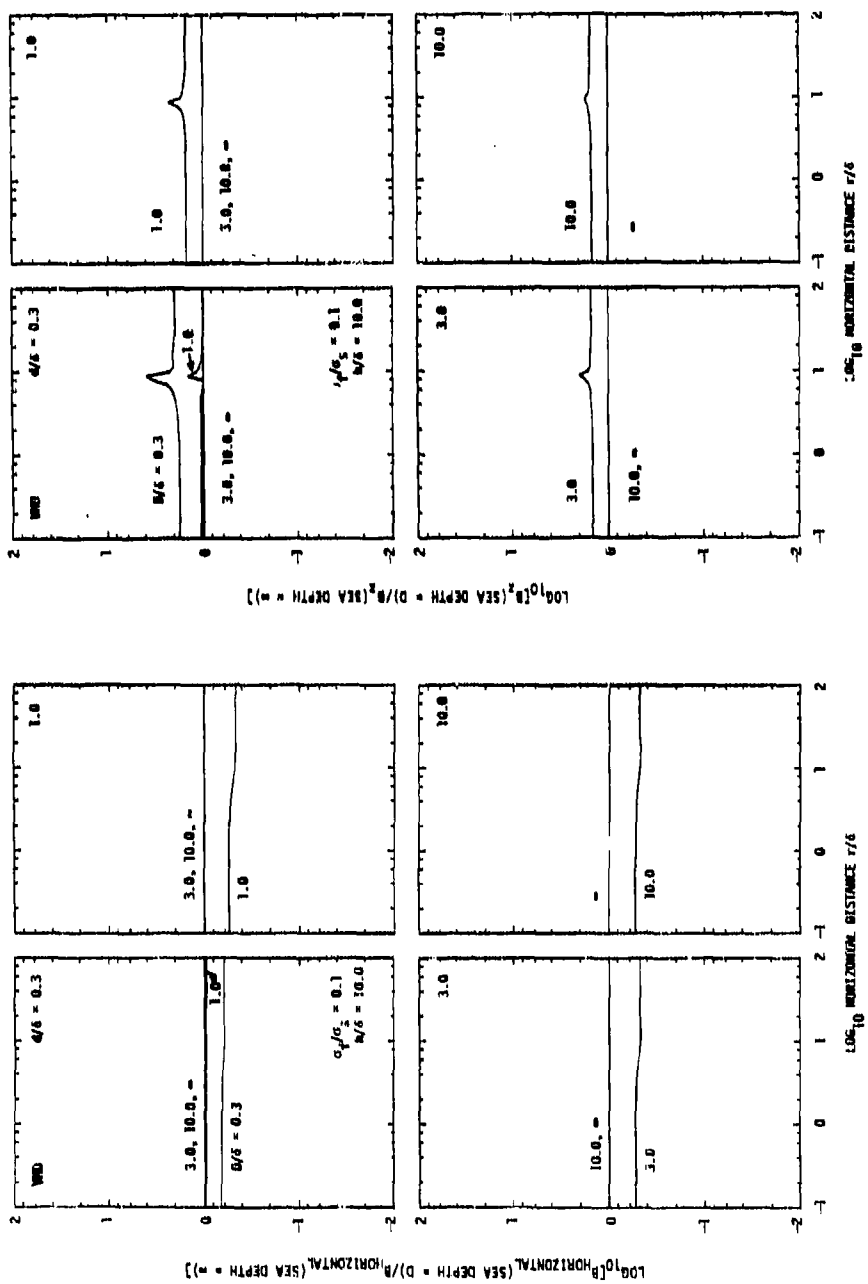


Figure 17. Curves illustrating the changes produced in the magnetic field component data presented in Figure 11 for a VMD located ten sea water skin depths above the surface of an infinitely deep sea ($h/\delta = 10.0$) when an electrically conducting sea floor (conductivity $\sigma_f = 0.1\ \sigma_s$, depth D) is introduced.

# APPENDIX 3

## Field Data For The

## HORIZONTAL ELECTRIC DIPOLE, $\phi = 0°$

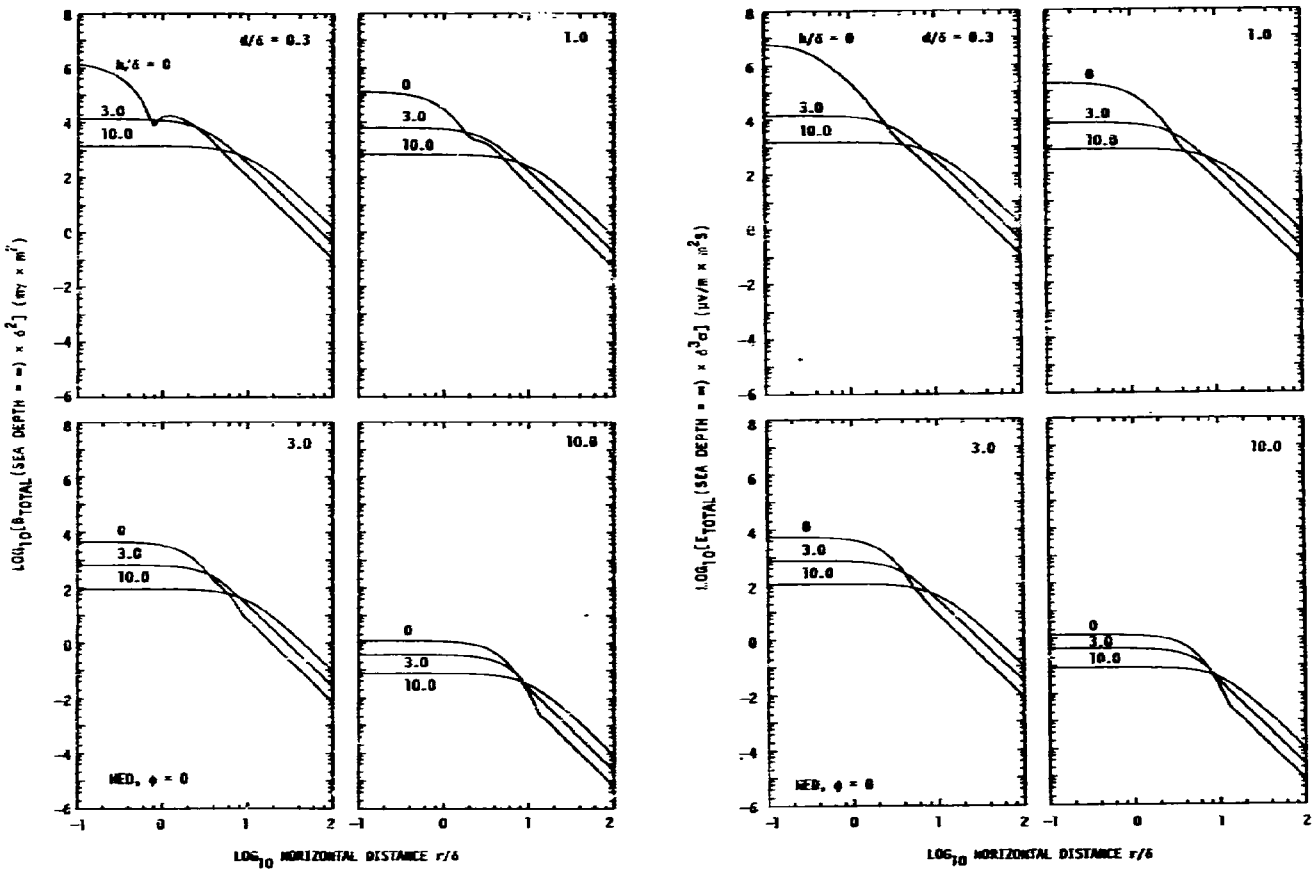


Figure 18. Variation with horizontal distance of the amplitudes of the total magnetic ($B_{TOTAL}$) and electric ($E_{TOTAL}$) fields produced in an infinitely deep sea by a horizontally directed harmonic electric dipole (HED) located on and above the surface of the sea. The fields are given for an azimuthal ($\phi$) of 0°.

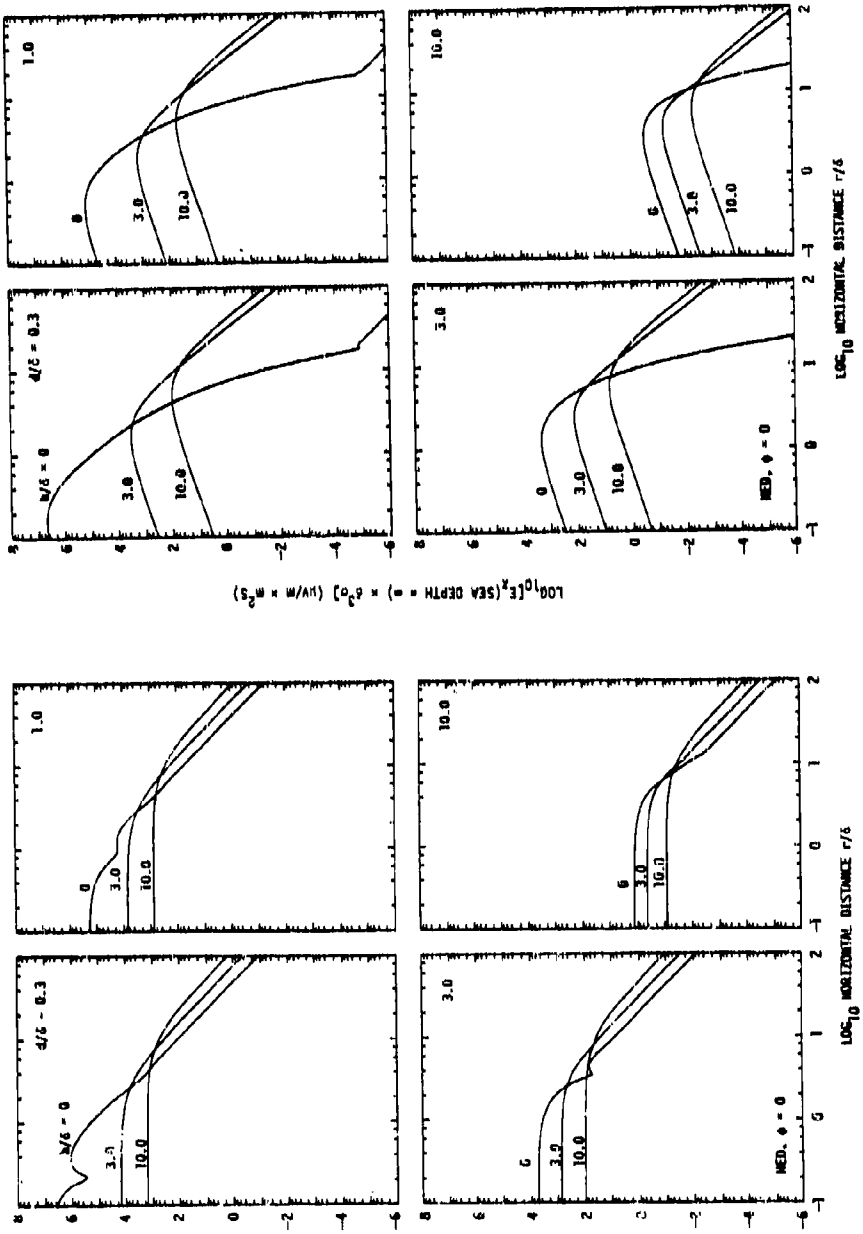


Figure 19. Variation with horizontal distance of the amplitudes of the two electric field components $E_{HORIZONTAL}$ and $E_z$ produced in an infinitely deep sea by a horizontally directed harmonic electric dipole (HED) located on and above the surface of the sea. The fields are given for an azimuthal ($\phi$) of 0°.

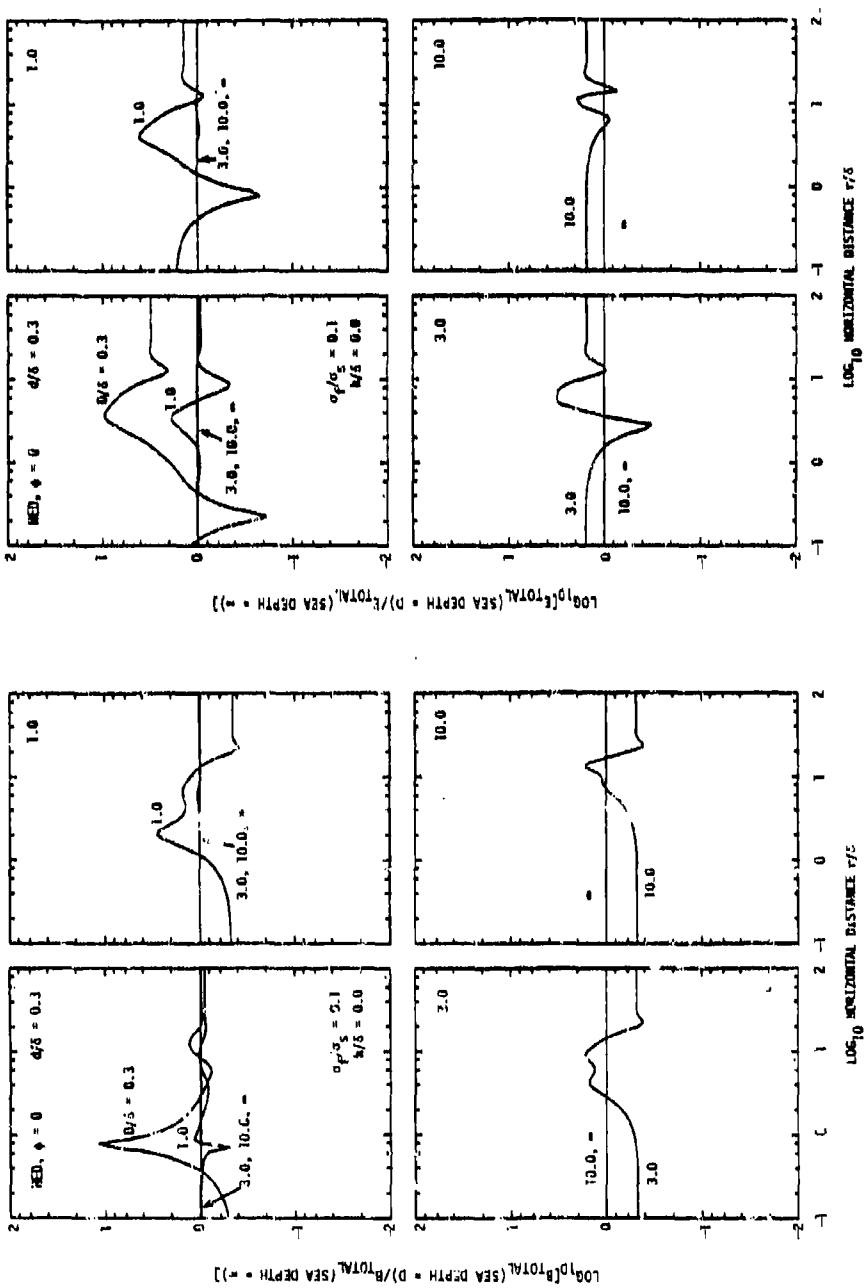


Figure 20. Curves illustrating the changes produced in the magnetic and electric field data presented in Figure 18 for an HED located on the surface of an infinitely deep sea when an electrically conducting sea floor (conductivity $\sigma_f = 0.1\ \sigma_s$, depth D) is introduced. Note that changes apply to the fields produced at an azimuthal angle ($\phi$) of 0°.

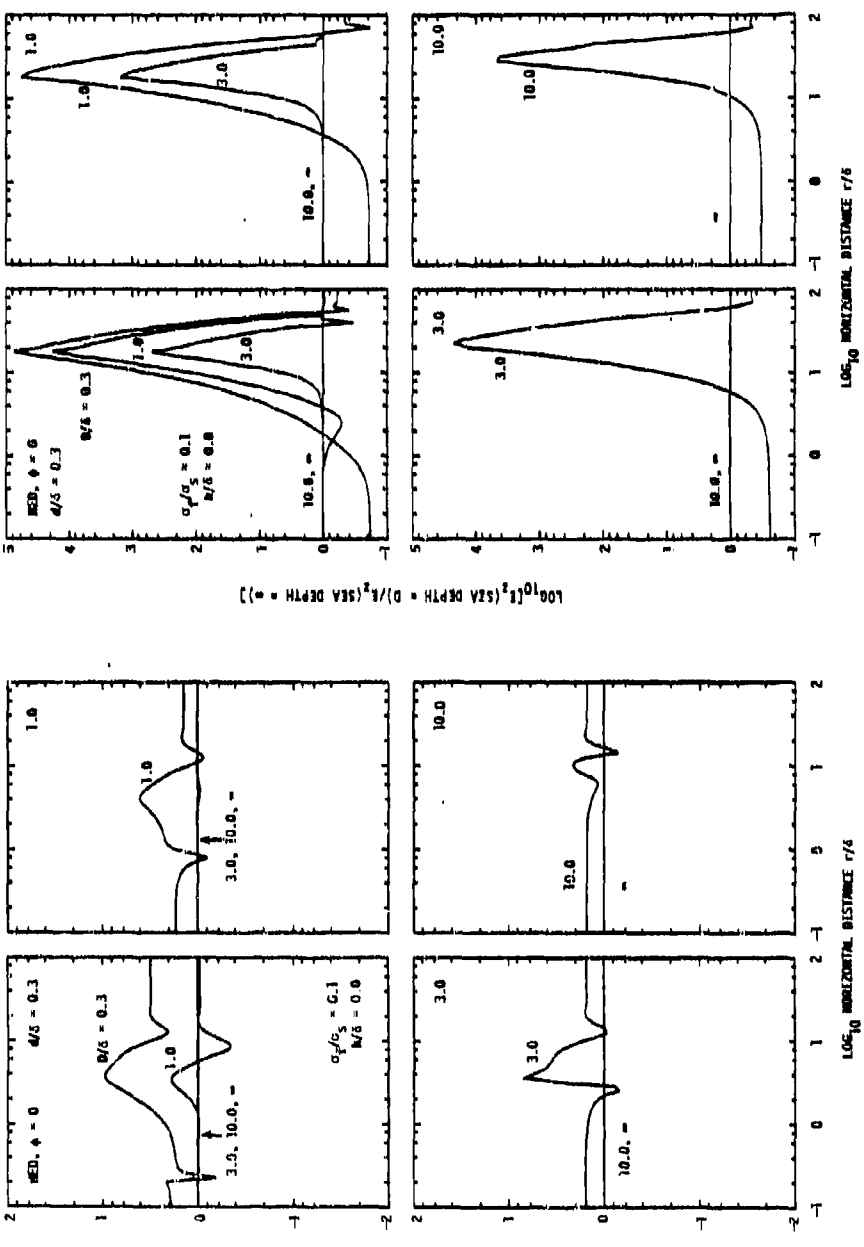


Figure 21. Curves illustrating the changes produced in the electric field component data presented in Figure 19 for an HED located on the surface of an infinitely deep sea when an electrically conducting sea floor (conductivity $\sigma_f = 0.1\ \sigma_s$, depth D) is introduced. Note that the changes apply to the fields produced at an azimuthal angle ($\phi$) of 0°.

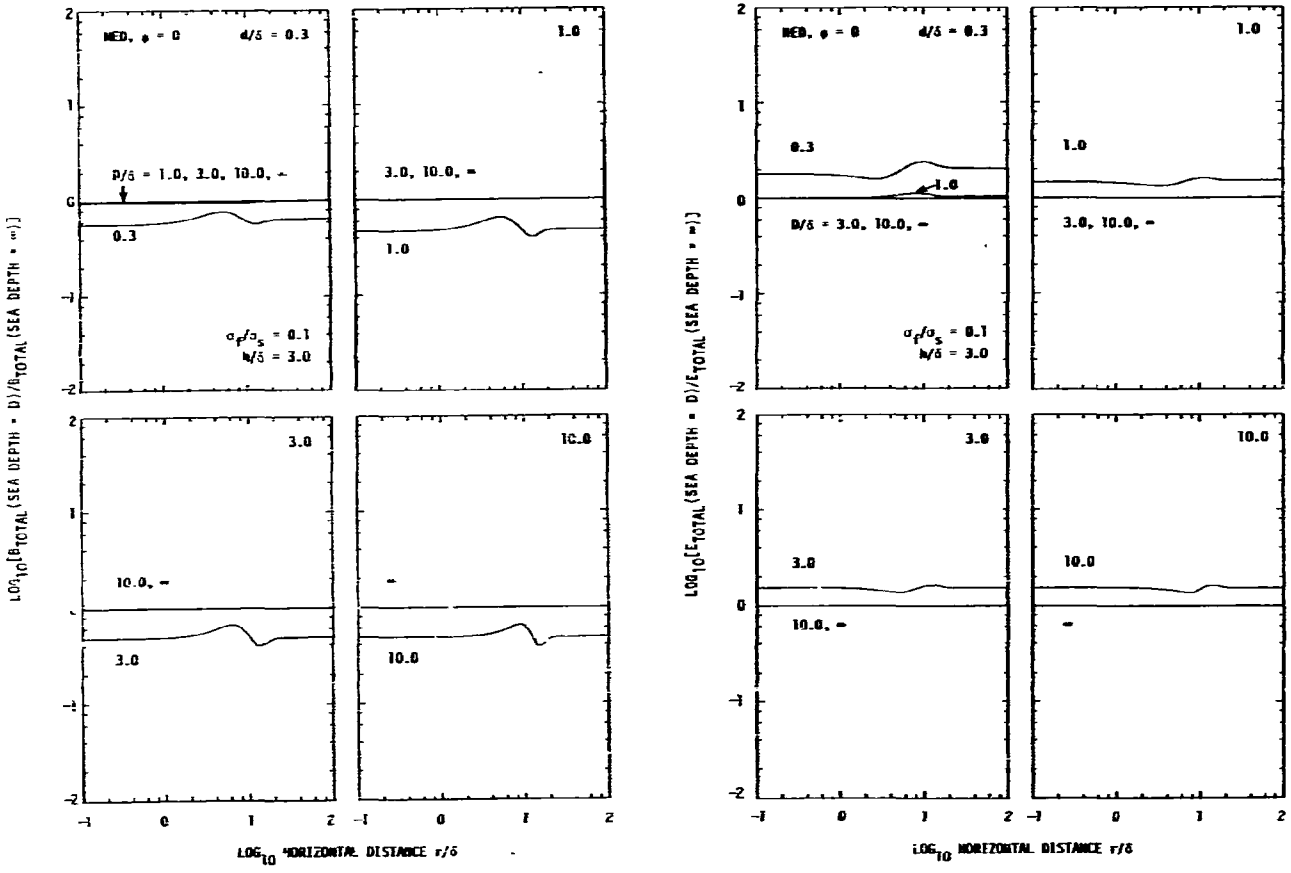


Figure 22. Curves illustrating the changes produced in the magnetic and electric field data presented in Figure 18 for an HED located three sea water skin depths above the surface of an infinitely deep sea ($h/\delta = 3.0$) when an electrically conducting sea floor (conductivity $\sigma_f = 0.1\ \sigma_s$, depth D) is introduced. Note that the changes apply to the fields produced at an azimuthal angle ($\phi$) of 0°.

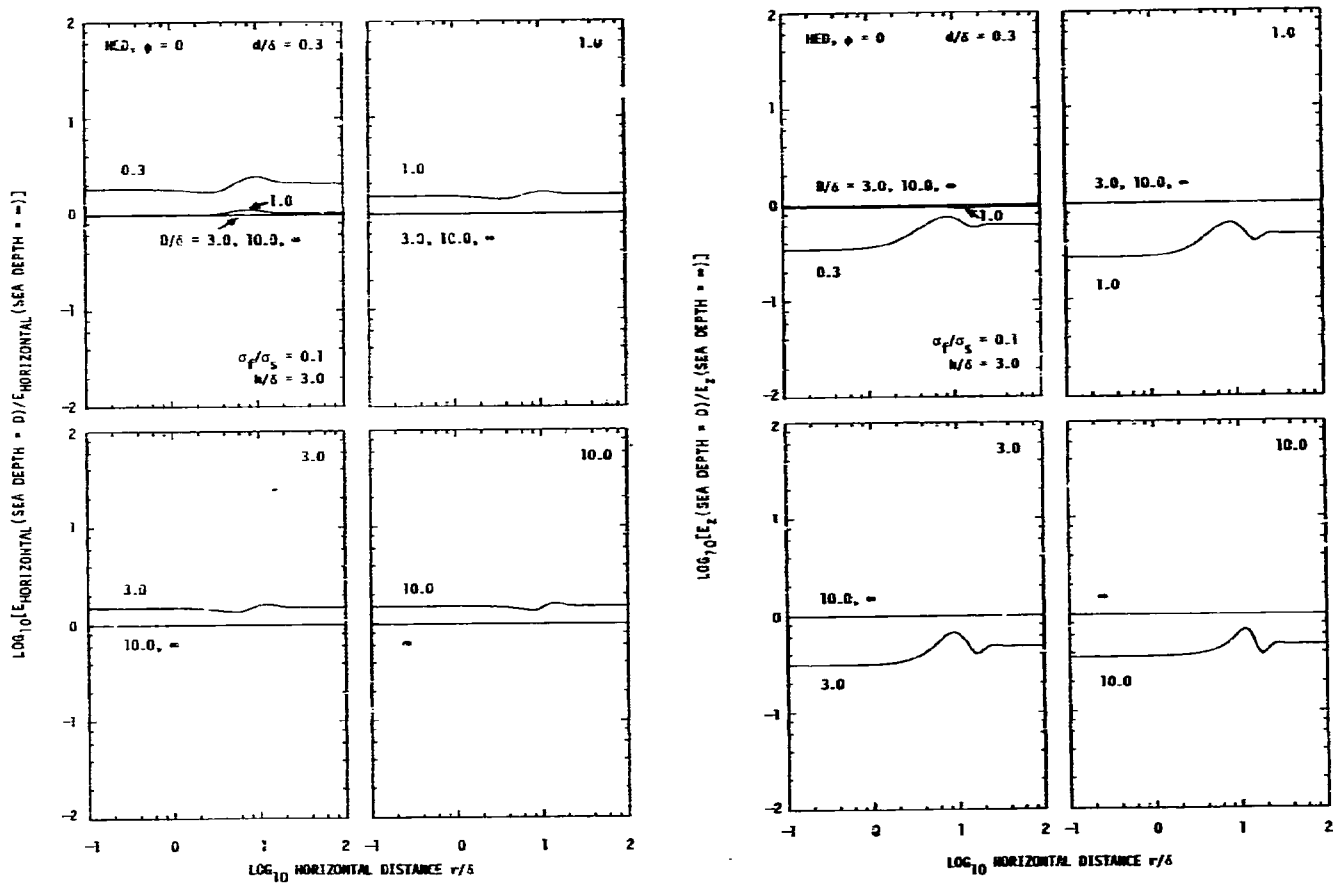


Figure 23. Curves illustrating the changes produced in the electric field component data presented in Figure 19 for an HED located three sea water skin depths above the surface of an infinitely deep sea ($h/\delta = 3.0$) when an electrically conducting sea floor (conductivity $\sigma_f = 0.1\ \sigma_S$, depth D) is introduced. Note that the changes apply to the fields produced at an azimuthal angle ($\phi$) of 0°.

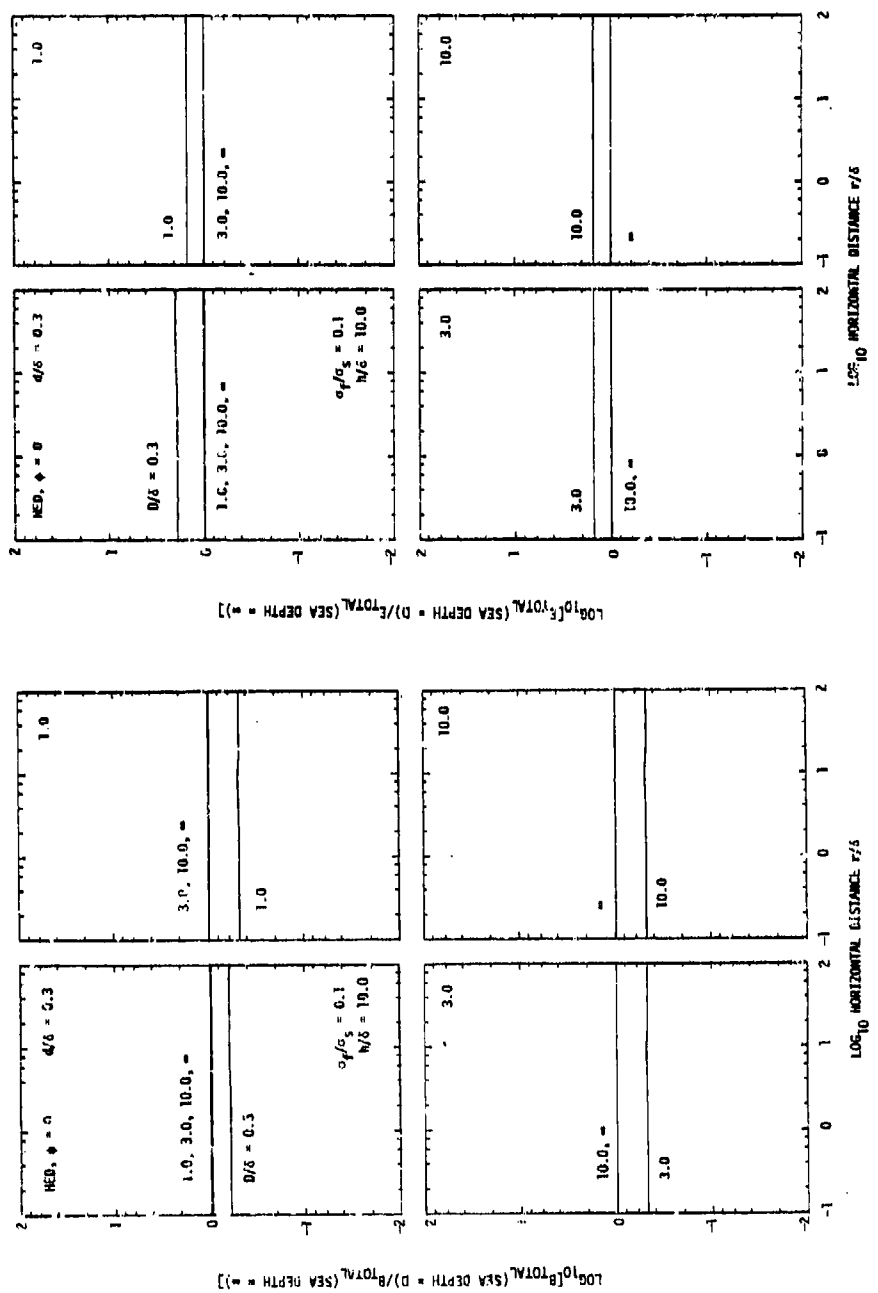


Figure 24. Curves illustrating the changes produced in the magnetic and electric field data presented in Figure 18 for an HED located ten sea water skin depths above the surface of an infinitely deep sea ($h/\delta = 10.0$) when an electrically conducting sea floor (conductivity $\sigma_f = 0.1\ \sigma_s$, depth D) is introduced. Note that the changes apply to the fields produced at an azimuthal angle ($\phi$) of 0°.

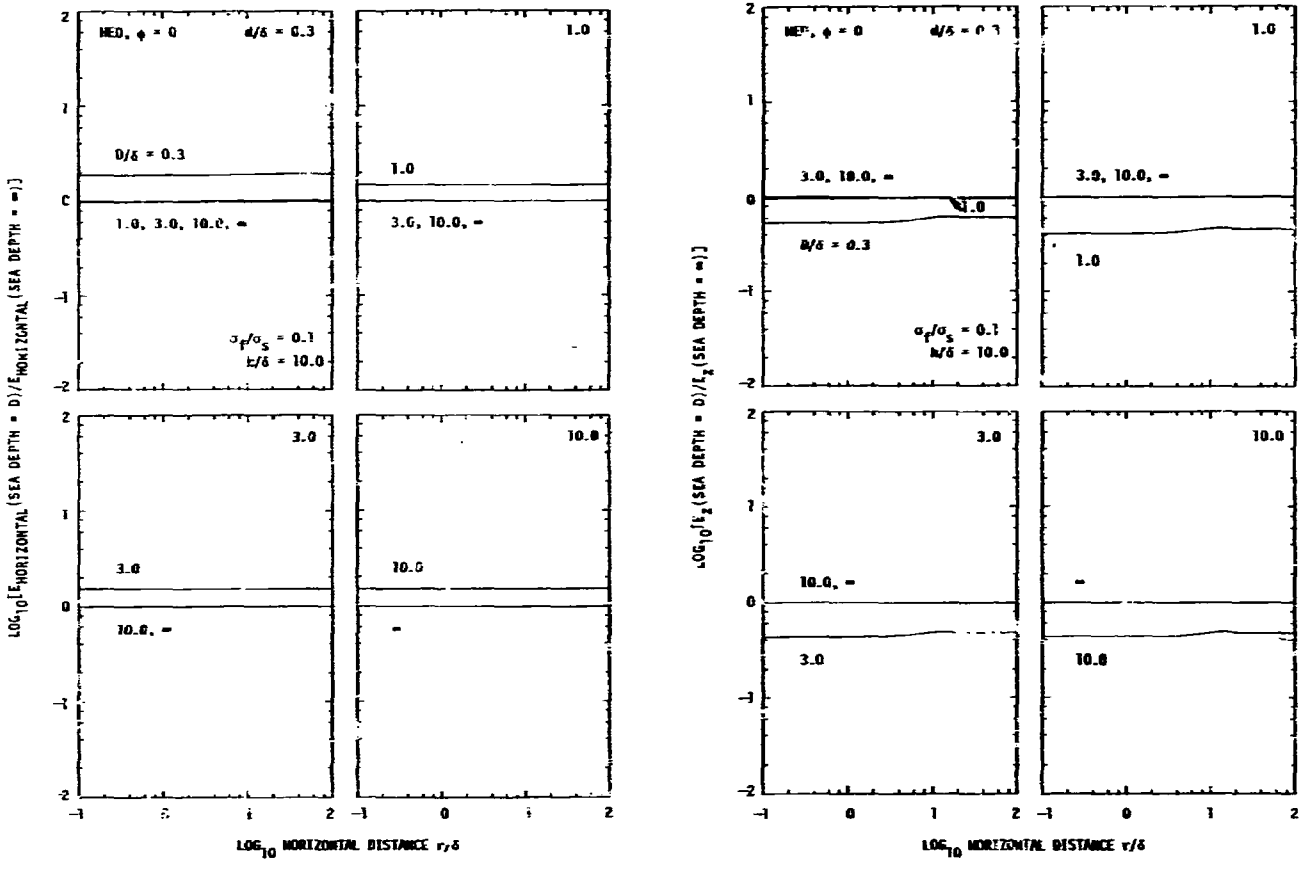


Figure 25. Curves illustrating the changes produced in the electric field component data presented in Figure 19 for an HED located ten sea water skin depths above the surface of an infinitely deep sea ($h/\delta = 10.0$) when an electrically conducting sea floor (conductivity $\sigma_f = 0.1\ \sigma_s$, depth D) is introduced. Note that the changes apply to the fields produced at an azimuthal angle ($\phi$) of 0°.

# APPENDIX 4

## Field Data For The

## HORIZONTAL ELECTRIC DIPOLE, $\phi = 90°$

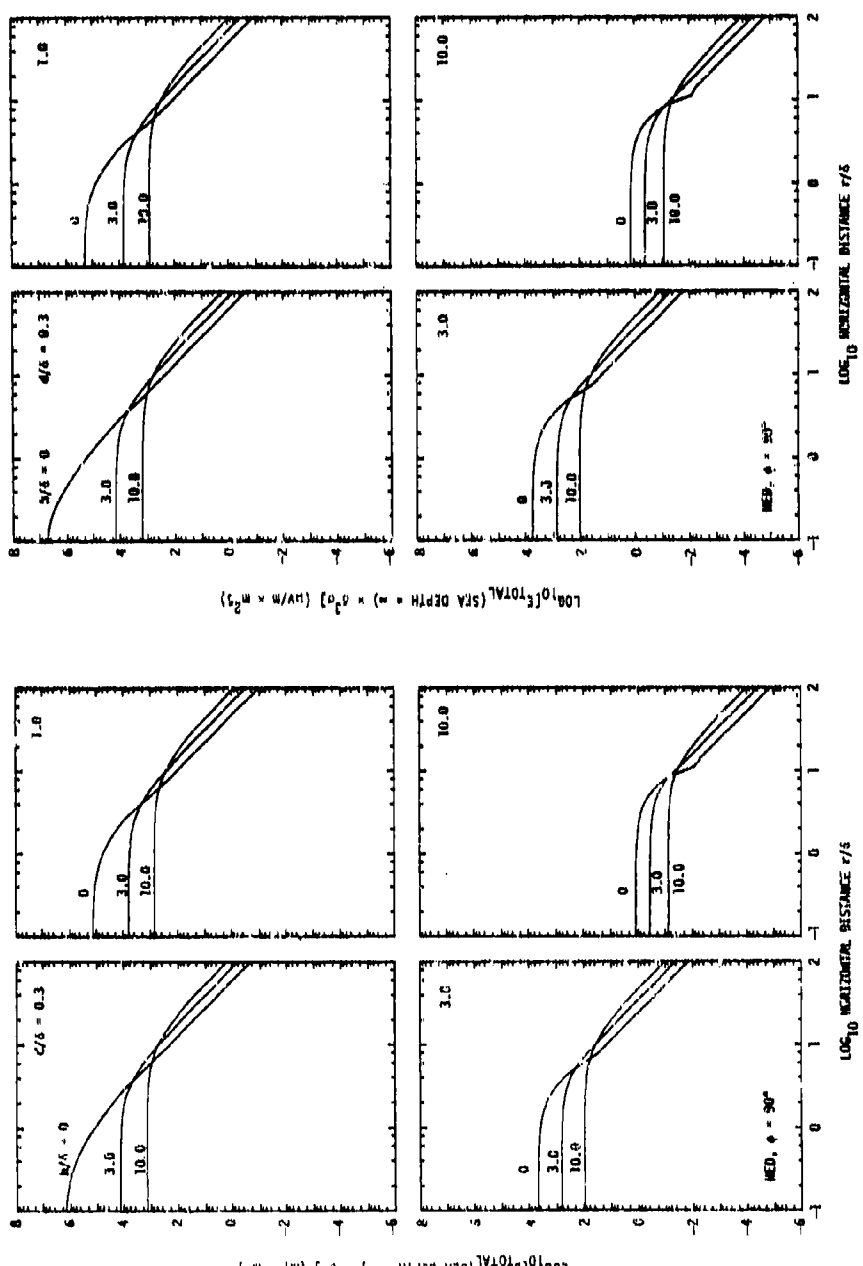


Figure . Variation with horizontal distance of the amplitudes of the total magnetic ($B_{TOTAL}$) and electric ($E_{TOTAL}$) fields produced in an infinitely deep sea by a horizontally directed harmonic electric dipole (HED) located on and above the surface of the sea. The fields are given for an azimuthal angle ($\phi$) of 90°.

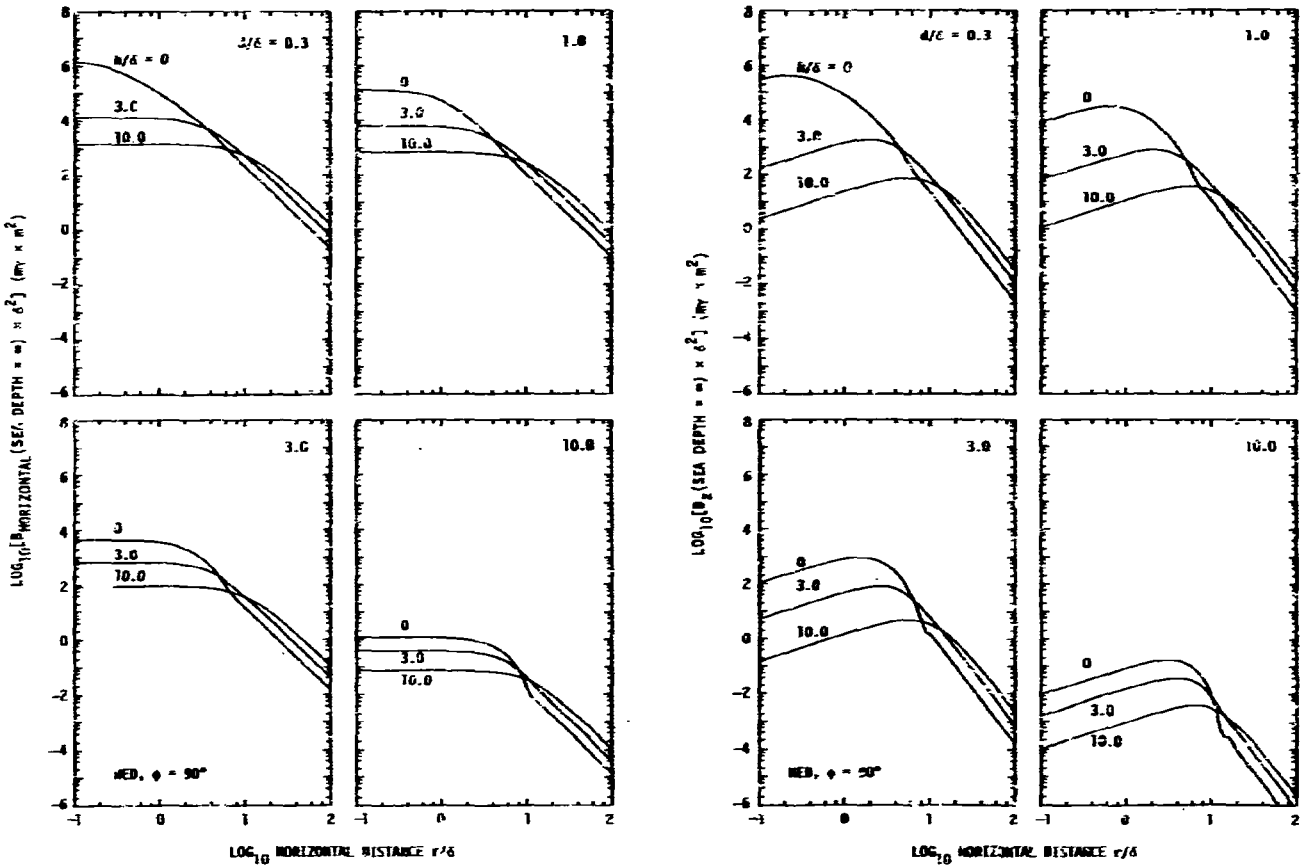


Figure 27. Variation with horizontal distance of the amplitudes of the two magnetic field components $B_{HORIZONTAL}$ and $B_z$ produced in an infinitely deep sea by a horizontally directed harmonic electric dipole (HED) located on and above the surface of the sea. The fields are given for an azimuthal angle ($\phi$) of 90°.

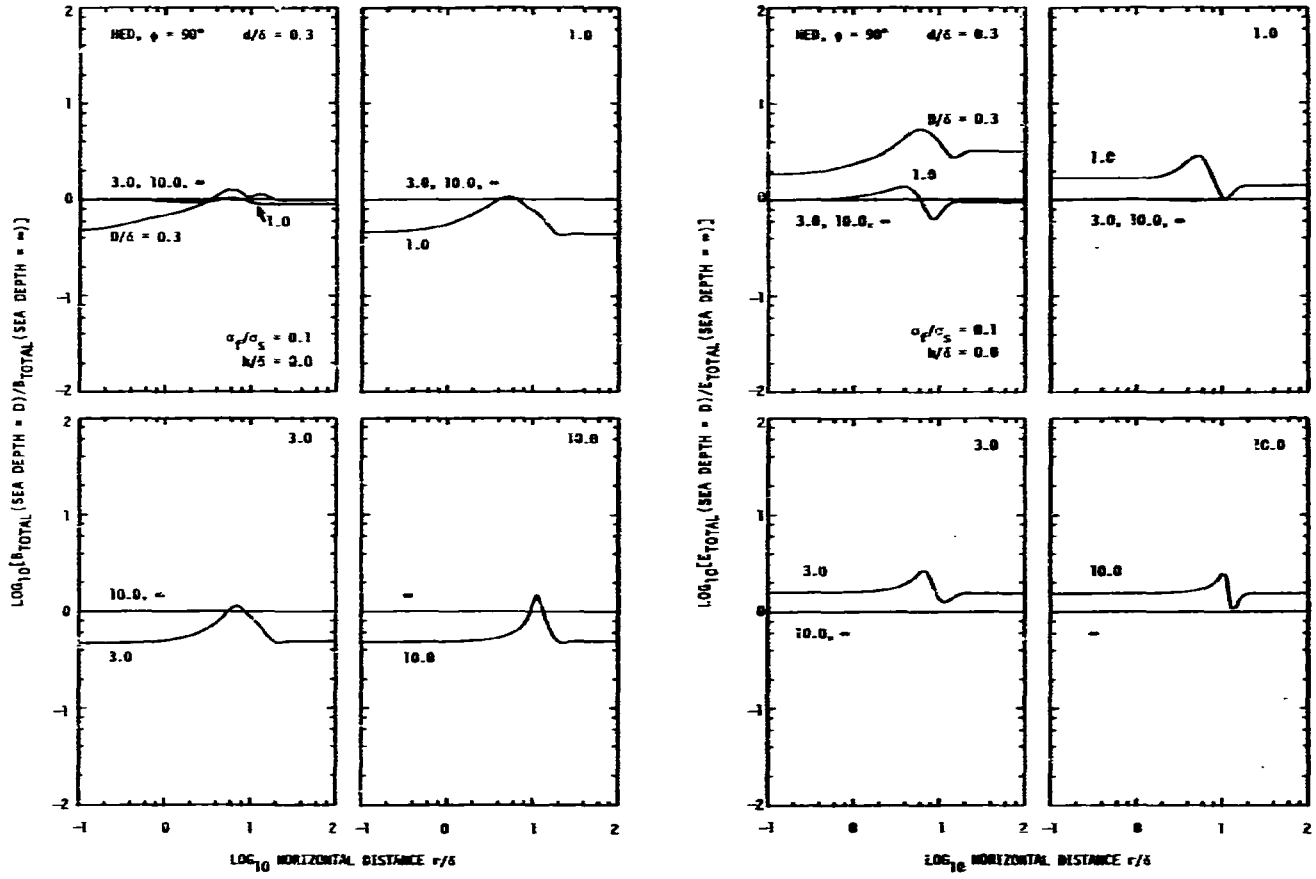


Figure 28. Curves illustrating the changes produced in the magnetic and electric field data presented in Figure 26 for an HED located on the surface of an infinitely deep sea when an electrically conducting sea floor (conductivity $\sigma_f = 0.1\ \sigma_s$, depth D) is introduced. Note that the changes apply to the fields produced at an azimuthal angle ($\phi$) of 90°.

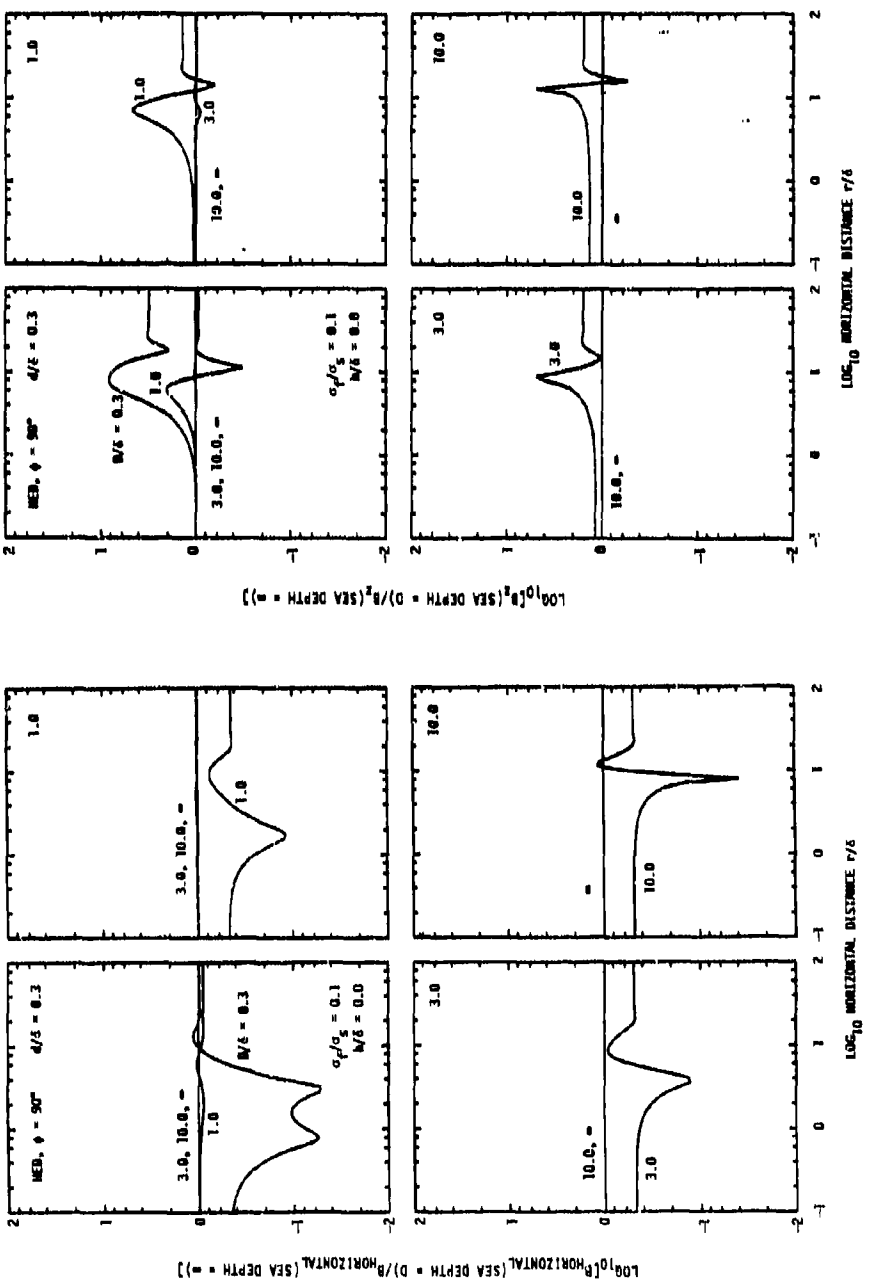


Figure 29. Curves illustrating the changes produced in the magnetic field component data presented in Figure 27 for an HED located on the surface of an infinitely deep sea when an electrically conducting sea floor (conductivity $\sigma_f = 0.1\ \sigma_s$, depth D) is introduced. Note that the changes apply to the fields produced at an azimuthal angle ($\phi$) of 90°.

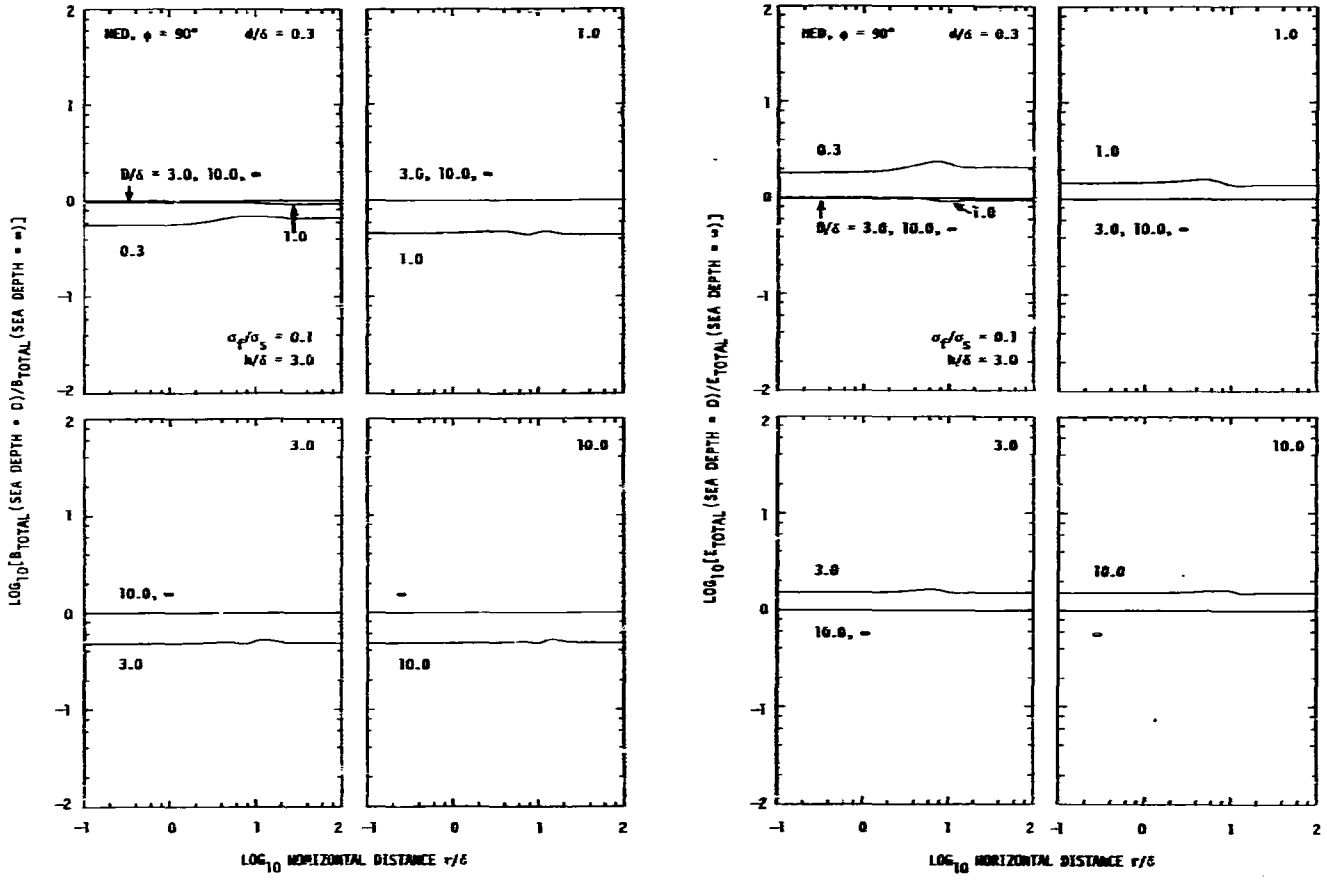


Figure 30. Curves illustrating the changes produced in the magnetic and electric field data presented in Figure 26 for an HED located three sea water skin depths above the surface of an infinitely deep sea ($h/\delta = 3.0$) when an electrically conducting sea floor (conductivity $\sigma_f = 0.1\ \sigma_S$, depth D) is introduced. Note that the changes apply to the fields produced at an azimuthal angle ($\phi$) of 90°.

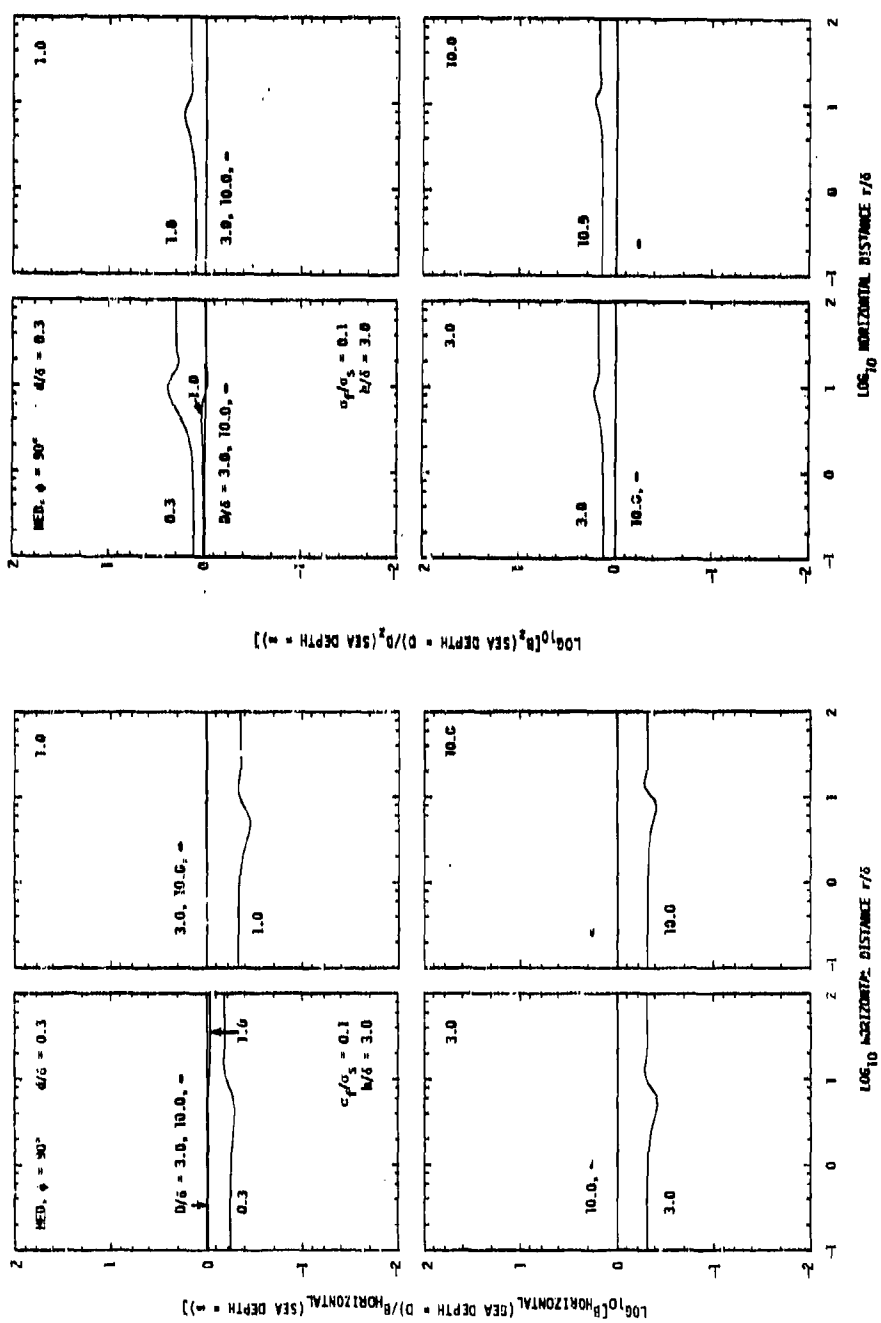


Figure 31. Curves illustrating the changes produced in the magnetic field component data presented in Figure 27 for an HED located three sea water skin depths above the surface of an infinitely deep sea ($h/\delta = 3.0$) when an electrically conducting sea floor (conductivity $\sigma_f = 0.1\ \sigma_s$, depth D) is introduced. Note that the changes apply to the fields produced at an azimuthal angle ($\phi$) of 90°.

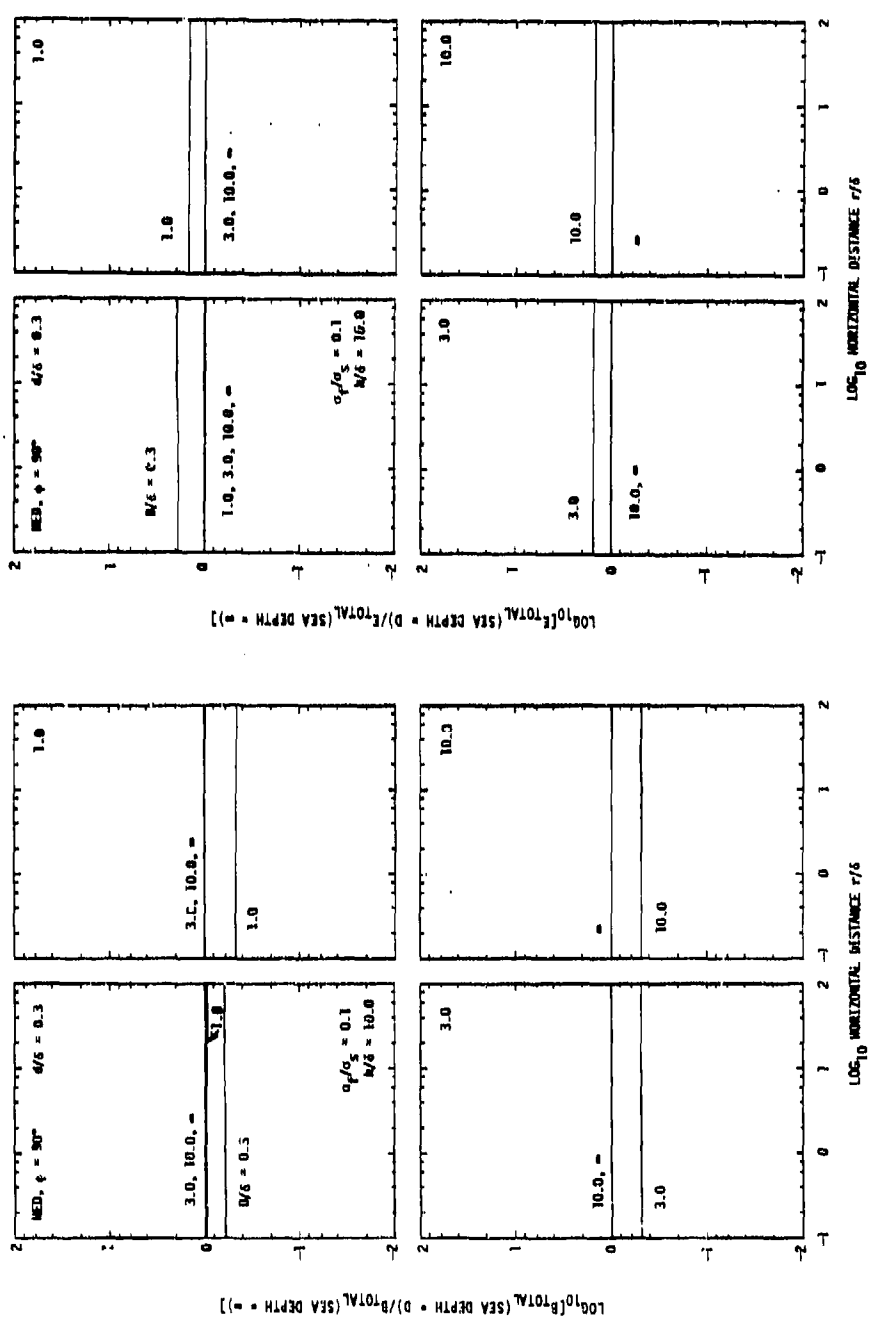


Figure 32. Curves illustrating the changes produced in the magnetic and electric field data presented in Figure 26 for an HED located ten sea water skin depths above the surface of an infinitely deep sea ($h/\delta = 10.0$) when an electrically conducting sea floor (conductivity $\sigma_f = 0.1\ \sigma_s$, depth D) is introduced. Note that the changes apply to the fields produced at an azimuthal angle ($\phi$) of 90°.

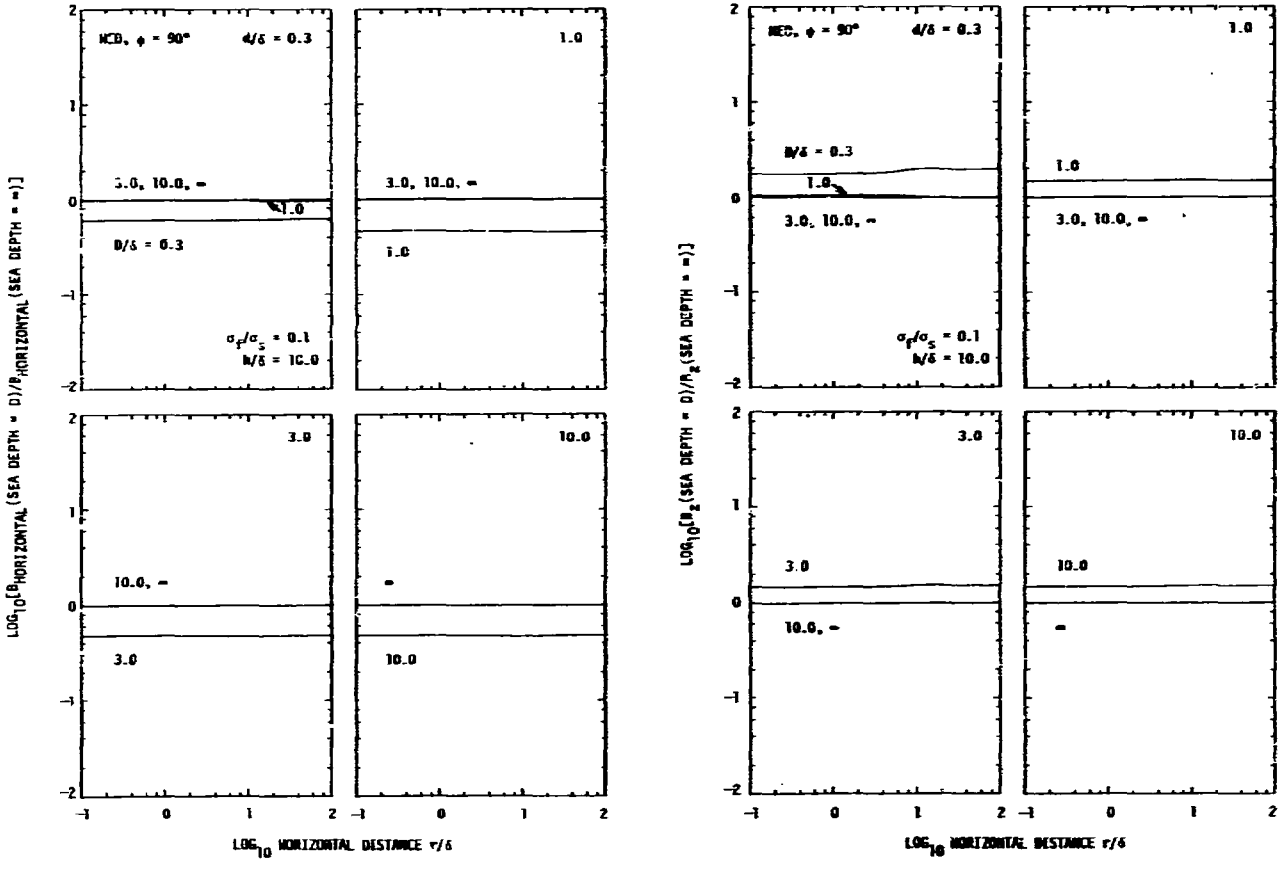


Figure 33. Curves illustrating the changes produced in the magnetic field component data presented in Figure 27 for an HED located ten sea water skin depths above the surface of an infinitely deep sea ($h/\delta = 10.0$) when an electrically conducting sea floor (conductivity $\sigma_f = 0.1\ \sigma_s$, depth D) is introduced. Note that the changes apply to the fields produced at an azimuthal angle ($\phi$) of 90°.

# APPENDIX 5

## Field Data For The

## HORIZONTAL MAGNETIC DIPOLE, $\phi = 0°$

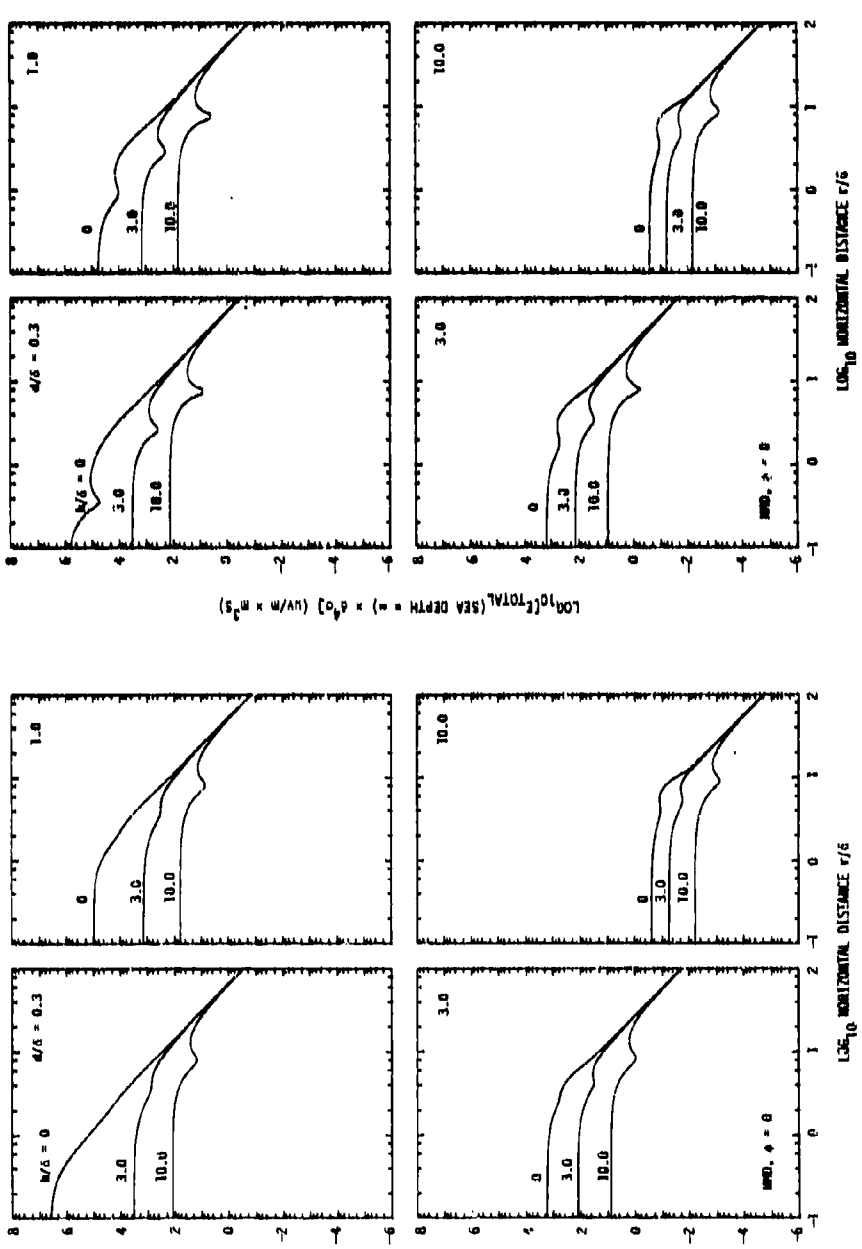


Figure 34. Variation with horizontal distance of the amplitudes of the total magnetic ($B_{TOTAL}$) and electric ($E_{TOTAL}$) fields produced in an infinitely deep sea by a horizontally directed harmonic magnetic dipole (HMD) located on and above the surface of the sea. The fields are given for an azimuthal angle ($\phi$) of 0°.

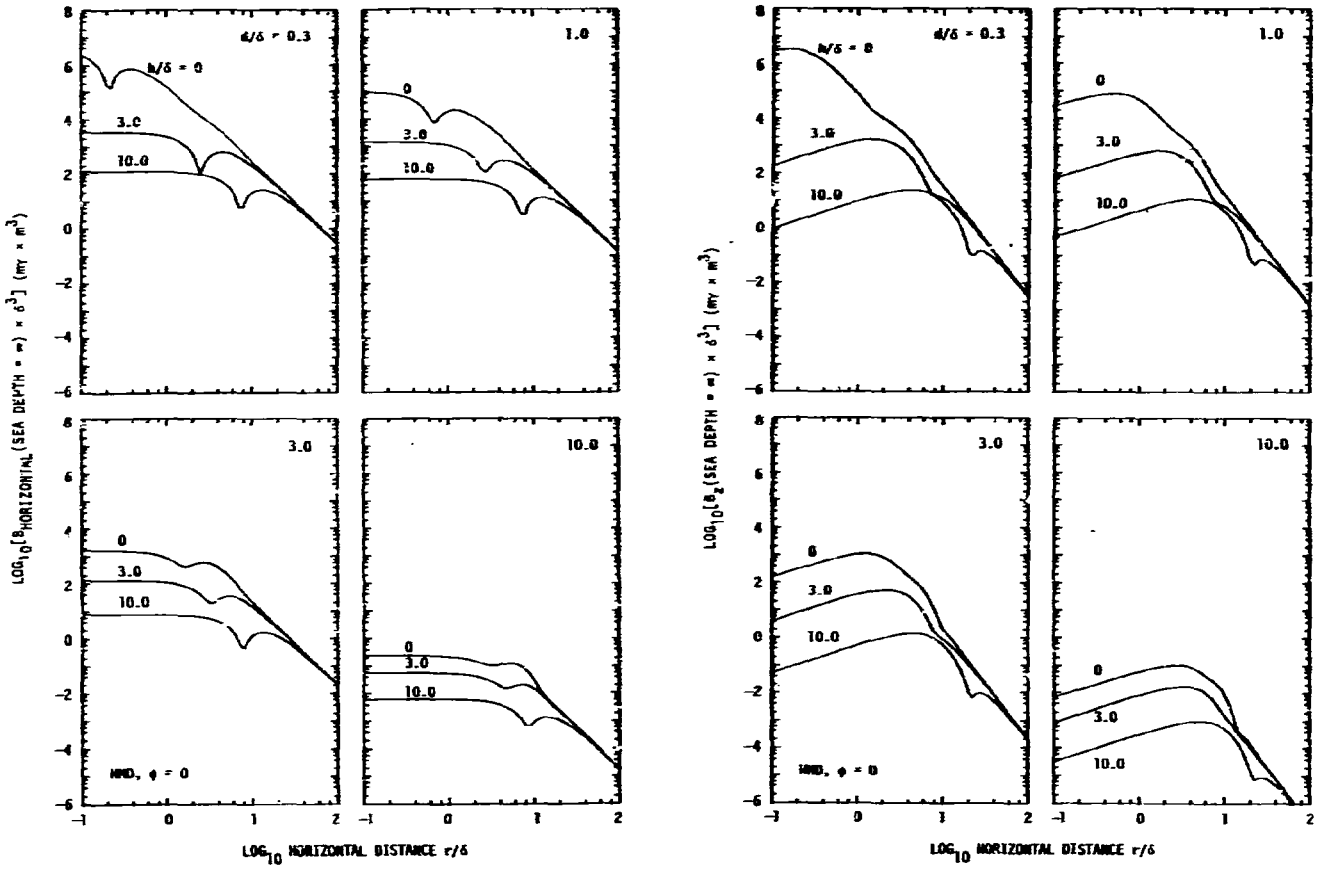


Figure 35. Variation with horizontal distance of the amplitudes of the two magnetic field components $B_{HORIZONTAL}$ and $B_Z$ produced in an infinitely deep sea by a horizontally directed harmonic magnetic dipole (HMD) located on and above the surface of the sea. The fields are given for an azimuthal angle ($\phi$) of 0°.

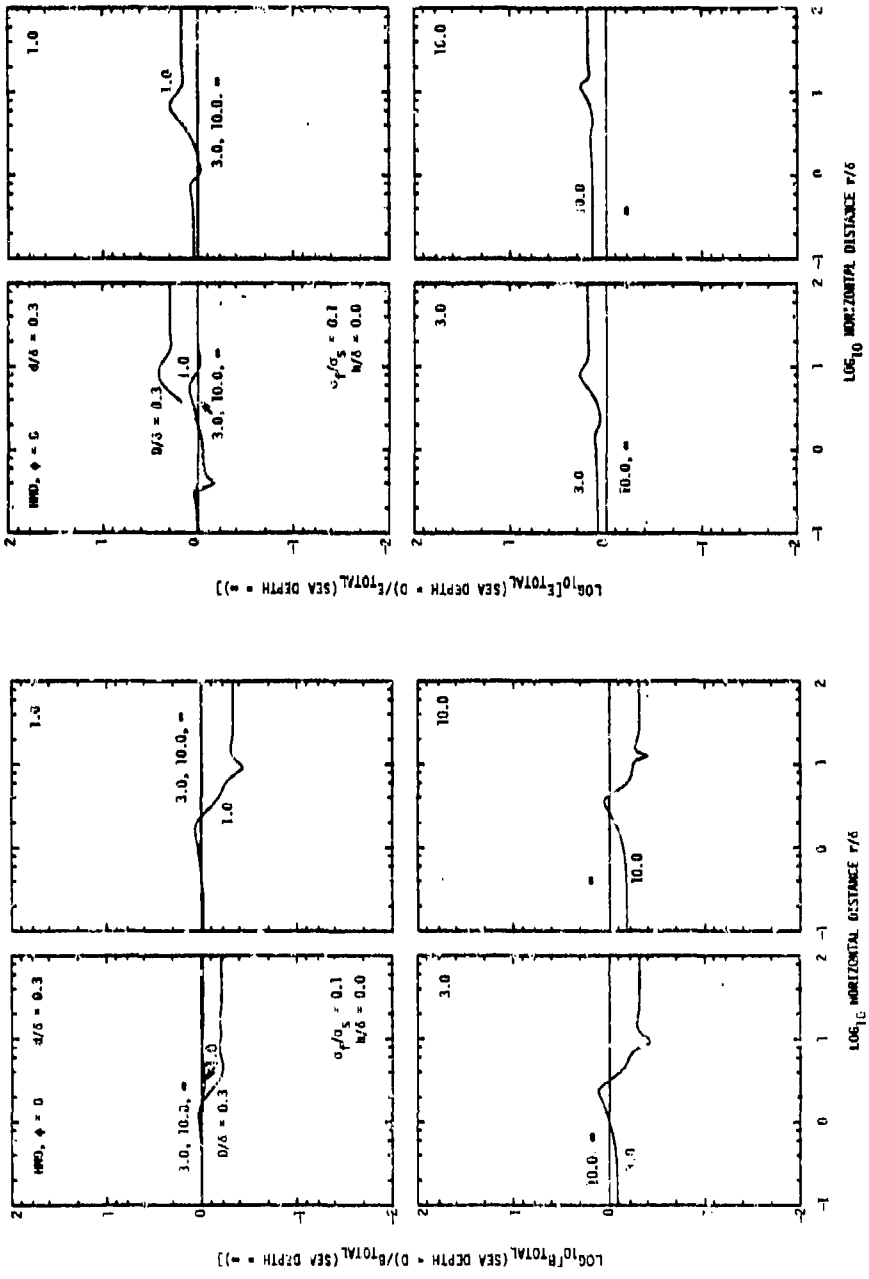


Figure 36. Curves illustrating the changes produced in the magnetic and electric field data presented in Figure 34 for an HMD located on the surface of an infinitely deep sea when an electrically conducting sea floor (conductivity $\sigma_f = 0.1\ \sigma_s$, depth D) is introduced. Note that the changes apply to the fields produced at an azimuthal angle ($\phi$) of 0°.

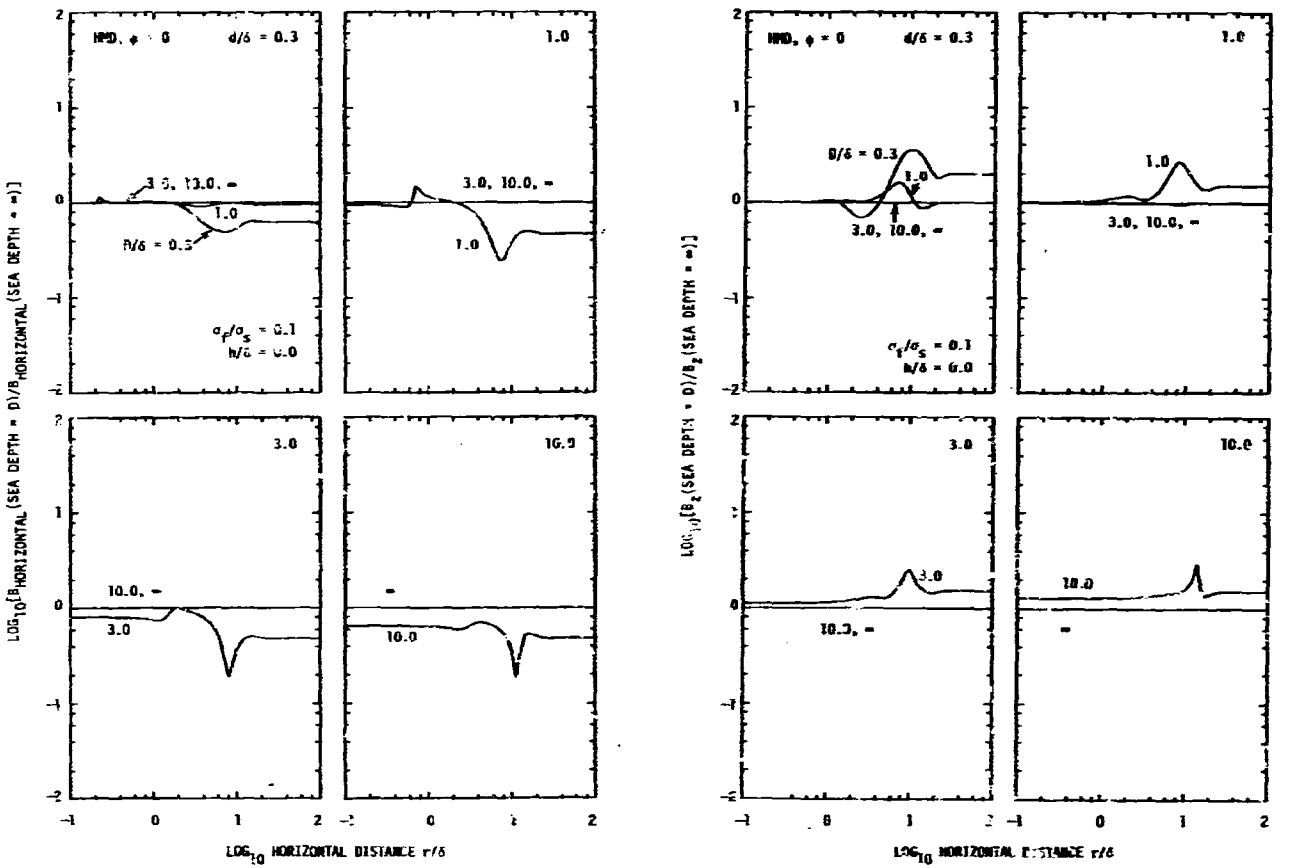


Figure 37. Curves illustrating the changes produced in the magnetic field component data presented in Figure 35 for an HMD located on the surface of an infinitely deep sea when an electrically conducting sea floor (conductivity $\sigma_f$ = 0.1 $\sigma_s$, depth D) is introduced. Note that the changes apply to the fields produced at an azimuthal angle ($\phi$) of 0°.

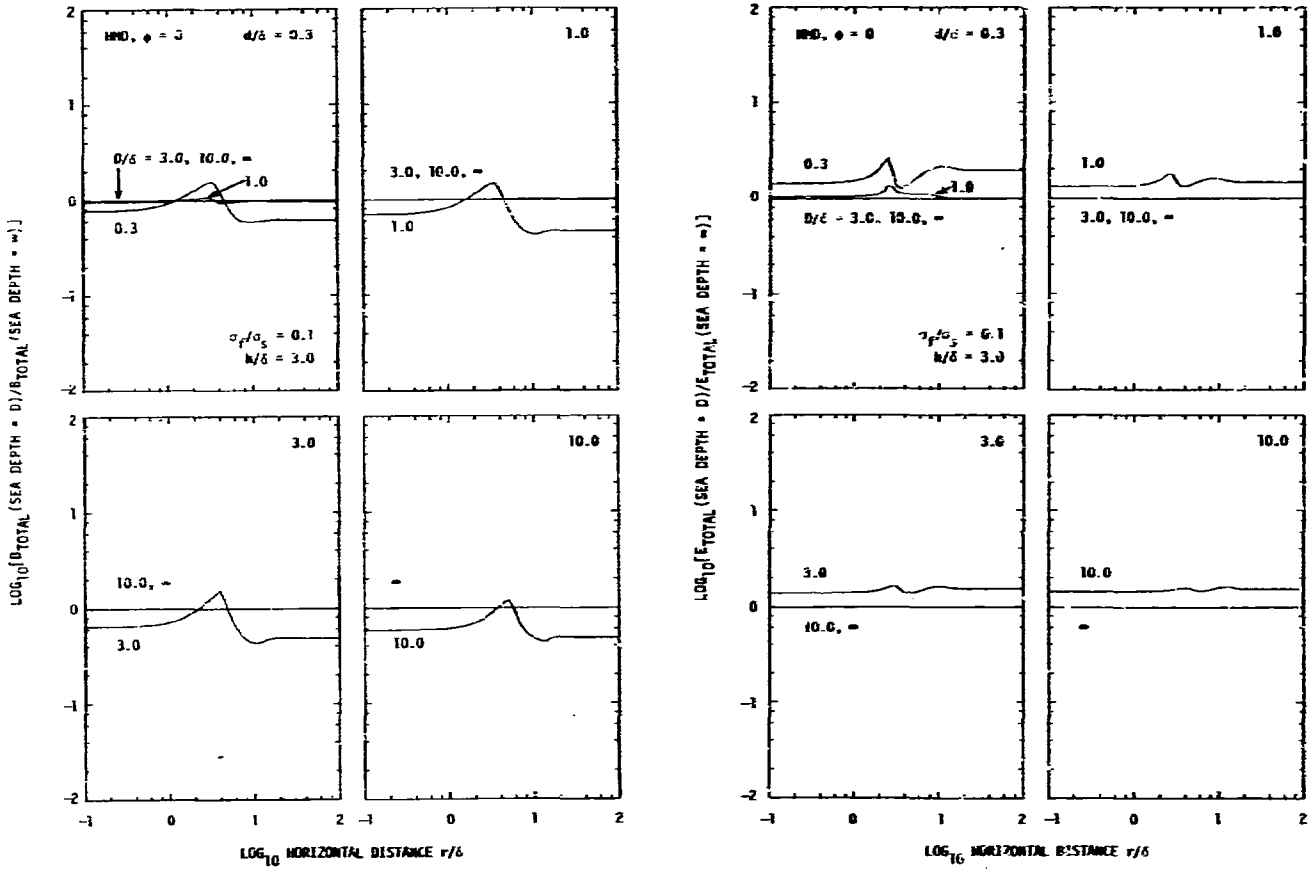


Figure 38. Curves illustrating the changes produced in the magnetic and electric field data presented in Figure 34 for an HMD located three sea water skin depths above the surface of an infinitely deep sea ($h/\delta = 3.0$) when an electrically conducting sea floor (conductivity $\sigma_f = 0.1\ \sigma_s$, depth D) is introduced. Note that the changes apply to the fields produced at an azimuthal angle ($\phi$) of 0°.

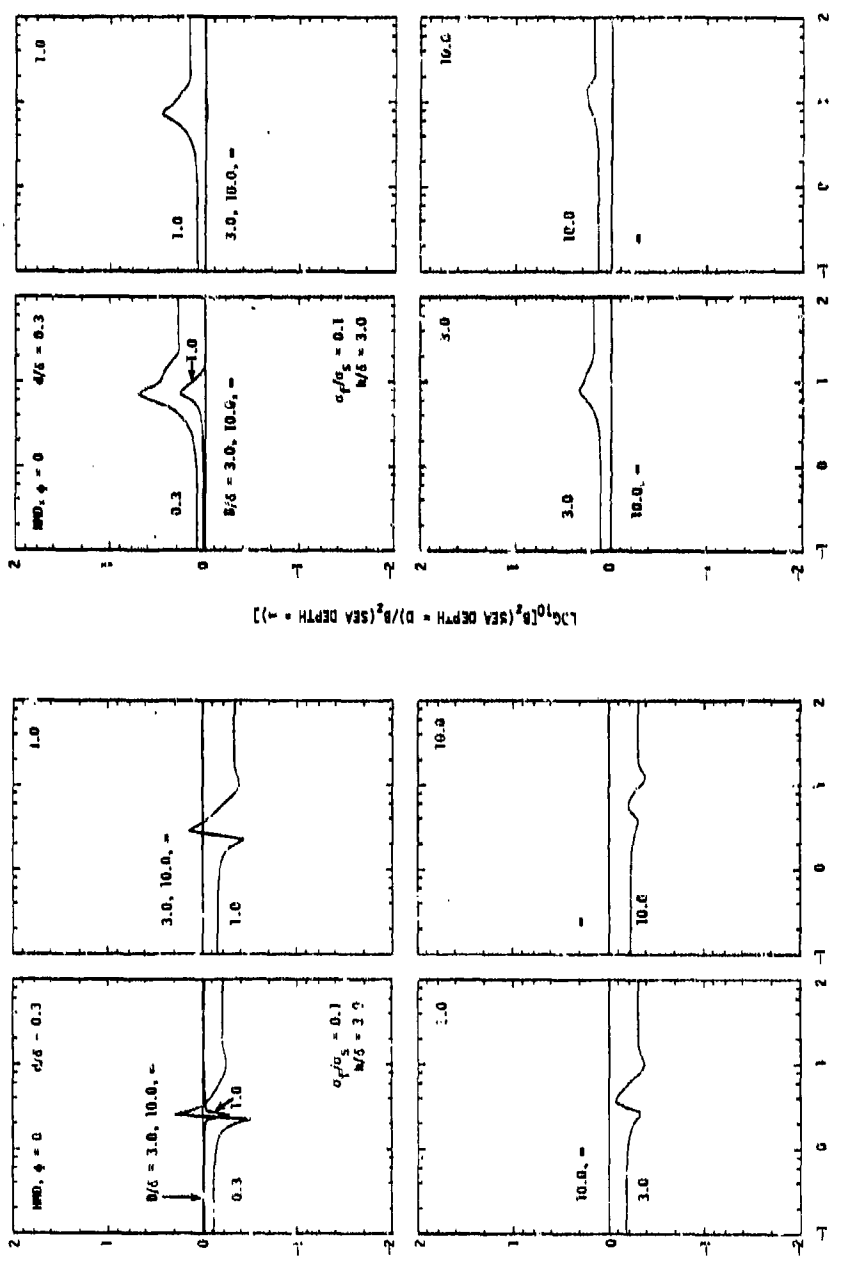


Figure 39. Curves illustrating the changes produced in the magnetic field component data presented in Figure 35 for an HMD located three sea water skin depths above the surface of an infinitely deep sea ($h/\delta = 3.0$) when an electrically conducting sea floor (conductivity $\sigma_f = 0.1\ \sigma_s$, depth D) is introduced. Note that the changes apply to the fields produced at an azimuthal angle ($\phi$) of 0°.

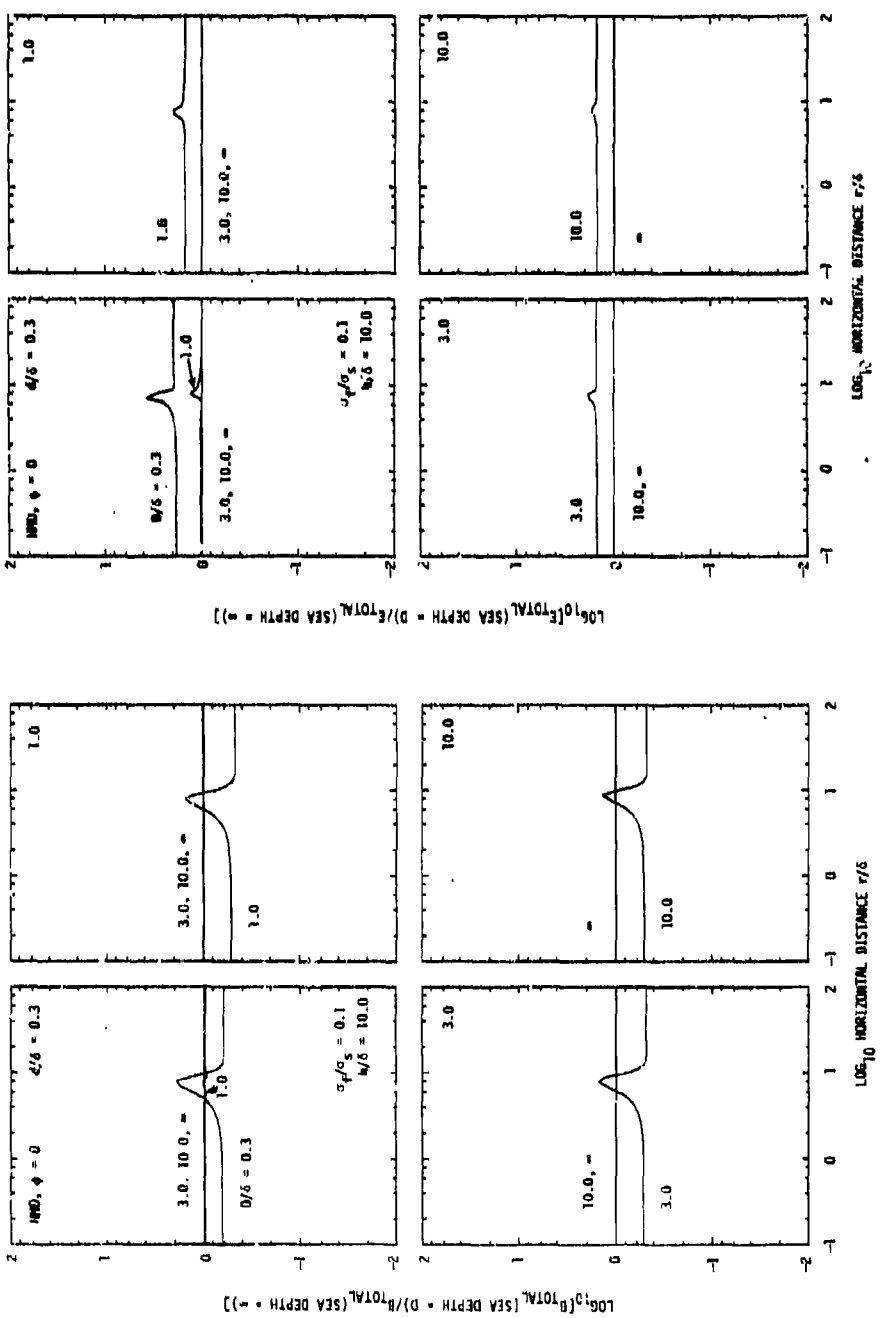


Figure 40. Curves illustrating the changes produced in the magnetic and electric field data presented in Figure 34 for an HMD located ten sea water skin depths above the surface of an infinitely deep sea ($h/\delta = 10.0$) when an electrically conducting sea floor (conductivity $\sigma_f = 0.1\ \sigma_s$, depth D) is introduced. Note that the changes apply to the fields produced at an azimuthal angle ($\phi$) of 0°.

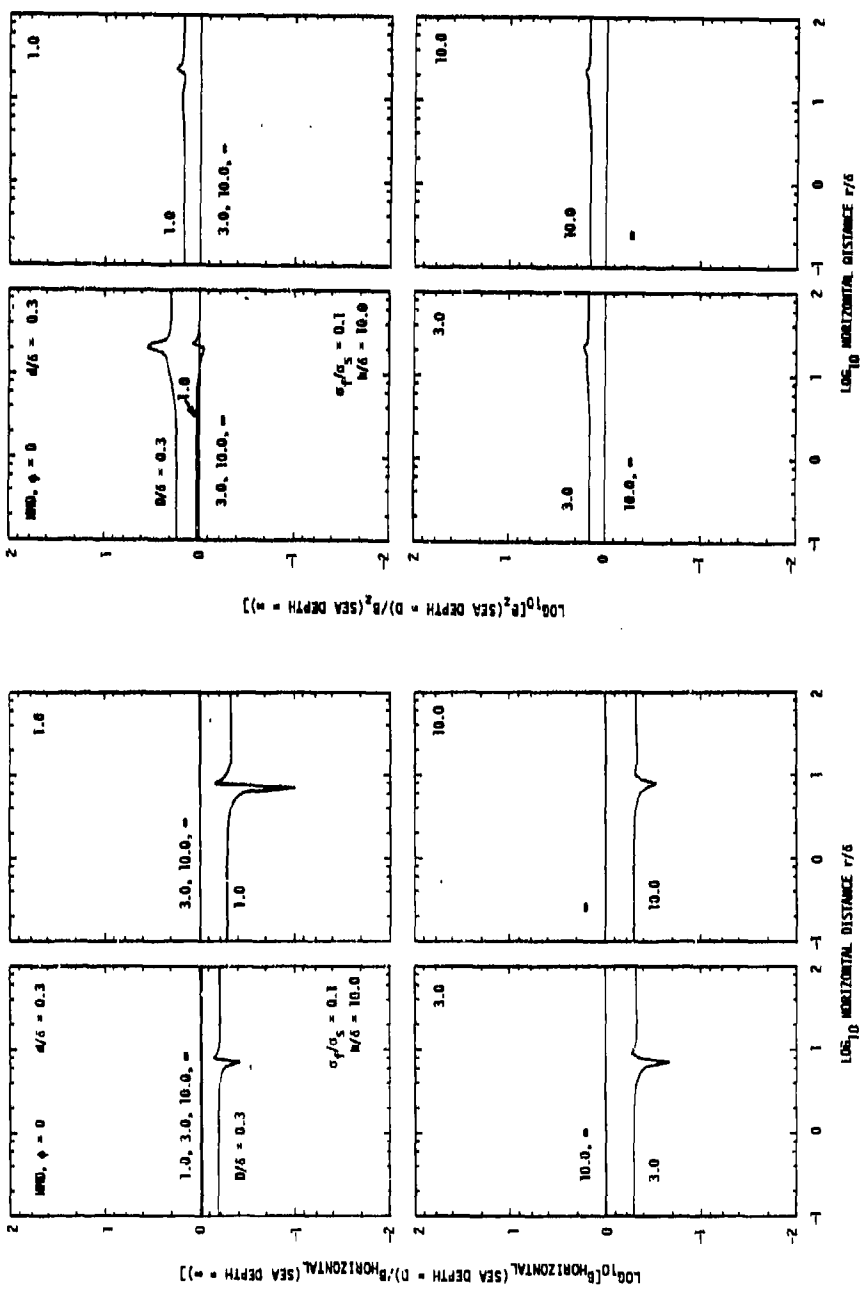


Figure 41. Curves illustrating the changes produced in the magnetic field component data presented in Figure 35 for an HMD located ten sea water skin depths above the surface of an infinitely deep sea ($h/\delta = 10.0$) when an electrically conducting sea floor (conductivity $\sigma_f = 0.1\ \sigma_S$, depth D) is introduced. Note that the changes apply to the fields produced at an azimuthal angle ($\phi$) of 0°.

# APPENDIX 6

## Field Data For The

## HORIZONTAL MAGNETIC DIPOLE, $\phi = 90°$

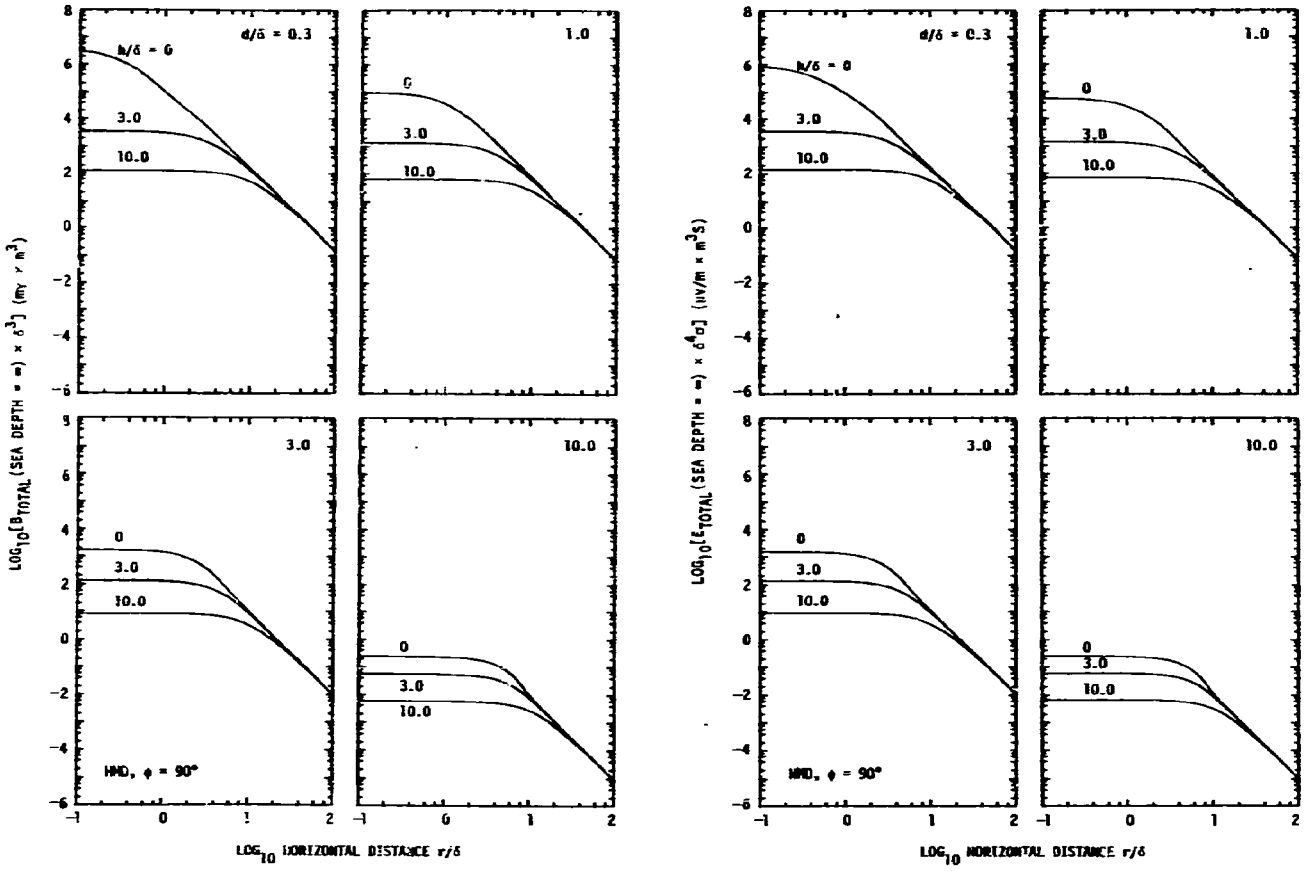


Figure 42. Variation with horizontal distance of the amplitudes of the total magnetic ($B_{TOTAL}$) and electric ($E_{TOTAL}$) fields produced in an infinitely deep sea by a horizontally directed harmonic magnetic dipole (HMD) located on and above the surface of the sea. The fields are given for an azimuthal angle ($\phi$) of 90°.

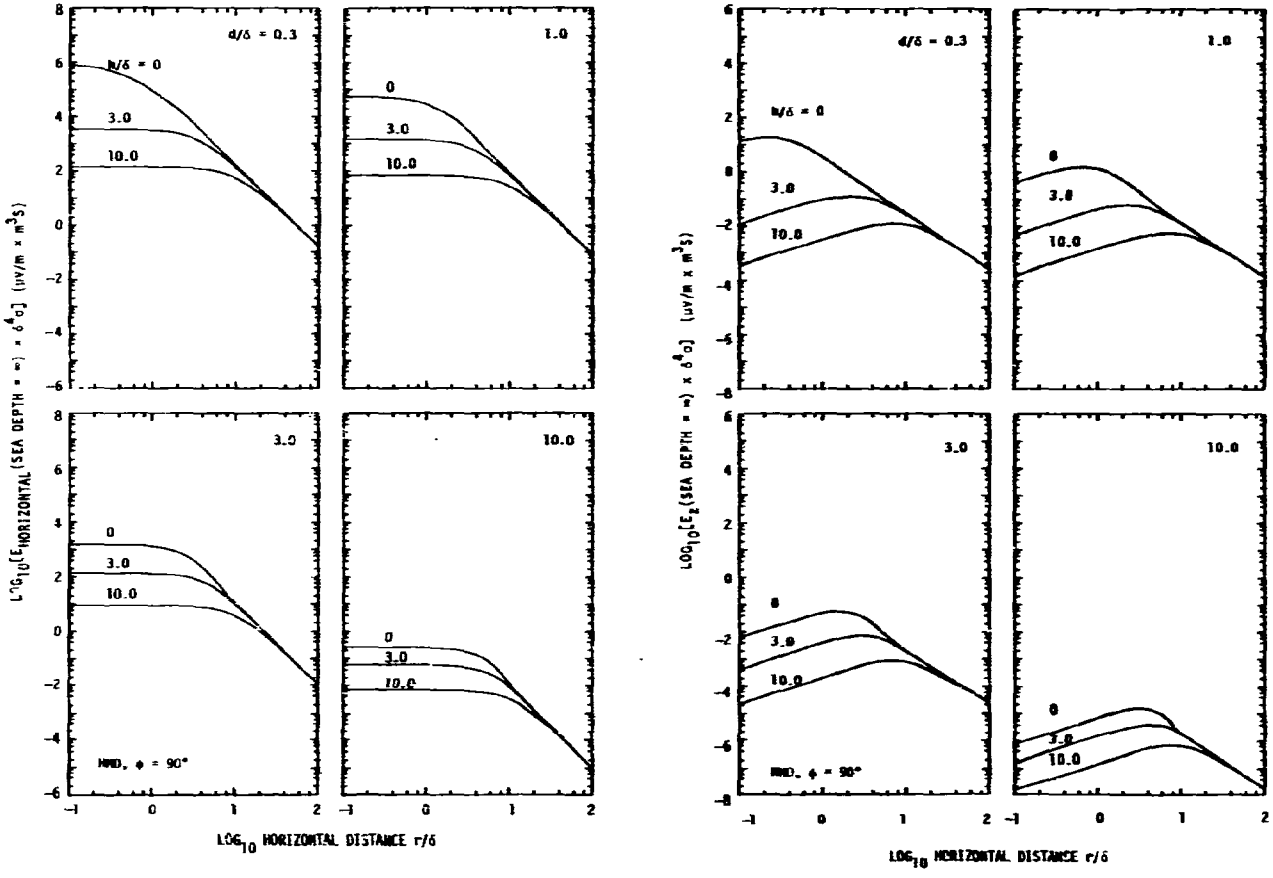


Figure 43. Variation with horizontal distance of the amplitudes of the two electric field components $E_{HORIZONTAL}$ and $E_z$ produced in an infinitely deep sea by a horizontally directed harmonic magnetic dipole (HMD) located on and above the surface of the sea. The components are given for an azimuthal angle ($\phi$) of 90°.

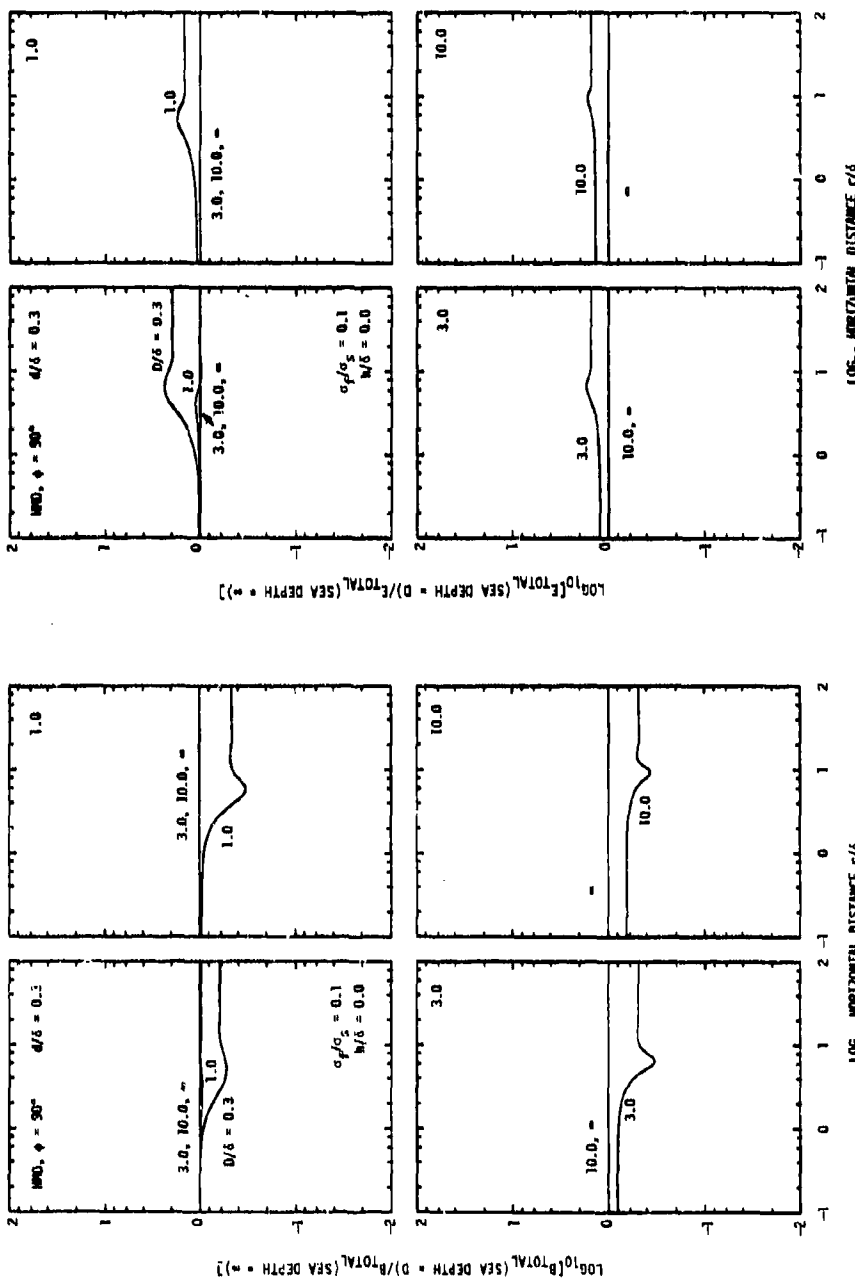


Figure 44. Curves illustrating the changes produced in the magnetic and electric field data presented in Figure 42 for an HMD located on the surface of an infinitely deep sea when an electrically conducting sea floor (conductivity $\sigma_f = 0.1\ \sigma_s$, depth D) is introduced. Note that the changes apply to the fields produced at an azimuthal angle ($\phi$) of 90°.

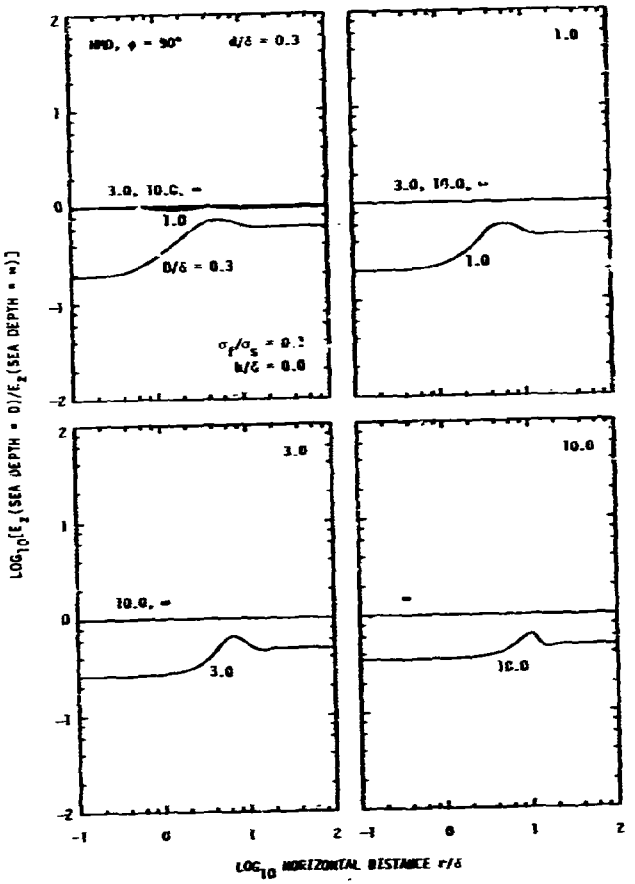


Figure 45. Curves illustrating the changes produced in the vertical electric field component ($E_Z$) data presented in Figure 43 for an HMD located on the surface of an infinitely deep sea when an electrically conducting sea floor (conductivity $\sigma_f$ = 0.1 $\sigma_S$, depth D) is introduced. Note that the changes apply to the fields produced at an azimuthal angle ($\phi$) of 90°.

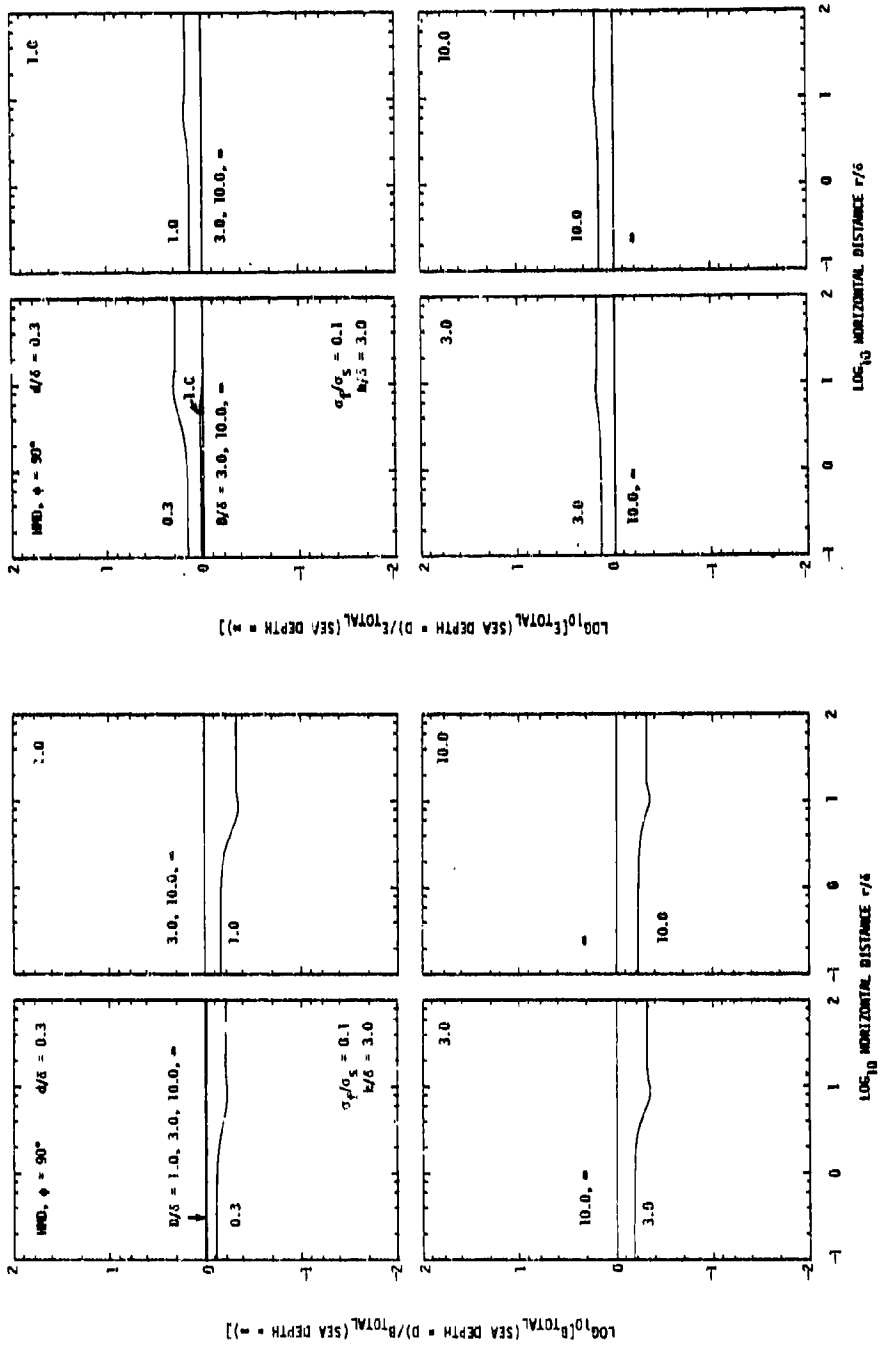


Figure 46. Curves illustrating the changes produced in the magnetic and electric field data presented in Figure 42 for an HMD located three sea water skin depths above the surface of an infinitely deep sea ($h/\delta = 3.0$) when an electrically conducting sea floor (conductivity $\sigma_f = 0.1\ \sigma_s$, depth E) is introduced. Note that the changes apply to the fields produced at an azimuthal angle ($\phi$) of 90°.

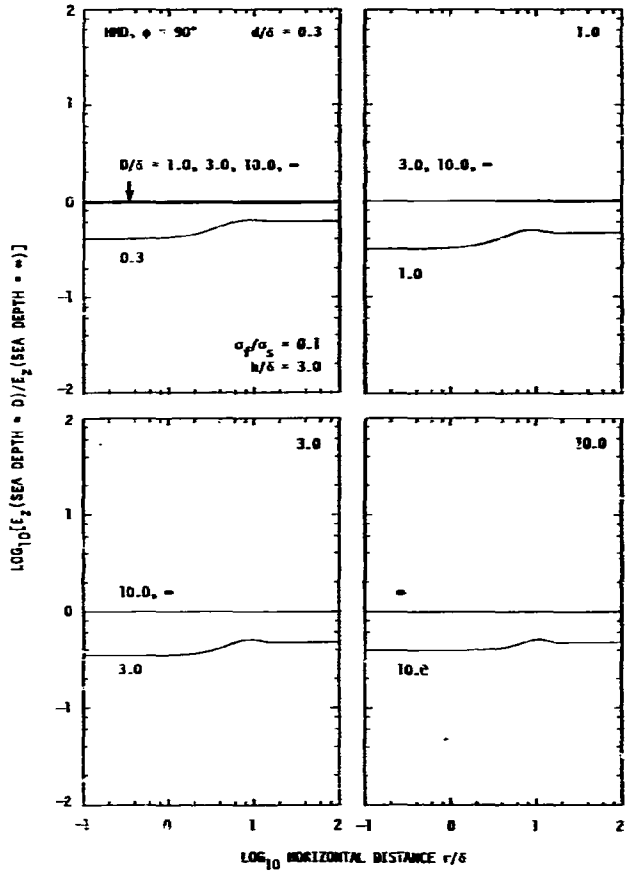


Figure 47. Curves illustrating the changes produced in the vertical electric field component ($E_Z$) data presented in Figure 43 for an HMD located three sea water skin depths above the surface of an infinitely deep sea ($h/\delta = 3.0$) when an electrically conducting sea floor (conductivity $\sigma_f = 0.1\ \sigma_s$, depth D) is introduced. Note that the changes apply to the fields produced at an azimuthal angle ($\phi$) of 90°.

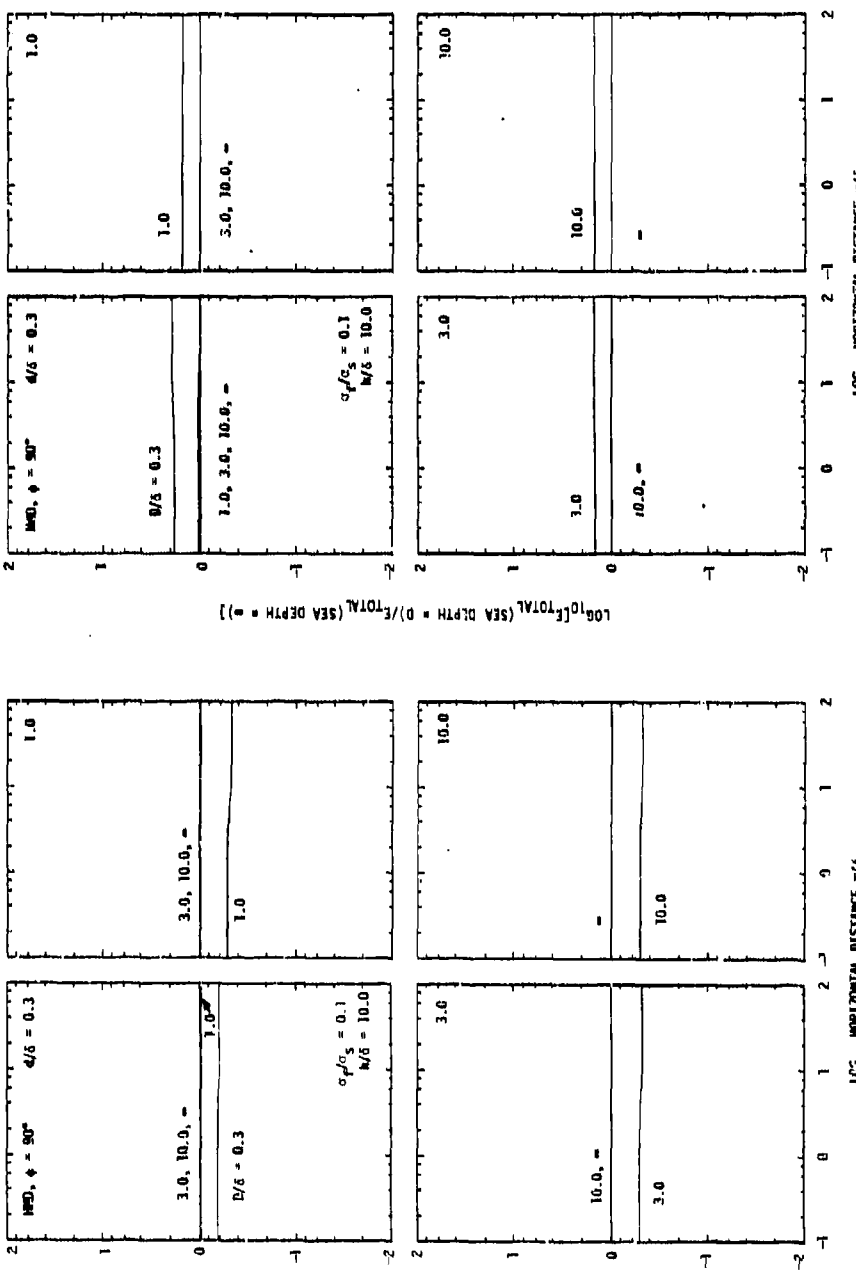


Figure 48. Curves illustrating the changes produced in the magnetic and electric field data presented in Figure 42 for an HMD located ten sea water skin depths above the surface of an infinitely deep sea (h/δ = 10.0) when an electrically conducting sea floor (conductivity $\sigma_f$ = 0.1 $\sigma_s$, depth D) is introduced. Note that the changes apply to the fields produced at an azimuthal angle (φ) of 90°.

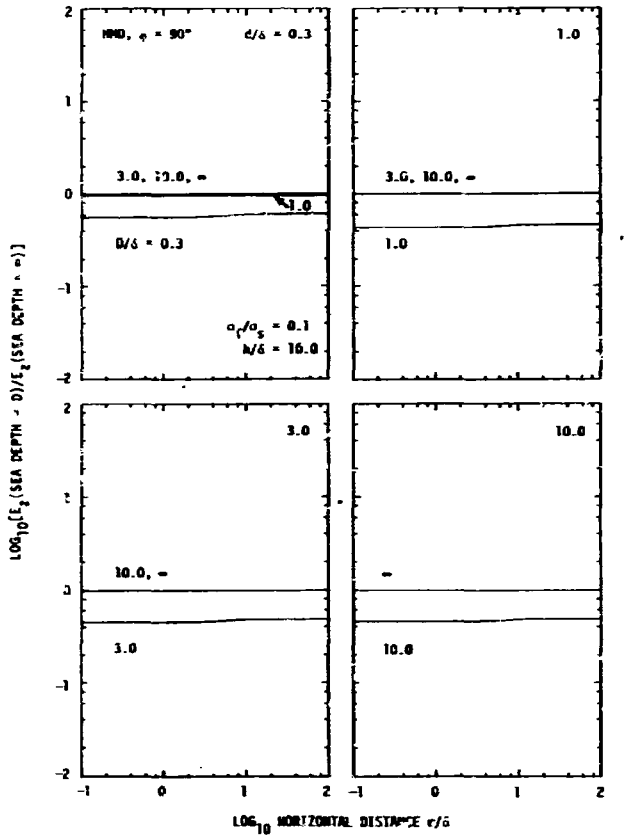


Figure 49. Curves illustrating the changes produced in the vertical electric field component ($E_z$) data presented in Figure 43 for an HMD located ten sea water skin depths above the surface of an infinitely deep sea ($h/\delta = 10.0$) when an electrically conducting sea floor (conductivity $\sigma_f = 0.1\ \sigma_s$, depth D) is introduced. Note that the changes apply to the fields produced at an azimuthal angle ($\phi$) of 90°.

# DISTRIBUTION LIST

| Organization | No. of Copies |
|---|---|
| Director<br>Defense Advanced Research<br>Projects Agency | |
| ATTN: Project Management | 2 |
| GSD, R. Alewine | 1 |
| STO, D.D. Lewis | 1 |
| 1400 Wilson Blvd<br>Arlington, VA 22209 | |
| Defense Technical<br>Information Center | 12 |
| Cameron Station<br>Alexandria, VA 22314 | |
| Office of Naval Research | |
| ATTN: Code 222 | 1 |
| Code 414 | 1 |
| Code 420 | 1 |
| Code 425 | 1 |
| 800 North Quincy Street<br>Arlington, VA 22217 | |
| Office of Naval Research<br>Resident Representative | 1 |
| University of California,<br>San Diego<br>La Jolla, CA 92093 | |
| Office of Naval Research<br>Resident Representative | 1 |
| Stanford University<br>Durand Building, Room 165<br>Stanford, CA 94305 | |
| Assistant Deputy Undersecretary<br>of Defense ($C^3$) | |
| ATTN: T.P. Quinn | 1 |
| Pentagon<br>Washington, D.C 20301 | |

| Organization | No. of Copies |
|---|---|
| Naval Research Laboratory<br>Information Technology Division | |
| ATTN: J.R. Davis | 1 |
| 4555 Overlook Avenue, SW<br>Washington, D.C. 20375 | |
| Naval Ocean Systems Center | |
| ATTN: Library | 1 |
| K.L. Grauer | 1 |
| C.F. Ramstedt | 1 |
| Y. Richter | 1 |
| 271 Catalina Boulevard<br>San Diego, CA 95152 | |
| Naval Electronic Systems<br>Command | |
| ATTN: PME-110-112 | 1 |
| PME-110-X1 | 1 |
| Department of the Navy<br>Washington, D.C. 20360 | |
| Naval Underwater Systems Center<br>New London Laboratory | |
| ATTN: P. Bannister | 1 |
| A. Bruno | 1 |
| J. Orr | 1 |
| E. Soderberg | 1 |
| New London, CT 06320 | |
| Naval Surface Weapons Center<br>White Oak Laboratory | |
| ATTN: J.J. Holmes | 1 |
| P. Wessel | 1 |
| Silver Spring, MD 20910 | |
| David W. Taylor Naval Ship<br>Research & Development Center | |
| ATTN: W. Andahazy | 1 |
| P. Field | 1 |
| Annapolis, MD 21402 | |

## DISTRIBUTION LIST (Continued)

| Organization | No. of Copies |
|---|---|
| Office of the Assistant Secretary of the Navy (R, E&S) | |
| ATTN: J. Hull | 1 |
| Washington, D.C. 20350 | |
| Naval Ocean R & D Activity | |
| ATTN: D.L. Durham | 1 |
| D.W. Handschumacher | 1 |
| K. Smits | 1 |
| NSTL Station | |
| Bay St. Louis, MS 39522 | |
| Naval Oceanographic Office | |
| ATTN: O.E. Avery | 1 |
| T. Davis | 1 |
| G.R. Lorentzen | 1 |
| NSTL Station | |
| Bay St. Louis, MS 39522 | |
| Naval Air Systems Command | |
| ATTN: B.L. Dillon | 1 |
| Washington, D.C. 20361 | |
| Naval Intelligence Support Center | |
| ATTN: G.D. Batts | 1 |
| W. Reese | 1 |
| 4301 Suitland Road | |
| Washington, D.C. 20390 | |
| Naval Postgraduate School | |
| Department of Physics and Chemistry | |
| ATTN: O. Heinz | 1 |
| Monterey, CA 93940 | |
| Naval Coastal Systems Center | |
| ATTN: R.H. Clark | |
| M.J. Wynn | 1 |
| Panama City, FL 32407 | |

| Organization | No. of Copies |
|---|---|
| Naval Air Development Center | |
| ATTN: J. Shannon | 1 |
| Warminster, PA 18974 | |
| Naval Ocean Systems Center | |
| ATTN: R. Buntzen | 1 |
| C. Fuzak | 1 |
| P. Hansen | 1 |
| 271 Catalina Boulevard | |
| San Diego, CA 95152 | |
| Director | |
| Defense Nuclear Agency | |
| ATTN: RAAE | 1 |
| DDST | 1 |
| RAEV | 1 |
| Washington, D.C. 20305 | |
| SRI International | |
| ATTN: D.M. Bubenik | 1 |
| J.B. Chown | 1 |
| J.G. Depp | 1 |
| R.C. Honey | 1 |
| W.E. Jaye | 1 |
| 333 Ravenswood Avenue | |
| Menlo Park, CA 94025 | |
| R. & D. Associates | |
| ATTN: C. Greifinger | 1 |
| P.O. Box 9695 | |
| Marina del Rey, CA 90291 | |
| Pacific-Sierra Research Corp. | |
| ATTN: E.C. Field, Jr. | 1 |
| 12340 Santa Monica Blvd | |
| Los Angeles, CA 90025 | |
| TASC | |
| ATTN: J. Czika, Jr. | 1 |
| 1700 N. Moore Street, Suite 1220 | |
| Arlington, VA 22209 | |

## DISTRIBUTION LIST (Continued)

| Organization | No. of Copies |
|---|---|
| Naval Weapons Center<br>ATTN: R.J. Dinger<br>China Lake, CA 93555 | 1 |
| Johns Hopkins University<br>Applied Physics Laboratory<br>ATTN: L.W. Hart<br>H. Ko<br>Johns Hopkins Road<br>Laurel, MD 20810 | 1<br>1 |
| La Jolla Institute<br>ATTN: K. Watson<br>La Jolla, CA 92407 | 1 |
| E.G. & G.<br>ATTN: L.E. Pitts<br>P.O. Box 398<br>Riverdale, MD 20840 | 1 |
| University of Texas, Austin<br>Geomagnetics and Electrical Geoscience Laboratory<br>ATTN: F.X. Bostick, Jr.<br>Austin, TX 78712 | 1 |
| Commander<br>Rome Air Development Center/EEPS<br>ATTN: P.A. Kossey<br>Hanscom AFB, MA 01731 | 1 |
| University of California<br>Scripps Institute of Oceanography<br>ATTN: C.S. Cox<br>La Jolla, CA 92093 | 1 |
| Lockheed Palo Alto Research Laboratory<br>ATTN: J.B. Cladis<br>W.L. Imhof<br>J.B. Reagan<br>M. Walt<br>3251 Hanover Street, Bldg 255<br>Palo Alto, CA 94304 | 1<br>1<br>1<br>1 |
| Chief<br>Air Force Technical Applications Center<br>HQUSAF<br>Patrick AFB, FL 32925 | 1 |
| Commander<br>Air Force Systems Command<br>Andrews AFB, MD 20331 | 2 |
| Commander<br>Air Force Geophysics Laboratory<br>ATTN: Technical Library<br>Hanscom AFB, MA 01731 | 1 |